DOI 10.14943/mem.fish.58.1-2.13

# Ecological Study on the Zooplankton Community in the Oyashio Region During the Spring Phytoplankton Bloom

Yoshiyuki ABE[1)]

(Received 26 August 2016, Accepted 17 October 2016)

**Table of Contents**



[1)] *Laboratory of Marine Biology (Plankton Laboratory), Division of Marine Bioresource and Environmental Science, Graduate School of Fisheries Science, Hokkaido University, 3-1-1 Minato-cho, Hakodate, Hokkaido, 041-8611, Japan*
(E-mail: y.abe@fish.hokudai.ac.jp)
(北海道大学大学院水産科学研究院海洋生物資源科学部門海洋生物学分野浮遊生物学領域)

**Key words**: Mesozooplankton, Macrozooplankton, Phytoplankton bloom, Oyashio region

## 1. Preface

In marine ecosystems, zooplankton play an important role in the transfer production of both the grazing food chain and the microbial food web for higher trophic levels (Raymont, 1983). In addition to the food mediator role, zooplankton accelerate the vertical material flux, termed "Biological pump" (Longhurst and Harrison, 1989; Longhurst, 1991). In high-latitude oceans (Arctic, subarctic, subantarctic and Antarctic), phytoplankton form spring blooms, and nearly half of the primary production is concentrated in a one- to two-month period. In the Oyashio region, western subarctic Pacific, nearly half of the annual primary production occurs from April to May (Saito et al., 2002; Liu et al., 2004; Ikeda et al., 2008). During the same period, zooplankton achieve faster growth (Kobari and Ikeda, 1999, 2001a, 2001b; Shoden et al., 2005). However, evaluation of the accurate growth rate of zooplankton is difficult using the sampling intervals (primarily once per month) usually used in previous studies (cf. Shoden et al., 2005 and references therein). For the evaluation of the accurate growth rate of zooplankton, high-frequency time-series sampling during the spring phytoplankton bloom is essential.

Previously, high-frequency time-series samplings were conducted at St. M in the North Atlantic Norwegian Sea over an 80-day period from March 23 to June 9, 1997 (Irigoien et al., 1998; Meyer-Harms et al., 1999; Niehoff et al., 1999; Hirche et al., 2001; Ohman and Hirche, 2001). In the eastern and western subarctic Pacific, high-frequency time-series samplings of zooplankton were achieved as a part of a series of iron fertilization effect studies (SEEDS I, SEEDS II and SERIES) (Tsuda et al., 2005, 2006, 2007, 2009; Fig. 1A).

Based on high-frequency time-series samplings at St. M in the Norwegian Sea, the egg production rates and composition of adult females of the dominant copepod species *Calanus finmarchicus* increase from pre-bloom to bloom peak and decrease during the post-bloom period (Niehoff et al., 1999). For *C. finmarchicus*, short-term changes in various population parameters, including feeding (Irigoien et al., 1998), reproduction (Niehoff et al., 1999), population structure (Hirche et al., 2001) and mortality (Ohman and Hirche, 2001), were evaluated during the spring phytoplankton bloom.

In terms of zooplankton fauna, dominant zooplankton species vary between the North Atlantic and North Pacific (Lalli and Persons, 1998). Although copepods dominate in both oceans, small-sized *Calanus* spp. (total length ca. 5 mm) dominate in the North Atlantic, and large-sized *Neocalanus* spp. (7-9 mm), with a 1-2 year generation period, dominate in the North Pacific (Conover, 1988). The utilization patterns of phytoplankton bloom during the spring also vary with oceans. Thus, *Calanus* spp. in the North Atlantic uses the phytoplankton bloom as an energy source for the reproduction of adults, while the reproduction of *Neocalanus* spp. in the North Pacific occur at deeper ocean layers without feeding, and these species utilize the phytoplankton bloom as an energy source for the development of newly recruited generations at the surface layer (Fig. 1B, C; Conover, 1988; Parsons and Lalli, 1988). These facts suggest that the zooplankton response to the spring phytoplankton bloom might vary between the North Atlantic and North Pacific.

Based on iron fertilization experiments in the North Pacific, the abundance of early copepodid stages increased in iron fertilization areas (SEEDS I, Tsuda et al., 2005). Conversely, in other experiments, the high abundance of copepods graze down the phytoplankton bloom (SEEDS II, Tsuda et al., 2007, 2009), and upward vertical migrations of subsurface resident copepods were observed for the phytoplankton bloom area (SERIES) (Tsuda et al., 2006). These results are clear responses of zooplankton to the phytoplankton bloom. However, because these zooplankton responses to the artificial bloom are enhanced through iron fertilization, it is likely that zooplankton responses might vary with the natural conditions. To evaluate zooplankton responses to the spring phytoplankton bloom under natural conditions, high-frequency time-series samplings were conducted in the Oyashio region during the spring phytoplankton bloom. This project, known as the "Ocean Ecodynamics Comparison in the Subarctic Pacific" (OECOS), was endorsed through the North Pacific Marine Science Organization (PICES) (Ikeda et al., 2010).

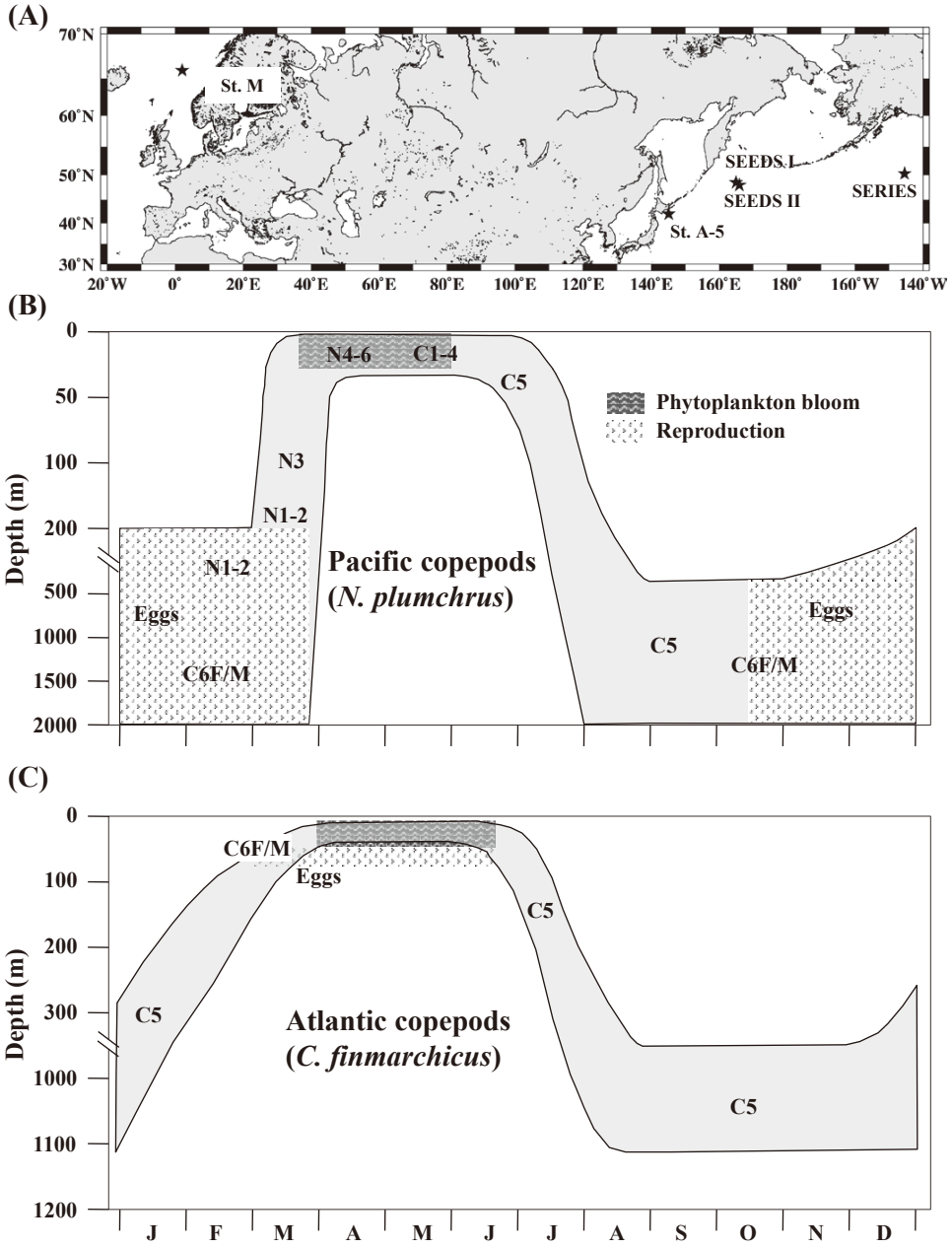


Fig. 1. Location of the stations where the high-frequency time-series observation on the mesozooplankton community during the phytoplankton bloom were performed (A). Life cycle patterns of the dominant epipelagic copepods in the subarctic Pacific *(Neocalanus plumchrus*) (B) and Atlantic (*Calanus finmarchicus*) (C). Life cycle diagrams were derived from Conover (1988), Kobari and Ikeda (2001b) and Fujioka et al. (2015).

The OECOS project was conducted at station A-5 in the Oyashio region from March 8 to May 1, 2007 using two consecutive cruises (T/S *Oshoro-Maru* [March] and *R/V Hakuho-Maru* [April - May]). During these cruises, high-frequency CTD casts, water sampling and various net samplings were conducted. Based on the OECOS project, various aspects of physical, chemical and biological changes during spring bloom were evaluated (Table 1). Within the findings of the OECOS project, three topics were highlighted: firstly, during the spring phytoplankton bloom, three water masses of different geographical origins exchange at the surface layer (Kono and Sato, 2010), and a high phytoplankton density was observed for Coastal Oyashio Water (COW) containing a high iron concentration originating from the Sea of Okhotsk (Nakayama et al., 2010). Secondly, the effects of feeding on the primary production of the two dominant taxa (*Neocalanus* copepods and euphausiids) were evaluated as 28% of the primary production for *Neocalanus* copepods (Kobari et al., 2010b) and 4.9% of the primary production for euphausiids (Kim et al., 2010b). Thirdly, diel migrant copepods (*Metridia* spp., *Gaetanus simplex* and *Pleuromamma scutullata*) cease diel vertical migration (DVM) and remain at

Table 1. Summary of the research subjects previously reported by the OECOS programme in the Oyashio region during March–April 2007.

| Subjects | References |
|---|---|
| Water mass exchange and their mixing ratio | Kono and Sato, 2010 |
| Iron and nutrient dynamics | Nakayama et al., 2010 |
| Spring bloom dynamics by satellite | Okamoto et al., 2010 |
| Pico- and nanophytoplankton community | Sato and Furuya, 2010 |
| Primary production | Isada et al., 2010 |
| Diatom species succession in relation with nutrient dynamics | Sugie et al., 2010a |
| Silica deposition in diatoms | Ichinomiya et al., 2010 |
| Resting spore formation and Si: N drawdown ratios of diatoms | Sugie et al., 2010b |
| Importance of intracellular Fe pools on diatoms growth | Sugie et al., 2011 |
| Bacteria biomass and production | Kobari et al., 2010a |
| Population structure of epipelagic copepods | Yamaguchi et al., 2010a |
| Vertical distribution of epipelagic copepods | Yamaguchi et al., 2010b |
| Feeding impact of epipelagic copepods | Kobari et al., 2010b |
| Growth of epipelagic copepods | Kobari et al., 2010c |
| Feedimg of *Oithona similis* on microplankton | Nishibe et al., 2010 |
| Ontogenetic vertical distribution of mesopelagic copepods | Abe et al., 2012 |
| Population dynamics of macrozooplanktonic euphausiids | Kim et al., 2010a |
| Metabolism and chemical composition of macrozooplanktonic euphausiids | Kim et al., 2010b |
| Population dynamics of macrozooplanktonic amphipods | Abe et al., 2016 |
| Population dynamics of macrozooplanktonic hydorozoans | Abe et al., 2014 |

deep ocean layers during the phytoplankton bloom period (Yamaguchi et al., 2010b; Abe et al., 2012).

For these findings, the causes of each issue have been described in the literature. However, synthesis studies addressing the entire plankton community from phytoplankton to macrozooplankton during the OECOS project have not previously been conducted. Thus, the interaction and relative importance of each topic issue remain unclear. Moreover, comparisons of the zooplankton responses to the phytoplankton bloom between the OECOS project and other studies (North Atlantic Norwegian Sea St. M: Irigoien et al., 1998; Meyer-Harms et al., 1999; Niehoff et al., 1999; Hirche et al., 2001; Ohman and Hirche, 2001, North Pacific SEEDS I: Tsuda et al., 2005; SEEDS II: Tsuda et al., 2007, 2009, SERIES: Tsuda et al., 2006) have not been made.

In the present study, short-term changes in phytoplankton (pico-, nano- and micro-size), protozooplankton and various species of meso- and macrozooplankton (abundance, biomass, population structure, vertical distribution, growth rates and feeding ecology) were evaluated during the OECOS period. The aim of the present study was to evaluate lower trophic levels during the spring phytoplankton bloom. To this end, reported and unpublished data were summarized, and new data on the population structure and feeding ecology of macrozooplankton during the OECOS period were added. Furthermore, Dr. Barbara Niehoff (AWI, Germany) and Prof. Atsushi Tsuda (AORI, Japan) provided additional zooplankton data on other high-frequency time-series samplings (SEEDS I, SEEDS II, SERIES and St. M), and comparisons with the OECOS data were achieved. The comparison of five time-series datasets revealed common patterns and different points, and the characteristics of zooplankton responses to the spring phytoplankton bloom were evaluated.

The present study is outlined in the following manner. In chapter 2, field sampling, analysis methods, physical environments, exchanges in water mass and temporal changes in phytoplankton, microzooplankton and mesozooplankton biomass are overviewed. In chapter 3, temporal changes in population structure of dominant meso- and macrozooplankton species are described. In chapter 4, temporal changes in vertical distribution of dominant copepod species are evaluated. In chapter 5, after multiplying individual masses, the abundance data of dominant meso- and macrozooplankton species are converted to carbon units, and subsequently, the growth rates are estimated in carbon units. In chapter 6, the feeding ecology of mesopelagic copepods and macrozooplankton are evaluated, and the zooplankton biomass and production are estimated for each species and compared between pre-bloom (March) and post-bloom (April) periods. In chapter 7, short-term changes in zooplankton during the spring phytoplankton bloom in the present study (OECOS) are compared with those in the other data sets (SEEDS I, SEEDS II, SERIES and St. M). Finally, based on these overviews, recommendations and future study directions are discussed.

## 2. Materials and Methods and Environmental Changes

### 2-1. Field sampling

Daily measurements of temperature, salinity and chlorophyll *a* (chl *a*) fluorescence data were obtained through CTD casts (SBE-9 plus, Sea Bird Electronics, Washington) at a single station (St. A-5, 42°00′N, 145°15′E, depth 4,000 m, Fig. 2) in the Oyashio region during March 9-14 and April 5 - May 1, 2007. The data were averaged every 1 m. Based on temperature and salinity data, the mixture ratios of the three water masses (Coastal Oyashio Water: COW; modified Kuroshio Water: MKW; Oyashio Water: OYW) in the 0-50 m water column were calculated (Kono and Sato, 2010).

To clarify the origin of the water mass at the surface layer of each sampling date, re-analyses of the hydrographic data (temperature, salinity, sea surface height and geostrophic velocity) were performed using a 1/10° grid high-resolution ocean model, referred to as the Fisheries Research Agency Regional Ocean Model (FRA-ROMS; Fisheries Research Agency of Japan, 2014, http://fm.dc.affrc.go.jp/fra-roms/index.html). FRA-ROMS is a ROMS (Rutgers University and UCLA, http://myroms.org/index.php) based on an ocean model that assimilates satellite sea surface heights and temperatures, and field study data in the North Pacific via a three-dimensional variation method that uses an empirical orthogonal function (EOF) joint mode (Fujii and Kamachi, 2003) to generate realistic re-analysis products. Lagrangian particle-tracking experiments were conducted using the FRA-ROMS velocity field. The positions of the particles, estimated based on an advection equation, were inversely related to time:

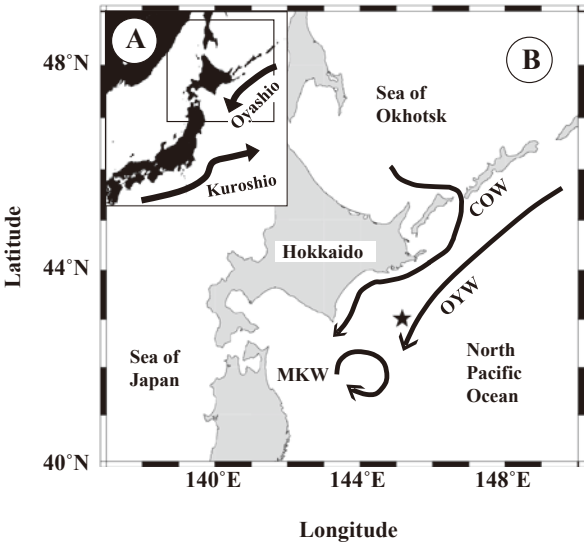


Fig. 2. Location of the Oyashio region (A) and sampling station (A-5, star) in the Oyashio region (B). The approximate directions of the current flows are shown with arrows (cf. Fig. 5). COW: coastal Oyashio water, MKW: modified Kuroshio water, OYW: Oyashio water.

$$\frac{dx}{dt} = -u(x, y, t), \frac{dy}{dt} = -v(x, y, t),$$

where (x (*t*), y (*t*)) is the position of a particle at time *t* and (*u*, *v*) is the velocity at the position (*x*, *y*) at time *t*. For this calculation, the time resolution was applied at 80 minutes. Through linear interpolation, (*u, v*) was estimated based on the flow velocity of the FRA-ROMS with a 1/10° horizontal resolution. We initially released particles at different depths (10, 20, 30, 50, 75, 100, 125, 150 and 200 m) at the sampling station (42°00′N, 145°15′E) and conducted a particle back-tracking experiment for the previous six months. We examined temporal changes at locations of the released particles to determine the origin of the water and evaluated the observed water temperature changes.

The water samples were collected from 11 depths (0, 5, 10, 20, 30, 40, 50, 75, 100, 125 and 150 m) using 12-L Niskin X bottles (General Oceanics) mounted on a CTD-RMS. Each 1-L water sample was filtered through a 20-μm mesh, Millipore polycarbonate membrane filter (2-μm) and a Whatman GF/F filter under low vacuum pressure. After filtration, each filter was immersed in 6 mL of *N,N*-dimethyl-formamide (DMF) for 6 hours at −5°C in the dark (Suzuki and Ishimaru, 1990). Subsequently, the chl *a* concentration was measured using a Turner Designs fluorometer (Turner Designs Co., TD-700) (Kobari et al., 2010a).

Water samples (1-L) collected at 5-m depth during April 6-30, 2007 were preserved in glutaraldehyde at a final concentration of 1% and subsequently settled and concentrated 10- to 20-fold using a siphon. Appropriate aliquots (1 mL) of the concentrated samples were transferred to glass slides, and diatom species were identified and counted using an inverted microscope. When the identification of diatom species was not possible using an inverted microscope, the samples were cleaned and desalted with DW, and subsequently the samples were filtered through a 0.2-μm Millipore polycarbonate membrane and dried. The dried filter was trimmed and mounted on a stub and subsequently ion-sputtered. The samples were observed using a scanning electron microscope (JMS-840A, JEOL Ltd., Tokyo), and species identification was conducted.

Water samples (200 mL) collected at 5-m depth during April 6-30, 2007 were preserved in Lugol's solution at a final concentration of 2% and subsequently settled and concentrated to 10 ml using a siphon. Appropriate aliquots (0.5-1 mL) of the concentrated samples were transferred to a counting chamber and microzooplankton (tintinnids, naked ciliates, other ciliates, athecate dinoflagellates, thecate dinoflagellates and diatom feeding dinoflagellates *Gyrodinium* spp.) were identified and enumerated under an inverted microscope. The species identification of ciliates was based on Montagnes and Lynn (1991) and Strüder-Kypke et al. (2001).

Mesozooplankton net samples were collected 23 times in daytime and 22 times at night using twin NORPAC nets (100-

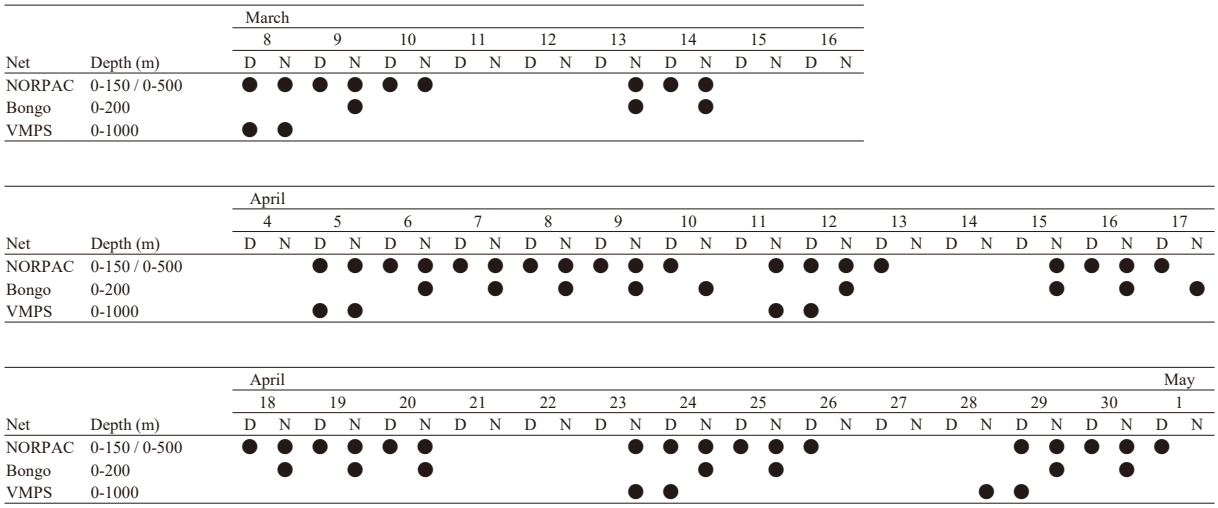


Fig. 3. A high-frequency time-series sampling of each plankton net (mesh sizes of twin-NORPAC: 100 and 335 μm, Bongo: 335 μm, VMPS: 60 μm) in the Oyashio region during the OECOS sampling period (March-May 2007). D: day, N: night.

and 335-μm mesh sizes, 45-cm diameter, Motoda, 1957) from 0 to 150 m and 0 to 500 m during March 9-14 and April 6 - May 1 (Fig. 3). The filtered water volumes were estimated from readings of a flowmeter (Rigosha Co. Ltd., Tokyo) mounted on a net ring. After collection, the samples were immediately preserved in v/v 5% borax-buffered formalin seawater.

To evaluate the vertical distribution of mesozooplankton, day and night vertical stratified samplings were obtained using a Vertical Multiple Plankton Sampler (VMPS: 60 μm mesh, 0.25 $m^2$ mouth opening; Terazaki and Tomatsu, 1997) from 9 strata between 0 and 1,000 m (0-25, 25-50, 50-75, 75-100, 100-150, 150-250, 250-500, 500-750 and 750-1,000 m) on March 8, and April 5, 11, 23 and 29, 2007 (Fig. 3). The volumes of filtered water ranged from 4.3 and 58.9 $m^3$. After the net was retrieved, the samples were immediately preserved in 5% borax-buffered formalin.

The macrozooplankton samples were collected at night (20:00-21:00 local time) on March 9, 13 and 14, and April 6, 7, 8, 9, 10, 12, 15, 16, 17, 18, 19, 20, 24, 25, 29 and 30, 2007 (Fig. 3). Bongo nets (70-cm mouth diameter, 315-μm mesh size) were obliquely towed from a 200-m depth to the surface (400-m wire out with 60° wire angle) at a speed of 2 knots. After collection, the samples were immediately preserved in v/v 5% borax-buffered formalin-seawater. The filtered water volumes were estimated from the readings of a flow meter (Rigosha Co. Ltd., Tokyo) mounted on a net ring.

## 2-2. Zooplankton sample analyses

### 2-2-1. Net sample analyses

In the land laboratory, NORPAC net samples (335-μm mesh) were split using a Motoda splitting device (Motoda, 1959), and a one-half aliquot was used to measure the wet mass, and another aliquot was used for microscopic analysis. For the wet mass measurement, the samples were transferred to a weighed 100-μm mesh and aspirated, and subsequently, the wet mass was measured using a microbalance (Mettler PM4000, precision 0.01 g) (Yamaguchi et al., 2010a). The remaining half aliquot of the samples was observed under a stereomicroscope for the identification and enumeration of 15 taxa (amphipods, appendicularians, chaetognaths, cnidarians, copepods, doliolids, euphausiids, mysids, ostracods, polychaetes, pteropods, salps, shellfish, fish and others). Amongst the night NORPAC net (100-μm mesh) samples collected at 0-500-m depth, copepodid C1-C6F/M stages of *Eucalanus bungii*, *Metridia pacifica*, *M. okhotensis*, *Neocalanus cristatus*, *N. flemingeri* and *N. plumchrus* were enumerated.

For VMPS samples, the species identification and enumeration were achieved for copepodid stages (C1-C6) of major epipelagic copepods (*E. bungii*, *M. pacifica*, *M. okhotensis*, *N. cristatus*, *N. flemingeri* and *N. plumchrus*) and mesopelagic copepods (*Gaetanus simplex*, *G. variabilis*, *Pleuromamma scutullata*, *Paraeuchaeta elongata*, *P. birostrata* and *Heterorhabdus tanneri*) using a stereomicroscope. Because of the difficulty identifying juvenile stages of *Gaetanus* species, C1-C4 individuals of *G. simplex* and *G. variabilis* were counted as *Gaetanus* spp.

From Bongo net samples, macrozooplanktonic euphausiids, amphipods, cnidarians and chaetognaths were quantified. For euphausiids, the three dominant species, *Euphausia pacifica*, *Thysanoessa inspinata* and *T. longipes*, were sorted. Eggs and nauplii were not observed in the samples. A few calyptopis larvae were observed, but were not quantified because of the lack of morphological characteristics for the identification of *Thysanoessa* spp. For furcilia larvae, juveniles, adult males and adult females, species identification was conducted according to Suh et al. (1993) for *E.*

*pacifica* and Endo and Komaki (1979) for *T. inspinata* and *T. longipes*. The furcilia larvae and juveniles of *T. inspinata* and *T. longipes* were sorted to species level based on the position of the carapace lateral denticle: middle margin for *T. inspinata* and posterior margin for *T. longipes* (Endo and Komaki, 1979). The adults were separated from juveniles based on the development of external secondary sexual characteristics: petasma for males and thelycum for females (Makarov and Denys, 1981). Adult females with attached spermatophores were also counted separately. The total length (*TL*, mm), from the tip of the rostrum to the distal end of the telson, was measured to the nearest 0.1 mm using an eyepiece micrometre under a dissecting microscope.

All amphipods detected in the Bongo net samples were sorted and enumerated at the species level. For the three most abundant species, *Cyphocaris challengeri*, *Primno abyssalis* and *Themisto pacifica*, the body length (*BL*, mm) was measured as the maximal distance between the tip of the head and the distal end of the uropod (or telson for *C. challengeri*) of the straightened body using an eye-piece micrometre with a precision of 0.05 to 0.10 mm. The segments in the first pleopod were counted to determine the instar stage of each amphipod. The specimens were separated into 5 categories according to the developmental stage and sex (juvenile, immature male, mature male, immature female and mature female) (Yamada and Ikeda, 2000, 2001a, 2001b, 2004; Yamada et al., 2002, 2004).

For cnidarians, the most abundant species *Aglantha digitale* were sorted and counted, and the results are expressed as abundance per $m^2$. Size measurements were made for bell height (*BH*) and gonad length (*GL*). For all individuals, the sizes were measured using an eye-piece micrometre with a precision of 0.5 mm (*BH*) or 0.05 mm (*GL*). Based on the ratio of *GL* to *BH*, *A. digitale* were separated into immature (*GL*/*BH* was < 10%) and mature (*GL*/*BH* was ≥10%) stages (McLaren, 1969).

For chaetognaths, all individuals were sorted and enumerated at the species level from Bongo net samples using a stereomicroscope. The species identification of chaetognaths was conducted according to Nagasawa and Marumo (1976) and Terazaki (1996). Concerning the third dominant chaetognath species (*Pseudosagitta scrippsae*), as the likelihood of the synonymy of *P. lyla* was suggested (Tokioka, 1974), we followed the taxonomic systematics of Alvariño (1962). For the three dominant chaetognaths (*Eukrohnia hamata, Parasagitta elegans* and *P. scrippsae*), the body length (*BL*, mm) was measured using a micrometre calliper or eye-piece micrometre mounted on a stereomicroscope with a precision of 0.05 to 0.10 mm. For the two most abundant species, *E. hamata* and *P. elegans*, the specimens were classified into five maturation stages (juvenile and stages I–IV) according to Thomson (1947), Terazaki and Miller (1986) and Johnson and Terazaki (2003).

**2-2-2. Gut content analyses**

For mesopelagic copepods, euphausiids and chaetognaths, gut content analyses were conducted. For mesopelagic copepods, the C6F specimens of *G. simplex*, *G. variabilis*, *P. scutullata*, *P. elongata*, *P. birostrata* and *H. tanneri* were sorted from the night VMPS samples obtained on March 8, and April 11 and 29. The gut was extracted from each prosome of the specimens using a stereomicroscope and dissected on a glass slide. The gut contents were identified and enumerated at the species or genus level using a dissecting microscope. For microplankton cells in the guts, the overall conditions of the cells were classified into three categories depending on the proportion of broken parts: 100% intact, 50–100% fragmented and 0–50% fragmented.

For carnivorous copepods (*P. elongata* and *H. tanneri*), most of the gut content was observed as mandible gnathobase (blade). From NORPAC net samples, C1–C6 stages of dominant copepod species (*G. simplex*, *G. variabilis*, *P. scutullata*, *P. elongata* and *H. tanneri*) were sorted, the mandible gnathobase was dissected and sketched, and the size of mandible blade (*MB*) was measured. The length of the mandible blade (*MB*) was measured at a precision of 1 μm, and the prosome length (*PL*, μm) was estimated from regressions (Dalpadado et al., 2008):

$$PL = 19.23\,MB - 376.3$$

The morphology of *MB* significantly varies with species (Arashkevich, 1969; Dalpadado et al., 2008). Based on the morphology and length of *MB*, species and stage identifications were obtained for each prey when possible.

For euphausiids, gut content analyses were conducted for 15 adult female/male specimens of the two dominant euphausiids, *E. pacifica* and *T. inspinata*. The specimens with mean *BL* at each sampling date were selected for the gut content analysis. Using a stereomicroscope, the gut of each specimen was removed from the carapace and dissected on a glass slide, and subsequently the food items were mounted using a cover glass. Taxonomic accounts of the food items were examined and enumerated using an inverted microscope (Nakagawa et al., 2001). The major copepod body parts in the gut contents were mandible gnathobase (blade). Based on the morphology and size of the gnathobase, the preys of the copepods were identified and enumerated at the species level according to copepodid stages (Dalpadado et al., 2008). The gut fullness was scored into 5 categories according to Nakagawa et al. (2001) (0; empty stomach, I; –25% full, II; 25–50% full, III; 50–75% full, IV; 75–100% full).

For chaetognaths, gut contents of the three dominant chaetognaths (*E. hamata*, *P. elegans* and *P. scrippsae*) were analysed. To avoid the effects of cod-end feeding, the food items observed forward of 1/4 of the gut were not enumerated (Øresland, 1987). For the copepods in the gut contents of chaetognaths, the copepodid stages were identified when pos-

sible. When the swimming legs or urosome of the copepods were damaged, their stages were estimated based on the *PL* of the dominant copepods in the Oyashio region (Ueda et al., 2008). The number of prey per chaetognaths (NPC, no. of prey ind.$^{-1}$, Nagasawa and Marumo, 1972) was calculated for each species at each sampling date.

**2–2–3. Biomass**

To estimate the biomass of each copepod species, the mean copepodid stage (*MCS*) was calculated for epi- and mesopelagic copepods (see 2–3–2). Based on the reported values of dry mass (*DM*) and the carbon: dry mass ratio (*C*: *DM*), regressions between the carbon mass (*CM*, μg) and the copepodid stage (*CS*) were calculated:

$$\mathrm{Log}_{10}\, CM = a \times CS + b$$

where *a* and *b* are fitted constants (Table 2). From these regressions and *MCS* values, the mean *CM* of each species was calculated, and subsequently the total mass was calculated after multiplying the mean *CM* by the abundance of each species.

For macrozooplankton taxa (euphausiids, amphipods, cnidarians and chaetognaths), based on the body size data, *BL* (mm) or *BH* (mm) (see 2–2–1), the wet mass (*WM*) of amphipods and the *DM* of euphausiids, cnidarians and chaetognaths were estimated using reported allometric equations, which varied with taxa (Table 2). Subsequently, the carbon biomass was estimated using reported ratios between *WM*, *DM* and *CM* (Table 2).

## 2–3. Data and statistical analyses

### 2–3–1. Correlation analysis with water mass-mixing ratio

Correlation analyses based on the water mass mixing ratio at 0–50 m (Kono and Sato, 2010) were conducted to determine the abundance (ind. m$^{-2}$) and biomass (mg C m$^{-2}$) of epipelagic copepods at 0–500 m (*E. bungii*, *M. pacifica*, *M. okhotensis*, *N. cristatus*, *N. flemingeri*, *N. plumchrus*), mesopelagic copepods at 0–1000 m (*G. simplex*, *G. variabilis*, *P. scutullata*, *P. elongata*, *P. birostrata* and *H. tanneri*) and macrozooplankton at 0–200 m (*E. pacifica*, *T. inspinata*, *C. challengeri*, *P. abyssalis*, *T. pacifica*, *A. digitale*, *E. hamata* and *P. elegans*).

Table 2. Regression formulae used for carbon biomass estimation for various zooplankton species in the Oyashio region. *WM*: wet mass in mg (mg WM ind.$^{-1}$), *DM*: dry mass in mg (mg DM ind.$^{-1}$), $DM_{\mu g}$: dry mass in μg (μg DM ind.$^{-1}$), *CM*: carbon mass in mg (mg C ind.$^{-1}$), $CM_{\mu g}$: carbon mass in μg (μg C ind.$^{-1}$), *CS*: copepodid stage, *BL*: body length (mm), *BH*: bell height (mm), *TL*: total length (mm). Regressions first reported in the present study are shown with the coefficient of determination ($r^2$).

| Taxa / Species | Formula | Reference |
|---|---|---|
| Copepods | | |
| *Eucalanus bungii* | Log $CM_{\mu g}$=0.3564 *CS*−0.2050, $r^2$=0.993 | Ueda et al., 2008 |
| *Metridia pacifica* | Log $CM_{\mu g}$=1.2407 *CS*−5.4079, $r^2$=0.999 | Ueda et al., 2008 |
| *Metridia okhotensis* | Log $CM_{\mu g}$=0.8372 *CS*−2.6382, $r^2$=0.999 | Padmavari, 2002; Ikeda et al., 2006 |
| *Neocalanus cristatus* | Log $CM_{\mu g}$=0.4920 *CS*+0.3798, $r^2$=0.999 | Ueda et al., 2008 |
| *Neocalanus flemingeri* | Log $CM_{\mu g}$=0.2716 *CS*+1.0328, $r^2$=0.729 | Ueda et al., 2008 |
| *Neocalanus plumchrus* | Log $CM_{\mu g}$=0.3974 *CS*+0.0306, $r^2$=0.981 | Ueda et al., 2008 |
| *Gaetanus* spp. | Log $CM_{\mu g}$=0.3331 *CS*+0.3293, $r^2$=0.882 | Yamaguchi and Ikeda, 2000; Ikeda et al., 2006 |
| *Pleuromamma scutullata* | Log $CM_{\mu g}$=0.6349 *CS*−1.7888, $r^2$=0.999 | Yamaguchi and Ikeda, 2000; Ikeda et al., 2006 |
| *Paraeuchaeta elongata* | Log $CM_{\mu g}$=0.3362 *CS*+1.0630, $r^2$=0.951 | Yamaguchi and Ikeda, 2002; Ikeda et al., 2006 |
| *Paraeuchaeta birostrata* | Log $CM_{\mu g}$=0.3369 *CS*+1.2355, $r^2$=0.995 | Yamaguchi and Ikeda, 2002; Ikeda et al., 2006 |
| *Heterorhabdus tanneri* | Log $CM_{\mu g}$=0.6976 *CS*−1.9922, $r^2$=0.999 | Yamaguchi and Ikeda, 2000; Ikeda et al., 2006 |
| Euphausiids | | |
| *Euphausia pacifica* | $DM$=0.0012$BL^{3.374}$, *CM*=0.3673 *DM*, *TL*= 1.292 *BL*+0.0762 | Kim et al., 2010a |
| *Thysanoessa inspinata* | $DM$=0.0043$BL^{3.057}$, *CM*=0.3808 *DM*, *TL*= 1.514 *BL*+0.575 | Kim et al., 2010a |
| Amphipods | | |
| *Cyphocaris challengeri* | $WM$=0.027 $BL^{2.71}$, *DM*=0.199 *WM*, *CM*=0.368 *DM* | Yamada and Ikeda, 2006 |
| *Primno abyssalis* | $WM$=0.023 $BL^{2.88}$, *DM*=0.226 *WM*, *CM*=0.543 *DM* | Yamada and Ikeda, 2006 |
| *Themisto pacifica* | $WM$=0.029 $BL^{2.82}$, *DM*=0.228 *WM*, *CM*=0.463 *DM* | Yamada and Ikeda, 2006 |
| Hydrozoans | | |
| *Aglantha digitale* | $\mathrm{Log}_{10}DM$=0.454$(\mathrm{Log}_{10}BH)^2$ + 1.883$\mathrm{Log}_{10}BH$ – 2.402, *CM*=0.204 *DM* | Takahashi and Ikeda, 2006; Runge et al., 1987 |
| Chaetognaths | | |
| *Eukrohnia hamata* | $\mathrm{Log}_{10}$ $DM_{\mu g}$=3.80 $\mathrm{Log}_{10}$ *BL*−0.79, *CM*=0.326 *DM* | Matsumoto, 2008; Ikeda and Takahashi, 2012 |
| *Parasagitta elegans* | $\mathrm{Log}_{10}$ $DM_{\mu g}$=2.91 $\mathrm{Log}_{10}$ *BL*−0.79, *CM*=0.477 *DM* | Imao, 2005; Omori, 1969 |

**2–3–2. Population structure of copepods**

To define the population structure of copepods, the mean copepodid stage (*MCS*) was calculated using the following equation (Marin, 1987):

$$MCS = \sum (i \times Ni) / N$$

where $Ni$ is the abundance (ind. $m^{-2}$) of $i$th copepodid stage ($i$ = 1 to 6) and $N$ is the total abundance of copepodid stages. The small and large *MCS* values indicate the dominance of early and late copepodid stages, respectively.

**2–3–3. Cohort analyses in macrozooplankton**

For macrozooplankton (euphausiids, amphipods, cnidarians and chaetognaths), cohort analyses were conducted based on the size-frequency histograms of *BL* or *BH* at each sampling date fitted to normal distribution curves. The length-frequency data were separated into multiple normal distribution curves using the free software "R" with an add-in package "mclust" (Fraley et al., 2012).

**2–3–4. Vertical distribution**

For copepods, to clarify the depth distribution of each copepodid stage, the depths containing 50% of the resident population (50% distributed layer: $D_{50\%}$, Pennak, 1943) were calculated. Additional calculations of $D_{25\%}$ and $D_{75\%}$ were also obtained for all copepodid stages. Day-night differences in the vertical distribution of each copepodid stage were evaluated using two-sample Kolmogorov-Smirnov tests (Sokal and Rohlf, 1995). To avoid errors resulting from small sample sizes in this DVM analysis, comparisons were obtained only for stages with > 20 ind. $m^{-2}$. Notably, the robustness of the Kolmogorov-Smirnov test for evaluating the DVM of zooplankton can be questionable in the case of large differences (>10-fold) in abundance between day and night (Venrick, 1986). However, because the day and night differences in the abundance observed in the present study were less than 5-fold, evaluations of DVM using the Kolmogorov-Smirnov test would be appropriate.

**2–3–5. Growth rate**

To calculate the mass-specific growth rate ($g$, $day^{-1}$), the individual mass (*CM*: μg C ind. $^{-1}$) was calculated based on the *MCS* using the regressions listed in Table 2 for the NORPAC net sampling date (epipelagic copepods) and the VMPS sampling date (mesopelagic copepods). For the *MCS* calculation, deep-sea resident stages (C6 stages of *Neocalanus* spp.) were omitted. For macrozooplankton taxa, based on the mean *BL* or *BH* of each cohort at each sampling date, individual mass (*CM*: μg C ind. $^{-1}$) was calculated using the equations listed in Table 2. To clarify the species showing growth during the study period, the linear regression

$$Y = aX + b,$$

where $Y$ is log-transformed individual mass ($\log_{10}$ [*CM*: μg C ind. $^{-1}$]), $X$ is Julian day starting on 1 March, and $a$ and $b$ are fitted constants, was applied. For species showing significant growth, the mass-specific growth rate was calculated using the following equation (Omori and Ikeda, 1984):

$$g = \ln (CM_{x+t} / CM_x) / t$$

where $CM_x$ is individual mass (μg C ind. $^{-1}$) at day $x$, and $t$ is the interval between sampling date (day).

**2–3–6. Production estimation**

To estimate the production of each zooplankton species during the OECOS period, the respiration rate ($R$: μl $O_2$ ind.$^{-1}$ $h^{-1}$) was estimated based on the empirical equation of Ikeda (2014):

$$\ln R = 23.097 + 0.813 \times \ln CM\ (\mu g\ C\ ind.^{-1}) - 6.248 \times 1000/T - 0.136 \times \ln D + Taxa$$

where $CM$ is individual carbon mass (μg C ind.$^{-1}$), $T$ is temperature at distribution layer of each species (K: absolute temperature), $D$ is distribution depth (m) and *Taxa* is a constant number that varies with taxa: 0 for copepods, 0.6 for euphausiids, 0.421 for amphipods, 0.425 for cnidarians and −0.345 for chaetognaths (Ikeda, 2014). Gross production ($P_g$) is expressed as the sum of the net production ($P_n$) and respiration ($R$):

$$P_g = P_n + R.$$

Assimilation efficiency ($A$) and gross growth efficiency ($K_1$) are expressed using the following equations:

$$A = (P_n + R) / F \text{ and } K_1 = P_n / F,$$

where ($F$) is the food requirement. For general zooplankton, $A$ and $K_1$ are 70% and 30%, respectively (Ikeda and Motoda, 1978). $P_n$ is expressed as:

$$P_n = 0.75 \times R.$$

From $R$, the individual growth rate ($P_N$: mg C ind.$^{-1}$ $day^{-1}$) was calculated using the following equation:

$$P_n = R \times 12/22.4 \times 0.75 \times 24/ 1{,}000,$$

where 12/22.4 is the carbon mass (12 g) in 1 mol (22.4 L) carbon dioxide, and ×24 is the time conversion factor from $h^{-1}$ to $day^{-1}$ and division by 1,000 is the unit conversion from μg to mg. The daily population production (mg C $m^{-2}$ $day^{-1}$) was estimated after multiplying $P_n$ by the abundance (ind. $m^{-2}$).

**2–4. Environmental changes during the OECOS period**

**2–4–1. Hydrography**

Temporal changes in temperature and salinity in the 0–1,000 m water column and the chl *a* and water mass composition in the 0–50 m water column from March 8 to May 1, 2007, are shown in Fig. 4. Throughout the study period, the temperature ranged from 2 to 6ºC, and the salinity ranged from 33.2 to 34.2 (Fig. 4A, B). The chl *a* contents showed three peaks (2–6 mg $m^{-3}$) on April 7, 11 and 23 (Fig. 4C). For the water mass mixing ratio in the 0–50 m water column, the OYW and MKW comprised approximately half of the water mass during March. Cold COW was observed in early April, and the

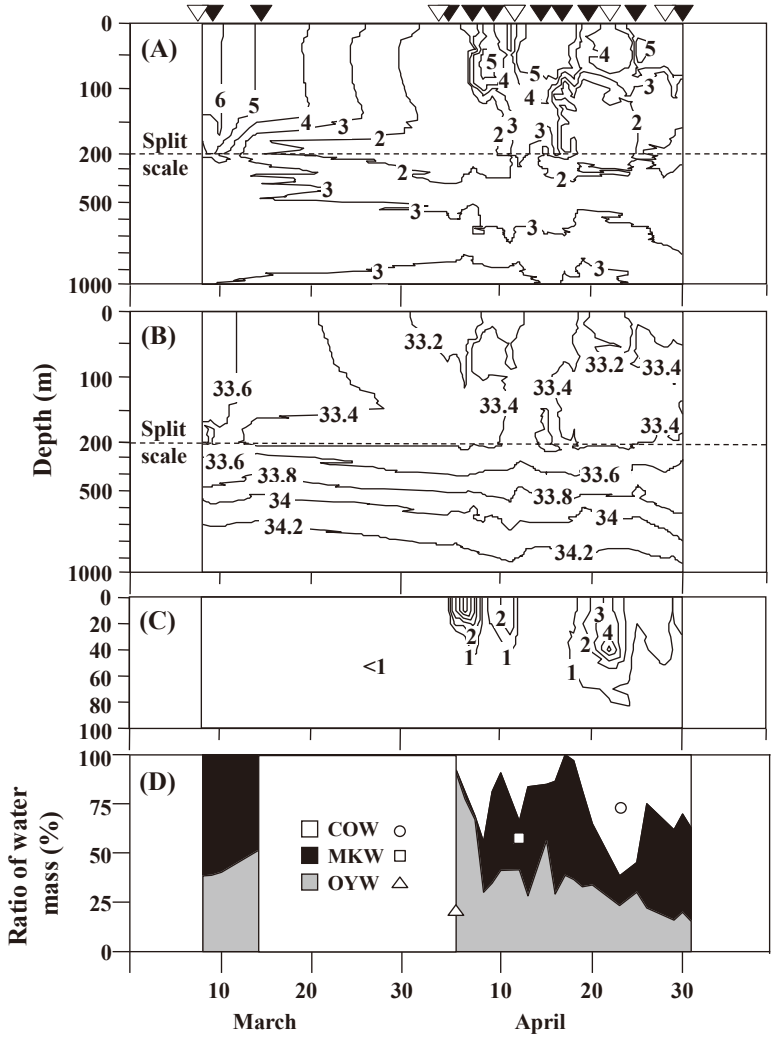


Fig. 4. Temporal changes in temperature (A, °C), salinity (B), chlorophyll *a* (C, mg $m^{-3}$) and the ratio of water mass at 0–50 m water column (D, %) in the Oyashio region during 9 March to 1 May 2007. Data in D were from Kono and Sato (2010). Solid and open triangles at the top abscissa indicate sampling timings of the Bongo net and VMPS, respectively. Symbols in D indicate the dates that FRA-ROMS analysis was performed for each water mass (cf. Fig. 5). COW; coastal Oyashio water, MKW; modified Kuroshio water; OYW; Oyashio water.

observed timings of COW corresponded with the chl *a* peaks described above (Fig. 4C, D). For the eleven Bongo net sampling dates, the dominant water masses varied, i.e., COW for April 20 and 25, OYW for March 14 and April 6 and MKW for March 9 and April 8, 10, 12, 15, 17 and 30 (Fig. 4D).

The FRA-ROMS analyses revealed that the estimated origin of each water mass varied. The origin of COW was the Sea of Okhotsk, while the origin of OYW was the east Kamchatka current, which flows along the southern edge of the Kurile chain (Fig. 5). During 2006-2007, clockwise warm water eddies were observed around the Oyashio region, and the origin of MKW was associated with this warm water eddy (Fig. 2B). The experienced water temperatures during the previous six months also significantly varied with the water mass ($p < 0.001$, one-way ANOVA) (Fig. 5). The estimated temperatures of COW, MKW and OYW were 1.5-6.0°C (4.0±1.4°C: mean ± 1 sd), 3.6-8.1°C (5.8±1.4°C) and 2.2-4.9°C (3.3±0.6°C), respectively.

### 2-4-2. Phytoplankton community

Temporal changes in the size-fractionated integrated mean chl *a* in the 0-150 m water column and the diatom cell density and species composition at 5-m depth are shown in Fig. 6. A chl *a* peak was observed on April 8 and dominated with a large-sized (> 20 μm) fraction after April (Fig. 6A). The HPLC-CHEMTAX analyses revealed that >74% of the chl *a* content was composed of diatoms in April 2007 (Isada et al., 2010). A diatom cell peak was observed on April 7 and dominated with centric diatoms throughout the study period. The dominant diatom taxa were *Thalassiosira* spp. before April 20 and subsequently changed to *Chaetoceros* spp. thereafter (Fig. 6B).

### 2-4-3. Microzooplankton community

Temporal changes in the microzooplankton abundance and

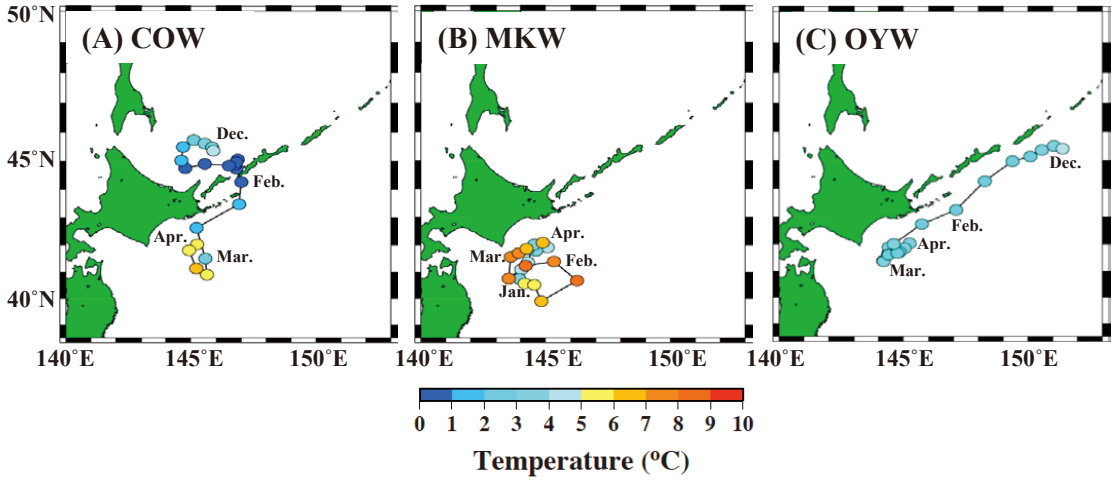


Fig. 5. Results of FRA-ROMS analyses, which back-calculated the origin of each water mass at each sampling date. (A) COW; coastal Oyashio water (25 April), (B) MKW; modified Kuroshio water (12 April), (C) OYW; Oyashio water (6 April). Colours indicate experienced temperatures.

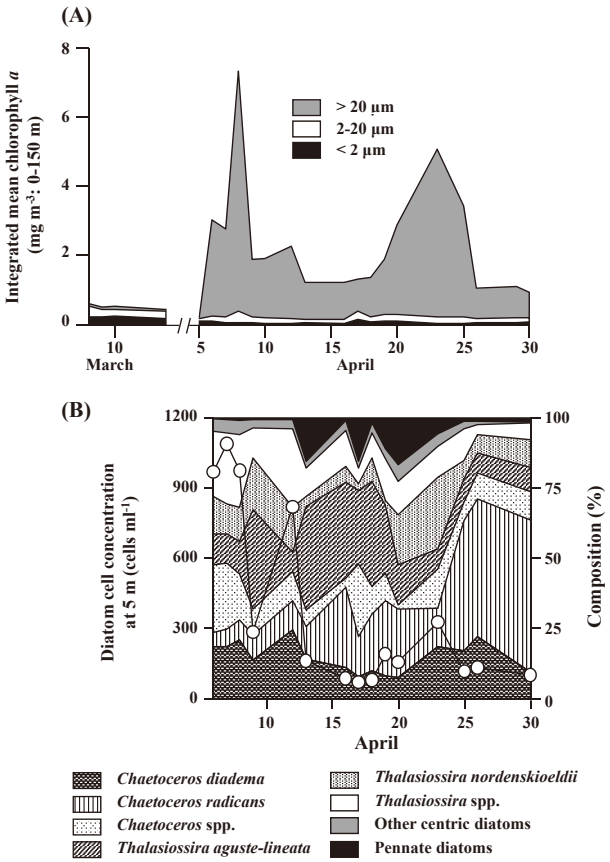


Fig. 6. Temporal changes in the integrated mean values of size-fractionated chlorophyll *a* in the 0-150 m water column (A) and the diatom cell concentration and taxonomic composition at the 5 m depth (B) in the Oyashio region from March-April 2007. Note that the diatom taxonomic data were only available for April.

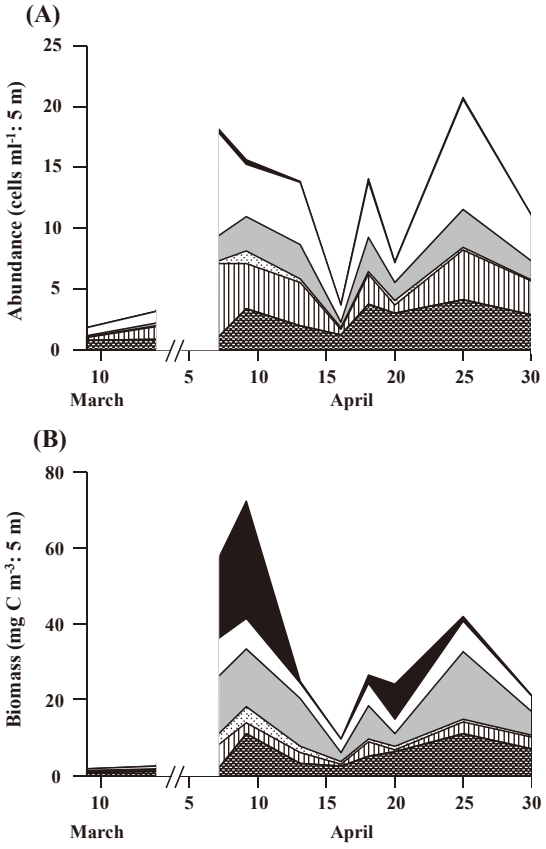


Fig. 7. Temporal changes in the abundance (A) and biomass (B) of the microzooplankton community at a 5 m depth in the Oyashio region during March-April 2007.

biomass and taxonomic accounts (ciliates, athecate dinoflagellates and thecate dinoflagellates) at 5-m depth from March 8 to April 30, 2007 are shown in Fig. 7. Peaks of microzooplankton abundance were observed on April 7 and 25, and athecate dinoflagellates were abundant (Fig. 7A). In terms

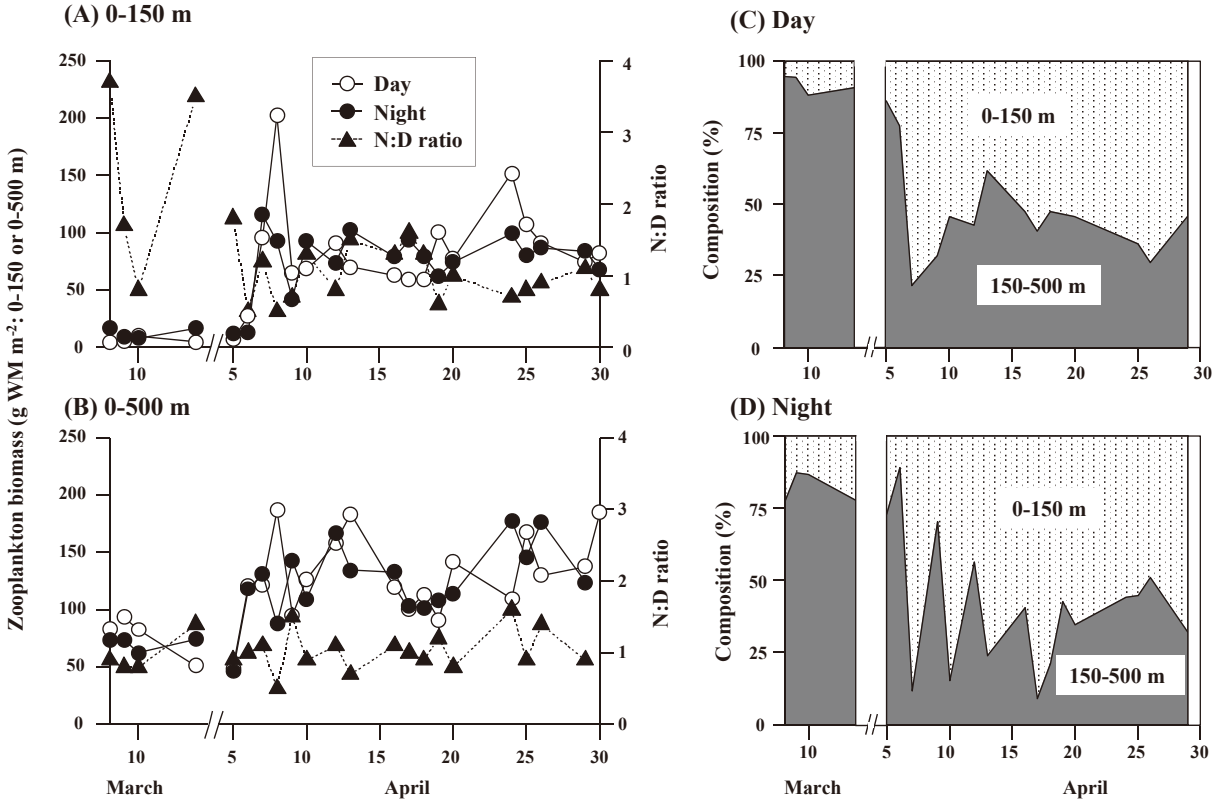


Fig. 8. Temporal changes in zooplankton wet biomass in the 0–150 m (A) and 0–500 m (B) water columns in the Oyashio region at day and night during 8–14 March and 6–30 April 2007. Night and day ratio (N: D ratio) were calculated for (A) and (B). Vertical distribution (0–150 m and 150–500 m) of the zooplankton biomass evaluated as differences in the standing stocks of two sampling layers (i.e., 150–500 m = [0–500 m] – [0–150 m]) is shown for day (C) and night (D).

of biomass, microplankton peaked on April 9, and the phagotrophic athecate dinoflagellate *Gyrodinium* sp. (diatom feeder) was dominant in biomass (Fig. 7B).

### 2–4–4. Mesozooplankton biomass

Temporal changes in the day and night mesozooplankton wet mass in the 0–150 m and 0–500 m water columns on March 8 and May 1, 2007 are shown in Fig. 8A (0–150 m) and 8B (0–500 m), respectively. The night: day ratio (N: D ratio) was also calculated. The vertical distribution (0–150 m and 150–500 m) of the zooplankton biomass, evaluated based on differences in the standing stocks (g WM $m^{-2}$) of the two sampling layers (i.e., the values at 150–500 m = [values at 0–500 m] – [values at 0–150 m]), is shown in Fig. 8C (daytime) and 8D (night time). Mesozooplankton wet mass of the 0–150 m water column ranged from 7.6 (mean day and night values in March 9) to 147.7 g WM $m^{-2}$ (April 8). The mesozooplankton wet mass was low during March but increased after April 8 and reached eight- and two-times higher values than those in March in the 0–150 m and 0–500 m water columns, respectively (Fig. 8A, B).

Concerning day–night differences in the 0–150 m water column, the biomass was higher at night than in the daytime in March, while no differences were detected in April (N: D ratio = 1, Fig. 8A). Day–night differences in the mesozooplankton biomass were not observed for the 0–500 m water column during the entire study period (Fig. 8B). Concerning the vertical distribution, most of the mesozooplankton biomass (92±3% [mean ± SD] for daytime, 82±5% for nighttime) was distributed at the 150–500 m layer prior to April 7, and gradually becoming shallower thereafter, while the biomass at 0–150 m exceeded that at the 150–500 m both day and night after April 13 (Fig. 8C, D).

## 3. Population Structure of Dominant Species

### 3–1. Results

### 3–1–1. Epipelagic copepods

Temporal changes in the abundance, biomass and copepodid stage composition of epipelagic copepods (*E. bungii*, *M. pacifica*, *M. okhotensis*, *N. cristatus*, *N. flemingeri* and *N. plumchrus*) in the 0–500 m water column in the Oyashio region from March to April 2007 are shown in Fig. 9.

For *E. bungii*, the abundance ranged from 4,369 to 26,654 ind. $m^{-2}$, the biomass ranged from 129.6 to 575.3 mg C $m^{-2}$, and the mean biomass was 288.1 ± 91.6 mg C $m^{-2}$ (mean ± SD) (Fig. 9A). Only late copepodid stages (C3–C6) were observed in March (Fig. 9A). The C3 composition gradually decreased from March to April 10. The C1 stage was

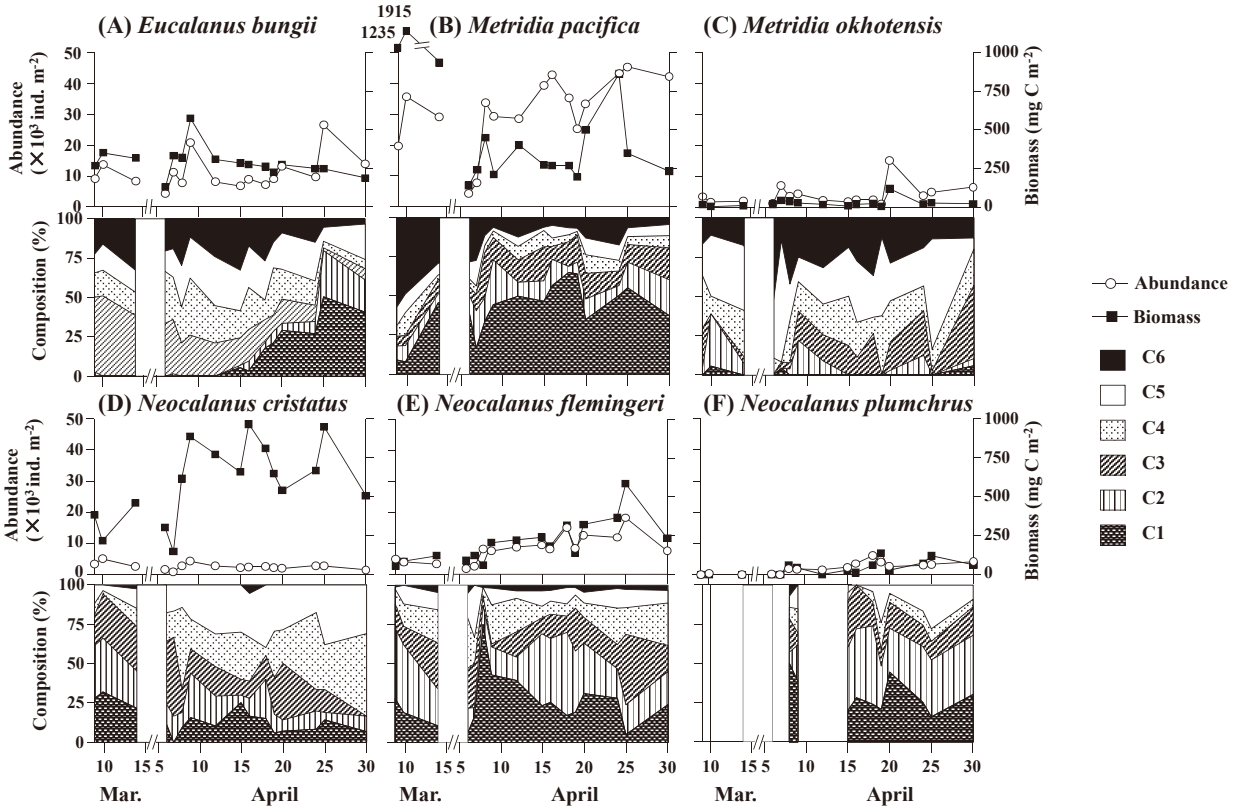


Fig. 9. Temporal changes in abundance, biomass and copepodid stage composition in regard to the abundance of epipelagic copepods, *Eucalanus bungii* (A), *Metridia pacifica* (B), *M. okhotensis* (C), *Neocalanus cristatus* (D), *N. flemingeri* (E) and *N. plumchrus* (F), in the 0–500 m water column in the Oyashio region during March to April 2007.

initially observed on April 12 and the total abundance rapidly increased, reaching nearly half of the population by April 25.

The abundance and biomass of *M. pacifica* ranged from 4,384 to 45,364 ind. $m^{-2}$ and 139.1 to 1915.4 mg C $m^{-2}$, respectively (Fig. 9B). The mean biomass of *M. pacifica* was at 529.3 ± 467.1 mg C $m^{-2}$. For the population structure, C6 dominated during early March, while all copepodid stages were observed throughout the study period (Fig. 9B). In April, the C6 composition decreased 12%, and the C1–C3 compositions increased 75%. Among these stages, the C1 stage comprised nearly half of the population in April.

The abundance and biomass of *M. okhotensis* ranged from 1,082 to 15,174 ind. $m^{-2}$ and 5.3 to 120.4 mg C $m^{-2}$, respectively. The mean biomass of *M. okhotensis* was 27.7 ± 26.0 mg C $m^{-2}$, which was extremely lower (ca. 1/20) than that of its congener *M. pacifica* (Fig. 9C). For the population structure, late copepodid stages (C4–C6) were dominant, and the most dominant stage was C5 (35%) followed by C6 (24%). C1 was extremely low throughout the study period, consistent with the findings for *M. pacifica*, as described above.

The abundance and biomass of *N. cristatus* ranged from 861 to 5,088 ind. $m^{-2}$ and 149.2 to 965.8 mg C $m^{-2}$, respectively (Fig. 9D). The mean biomass of *N. cristatus* was 595.9 ± 242.1 mg C $m^{-2}$. For the population structure, C1–C3 were predominant (composing >75%) in March, but decreased from March to late April, composing only 20% by late April. However, the composition of C4–C5 stages increased from March to April, and C4 composed 52% of the population by the end of April.

The abundance and biomass of *N. flemingeri* ranged from 1,931 to 18,300 ind. $m^{-2}$ and 54.6 to 585.7 mg C $m^{-2}$, respectively (Fig. 9E). The mean biomass of *N. flemingeri* was 208.9 ± 134.8 mg C $m^{-2}$. For *N. flemingeri*, all copepodid stages were observed. Throughout the study period, C1–C3 stages composed 65–85% of the population. Among the species, the C1 composition peaked on April 8 (75%), C2 was high on April 18 (53%) and C3 was high on April 25 (45%). Thus, a succession in dominant stages within the C1–C3 stage composition was observed for *N. flemingeri* in April.

The abundance and biomass of *N. plumchrus* ranged from 0 to 6,027 ind. $m^{-2}$ and 0 to 138.2 mg C $m^{-2}$, respectively (Fig. 9F). The mean biomass of *N. plumchrus* was 39.0 ± 42.6 mg C $m^{-2}$. These values were the lowest within the sympatric *Neocalanus* spp. (Fig. 9F). For the population structure of *N. plumchrus* (which commonly occurred after 15 April), C1–C3 stages composed 59–100% and showed slight temporal changes.

### 3–1–2. Mesopelagic copepods

Temporal changes in the abundance, biomass and copepo-

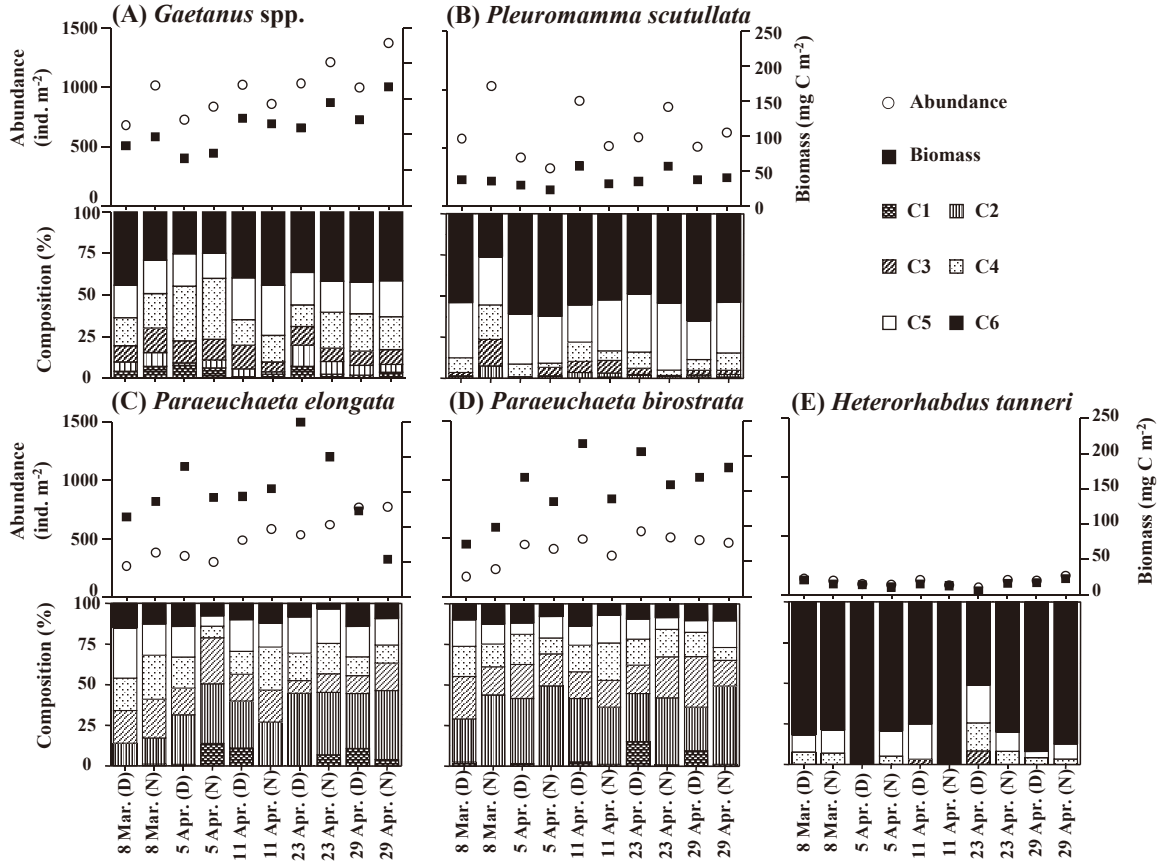


Fig. 10. Temporal changes in abundance, biomass and numerical copepodid stage composition of mesopelagic copepods, *Gaetanus* spp. (A), *Pleuromamma scutullata* (B), *Paraeuchaeta elongata* (C), *P. birostrata* (D) and *Heterorhabdus tanneri* (E), in the 0–1,000 m water column in the Oyashio region during March to April 2007. (D): day, (N): night.

did stage composition (in abundance) of mesopelagic copepods are shown in Fig. 10. These mesopelagic copepod data were computed using day and night vertical stratified samplings through VMPS from 9 strata in the 0–1,000 m water column, and expressed in units per 1-$m^2$ water column.

The abundance and biomass of *Gaetanus* spp. ranged from 359 to 910 ind. $m^{-2}$ and 66.5 to 166.9 mg C $m^{-2}$, respectively (Fig. 10A). The mean biomass of *Gaetanus* spp. was 110.2 ± 29.8 mg C $m^{-2}$. *Gaetanus* spp. primarily comprised *G. simplex* and *G. variabilis*, and C4–C6 composed 75–90% of the population throughout the study period.

The abundance and biomass of *P. scutullata* was 326–1,031 ind. $m^{-2}$ and 23.7 – 58.0 mg C $m^{-2}$, respectively (Fig. 10B). The mean biomass of *P. scutullata* was 39.2 ± 10.4 mg C $m^{-2}$. For the population structure, C5 and C6 dominated, and C6 comprised more than 50% of the population of *P. scutullata*, except for the night March 8 (Fig. 10B).

The abundance of *P. elongata* was 261–771 ind. $m^{-2}$ and significantly increased throughout the study period ($r$=0.90 for correlation between abundance and Julian day, $p$<0.01, Fig. 10C). The biomass of *P. elongata* was 53.3 – 249.4 mg C $m^{-2}$ with a mean value of 150.2 ± 50.4 mg C $m^{-2}$ (Fig. 10C). The population structure of *P. elongata* primarily comprised C1–C3, particularly dominated with C2 (14–45%).

The abundance and biomass of *P. birostrata* ranged from 174 to 559 ind. $m^{-2}$ and 75.0 to 217.9 mg C $m^{-2}$, respectively (Fig. 10D). The mean biomass of *P. birostrata* was 155.5 ± 42.5 mg C $m^{-2}$. The abundance of *P. birostrata* significantly increased during the study period ($r$=0.54 correlation with Julian day, $p$<0.05). The population structure of *P. birostrata* was similar to that of *P. elongata* and primarily comprised C1–C3 (52 –69% of total population). Among these stages, C2 was the most abundant (27–49%).

The abundance and biomass of *H. tanneri* ranged from 60 to 138 ind. $m^{-2}$ and 5.3 to 22.7 mg C $m^{-2}$, respectively (Fig. 10E). The mean biomass of *H. tanneri* was 15.1 ± 4.7 mg C $m^{-2}$. For Heterorhabdidae, inter-molt growth was more than 900% in body mass, thus the smallest C1 and C2 of *H. tanneri* are difficult to collect using the ordinary mesh size of the plankton net (Yamaguchi and Ikeda, 2000b). Because early copepodid stages (C1–C2) were not collected in the present study, the population structure was skewed for late copepodids, particularly for the predominance of C6.

### 3–1–3. Macrozooplankton

The data on macrozooplanktonic taxa (euphausiids, amphipods, cnidarians and chaetognaths) were derived from Bongo

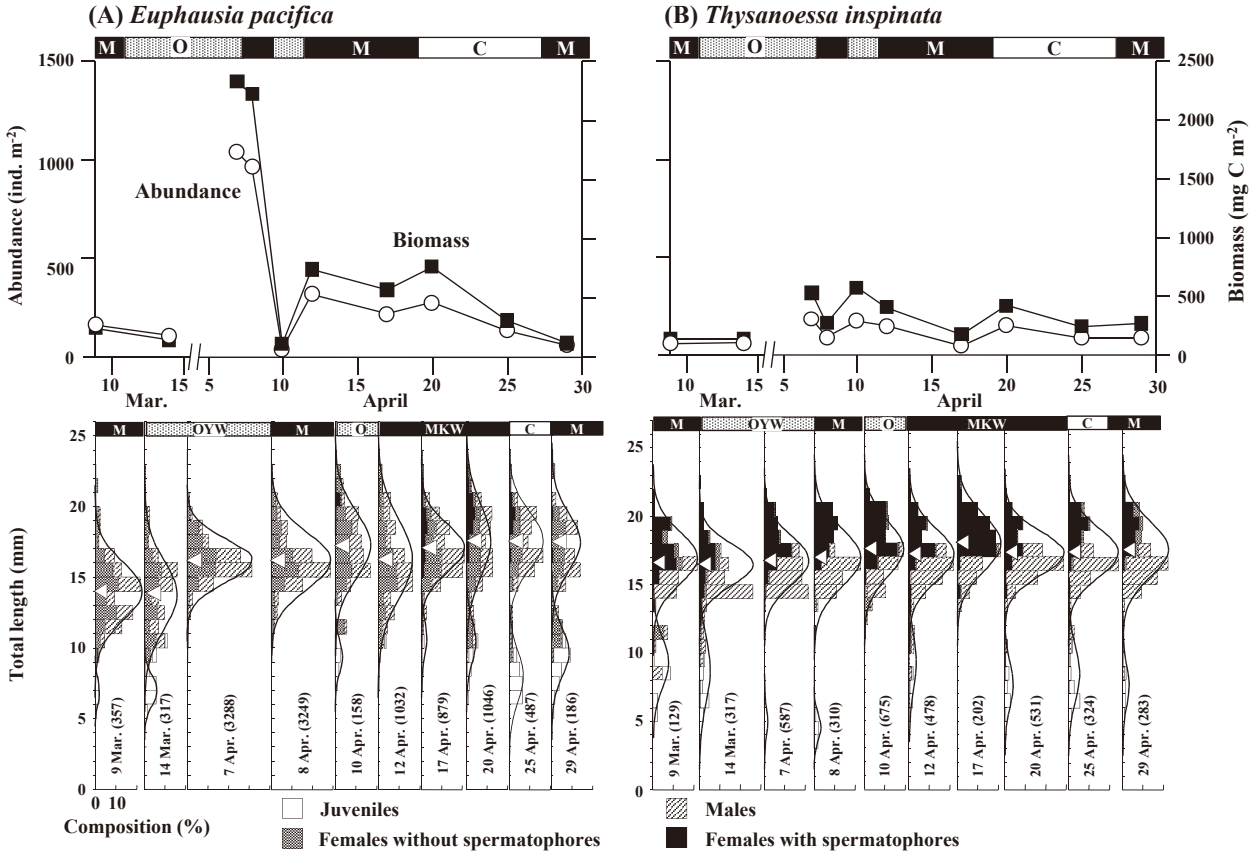


Fig. 11. Temporal changes in abundance, biomass and total length (*TL*) histogram in macrozooplanktonic euphausiids, *Euphausia pacifica* (A) and *Thysanoessa inspinata* (B), in the 0–200 m water column in the Oyashio region during March–April 2007. The values in the parentheses indicate measured individual numbers. Triangles indicate the mean *TL*s of the dominant cohort. For the dominant water masses, C; coastal Oyashio water, M; modified Kuroshio water, O; Oyashio water.

net samplings at night from the 0–200 m water column. For euphausiids, two species, *E. pacifica* (63.3% of total euphausiids species) and *T. inspinata* (33.6%), were dominant. Temporal changes in abundance, biomass and total length (*TL*) histograms are shown in Fig. 11.

The abundance and biomass of *E. pacifica* ranged from 40 to 1,040 ind. $m^{-2}$ (mean ± 1 sd: 335 ± 346 ind. $m^{-2}$) and 116 to 2,330 mg C $m^{-2}$, respectively (Fig. 11A). The mean biomass of *E. pacifica* was 755 ± 796 mg C $m^{-2}$. The abundance of *E. pacifica* peaked from April 7–8, consistent with the timing of the chl *a* peak. For *E. pacifica*, the *TL* ranged from 5.2 to 25.4 mm. Based on the cohort analyses, two cohorts were identified. The mean *TL* of the large-sized cohort was 13.8–17.6 mm, while that of the small-sized cohort was 6.9–10.5 mm. Numerically, the large-sized cohort was predominant in the *E. pacifica* population (Fig. 11A). The small-sized cohort primarily comprised juveniles, and the large-sized cohort comprised females, without spermatophores and adult males. After April 17, females with spermatophores were observed in 3.8%–17.2% of the population. Based on the mean *TL* of each cohort, the daily growth rate in *TL* was calculated as 0.082 mm *TL* $day^{-1}$.

The abundance and biomass of *T. inspinata* ranged from 50 to 186 ind. $m^{-2}$ (mean ± SD: 111 ± 47 ind. $m^{-2}$) and 135 to 576 mg C $m^{-2}$, respectively. The mean biomass of *T. inspinata* was 317 ± 150 mg C $m^{-2}$, ca. 1/2 – 1/3 of that of *E. pacifica* (Fig. 11B). The *TL* of *T. inspinata* ranged from 3.7 to 26.7 mm. Based on the cohort analyses, two size cohorts were recognized. The mean *TL* of the large- and small-sized cohorts was 16.5–18.1 mm and 4.9–9.3 mm, respectively (Fig. 11B). The large-sized cohort was dominant in population number. The small-sized cohort comprised juveniles, and the large-sized cohort comprised adult males and adult females with spermatophores. Notably, the *TL*s of adult females with spermatophore were consistently larger than those of adult males within the large-sized cohort. Based on the mean *TL* of each cohort, the growth rate of *T. inspinata* was 0.022 mm *TL* $day^{-1}$.

For amphipods, 13 species belonging to 9 genera were observed throughout the sampling period. Among these species, four species, *C. challengeri, P. abyssalis T. pacifica* and *T. japonica*, were predominant, accounting for 85% of the abundance and 84% of the biomass. For the two numerically dominant amphipod species, *C. challengeri* and *T. paci-*

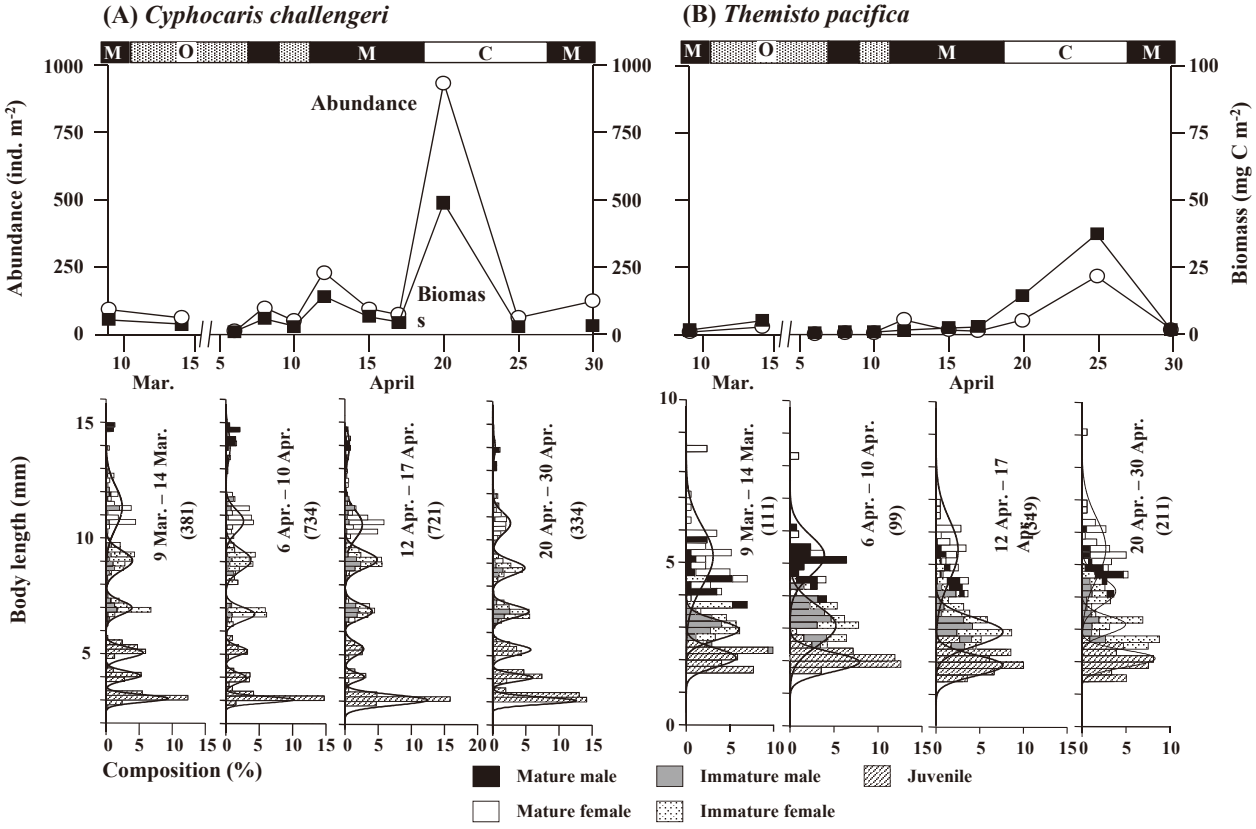


Fig. 12. Temporal changes in abundance, biomass and body length histograms of macrozooplanktonic amphipods, *Cyphocaris challengeri* (A) and *Themisto pacifica* (B), in the 0–200 m water column in the Oyashio region during March–April 2007. The dominant water masses at each sampling date are shown as upper bars. The values in the parentheses indicate the sample size. Smooth curves in histograms indicate cohort analysis. For the dominant water masses, C; coastal Oyashio water, M; modified Kuroshio water, O; Oyashio water.

*fica,* temporal changes in abundance, biomass and body length (*BL*) histograms are shown in Fig. 12.

The abundance of *C. challengeri* ranged from 14 to 934 ind. $m^{-2}$ (mean ± SD: 168 ± 248 ind. $m^{-2}$) (Fig. 12A). The biomass ranged from 11.2 to 488.9 mg C $m^{-2}$ with mean biomass at 91.1 ± 129.9 mg C $m^{-2}$. Both the abundance and biomass were low during March, while high values were observed on April 12 and 20. For *C. challengeri*, the *BL* ranged from 2.4 – 15.0 mm, and this species was classified into 7 cohorts. Each cohort corresponded with the differences in instar number. Thus, based on smaller sizes, each cohort comprised instar 4, instar 5, instar 6, instar 7, instar 8, instar 9 and instars 10–12, respectively. The minimum *BL* of mature females and males was 9.81 mm and 13.00 mm, respectively.

The abundance and biomass of *T. pacifica* ranged from 4 to 216 ind. $m^{-2}$ (mean ± SD: 39.3 ± 39.6 ind. $m^{-2}$) and 0.7 to 37.5 mg C $m^{-2}$ (6.4 ± 10.6 mg C $m^{-2}$), respectively (Fig. 12B). Both the abundance and biomass were low from March to April 10, but was higher on April 20 and 25. For *T. pacifica*, cohort analyses were conducted with pooled *BL* data at 5–10 day intervals. The *BL* of *T. pacifica* ranged from 1.4 to 9.2 mm, and this species was separated into 3 or 4 cohorts. The smallest *BL* cohort (mean *BL*: 1.9 – 2.1 mm) comprised juveniles, while the middle-sized cohort (mean *BL*: 2.8 – 4.5 mm, note that two cohorts were identified from April 20 – 30) comprised immature females/males, and the large-sized *BL* cohort (mean *BL*: 5.1 – 5.5 mm) comprised mature females and males.

The abundance and biomass of cnidarian *A. digitale* ranged from 16 to 316 ind. $m^{-2}$ (mean ± SD: 115 ± 88 ind. $m^{-2}$) and 4.1 to 81.3 mg C $m^{-2}$ (24.5 ± 23.4 mg C $m^{-2}$), respectively (Fig. 13). Both the abundance and biomass were low in March and high in April. The *BH* of *A. digitale* ranged from 4 to 18 mm. Based on the cohort analysis, two cohorts were identified for *A. digitale* throughout the study period. The mean *BH*, of the small- and large-sized cohorts was 6.2–9.1 mm and 10.5–13.1 mm, respectively. The composition of the mature specimens in the population ranged from 8% to 49% and was less than 8.3% from March 9 to April 10 but rapidly increased to 30.4% on April 15 and subsequently remained high until end of the study period (14–49%).

Throughout the study period, three chaetognath species belonging to three genera were observed (*E. hamata*, *P. elegans* and *P. scrippsae*). For *E. hamata* and *P. elegans*, two numerically dominant chaetognaths (>95% in total chaeto-

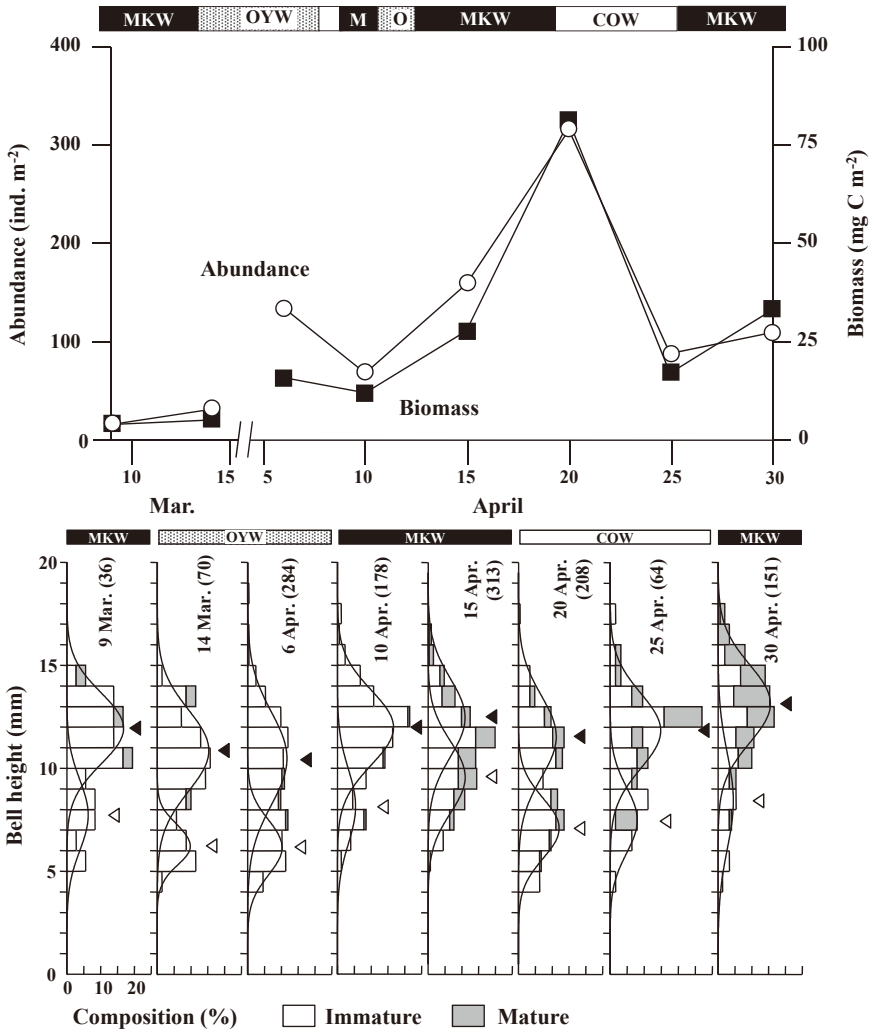


Fig. 13. Temporal changes in abundance, biomass and bell height (*BH*) histogram of macrozooplanktonic hydromedusa *Aglantha digitale* in the 0–200 m water column in the Oyashio region during March–April 2007. For histogram analysis, immature and mature specimens were separated. Open and solid triangles indicate the mean *BH* values of small- and large-sized cohorts, respectively. The values in the parentheses indicate measured individual numbers. For dominant water masses, COW; coastal Oyashio water, MKW; modified Kuroshio water, OYW; Oyashio water.

gnath abundance), temporal changes in abundance, biomass and *BL* histograms are shown in Fig. 14.

The abundance and biomass of *E. hamata* ranged from 113 to 2,543 ind. $m^{-2}$ (mean ± SD: 1,050 ± 594 ind. $m^{-2}$) and 10.2 to 208.9 mg C $m^{-2}$ (92.2 ± 53.8 mg C $m^{-2}$), respectively (Fig. 14A). Both the abundance and biomass were low in March and high after April 8. The *BL* of *E. hamata* ranged from 5.8 to 23.7 mm. Based on the cohort analyses, the *BL* at each sampling date was separated into three cohorts. The mean *BL* of each cohort was 7.9 – 10.7 mm (small-sized cohort), 10.5 – 13.2 mm (middle-sized cohort) and 12.6 – 15.4 mm (large-sized cohort). The small-sized cohort primarily comprised juveniles and stage I individuals, while both the middle- and large-sized cohorts comprised stage I individuals. Juveniles were abundant from March 9–14 and April 12–15.

The abundance and biomass of *P. elegans* ranged from 52.4 to 380.4 ind. $m^{-2}$ (means ± SD: 176.0 ± 92.4 ind. $m^{-2}$) and 45.7 to 471.6 mg C $m^{-2}$ (193.6 ± 123.5 mg C $m^{-2}$), respectively (Fig. 14B). The *BL* of *P. elegans* ranged from 11.0 to 41.3 mm, and small specimens (< 10 mm) were not observed during the study period. The large body sizes of *P. elegans* were comparable to the occurrences of the small body sizes of *E. hamata*. Because of the large body sizes of *P. elegans*, the abundance of *P. elegans* was lower than that of *E. hamata*, and the total biomass of *P. elegans* was higher than that of *E. hamata* (Fig. 14A, B). Based on the cohort analyses, the *BL* histogram of *P. elegans* was divided into three cohorts throughout the study period. The mean *BL* of each cohort ranged from 15.1 – 22.1 mm (small-sized cohort), 21.4 – 28.1 mm (middle-sized cohort) and 26.4 – 31.3 mm (large-sized cohort). The small-, middle- and large-sized cohorts comprised stage I, stage II and stage III individuals, respectively. At end of the study period (April 30), stage IV

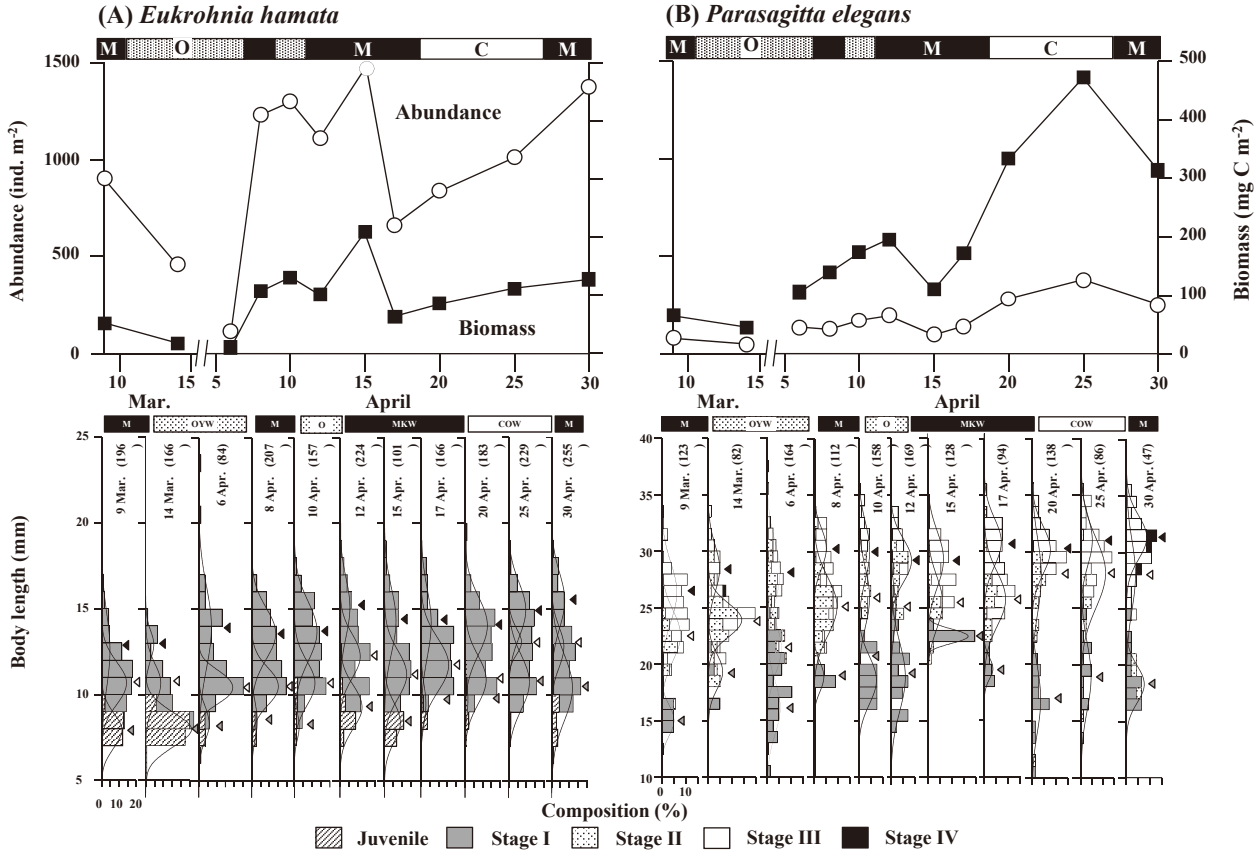


Fig. 14. Temporal changes in abundance, biomass and body length (*BL*) histograms of macrozooplanktonic chaetognaths, *Eukrohnia hamata* (A) and *Parasagitta elegans* (B), in the 0–200 m water column in the Oyashio region from March–April 2007. The dominant water masses at each sampling date are shown as horizontal bars. The values in the parentheses indicate measured individual numbers. The positions of triangles indicate mean BL of each cohort. For the dominant water masses, C; coastal Oyashio water, M; modified Kuroshio water, O; Oyashio water.

(mature specimens) was observed for the large-sized cohort (Fig. 14B).

### 3–1–4. Correlations with water mass exchanges

The results of the correlation analyses between the mixture ratio of water mass and abundance or the biomass of epi-, mesopelagic copepods and macrozooplankton are shown in Table 3. For epipelagic copepods, positive correlations were observed between the COW and the abundance and biomass of *N. flemingeri* and the biomass of *N. plumchrus*. Negative correlations were observed between the OYW and the abundance of *M. pacifica*, *N. cristatus*, *N. flemingeri* and *N. plumchrus* and the biomass of *N. cristatus*. For MKW, no correlations were detected for any species.

For mesopelagic copepods, a negative correlation was observed between MKW and the abundance of *H. tanneri*. Except for this interaction, no correlations were detected between the water masses and the abundance/biomass of mesopelagic copepods.

For macrozooplankton, positive correlations were observed between the COW and the abundance and biomass of the amphipod *T. pacifica*, cnidarian *A. digitale* and chaetognath *P. elegans* (except for the biomass of *A. digitale*). Negative correlations were observed between the MKW and the abundance of the euphausiid *T. inspinata* and chaetognath *E. hamata*. Negative correlations were also observed between the OYW and the abundance of the amphipod *P. abyssalis* and the biomass of the chaetognath *E. hamata*. For euphausiids or amphipods, correlations with the mixture ratio of the water mass were less than those of the other macrozooplankton taxa.

## 3–2. Discussion

### 3–2–1. Population structure of each zooplankton species

Tsuda et al. (2004) and Shoden et al. (2005) studied the life cycles of *E. bungii* in the Oyashio region. *E. bungii* has a one generation per year life cycle with diapause at C3–C6 stages. This species ascends from a deep ocean layer to the surface between February and April, and reproduction and growth occur during the spring phytoplankton bloom in the Oyashio region (Shoden et al., 2005). During the OECOS period, the population initially comprised C3–C6 stages, and following the phytoplankton bloom (Fig. 4C), rapid increases of C1 and C2 stages were observed (Fig. 9A). The rapid increases of C1 and C2 stages after April 15 might reflect

Table 3. Correlation coefficient ($r$) matrix between the mixture ratio of water mass (COW: coastal Oyashio water, MKW: modified Kuroshio water, OYW: Oyashio water) and abundance (ind. $m^{-2}$) or biomass (mg C $m^{-2}$) of epipelagic copepods (Eb: *Eucalanus bungii*, Mp: *Metridia pacifica*, Mo: *M. okhotensis*, Nc: *Neocalanus cristatus*, Nf: *N. flemingeri*, Np: *N. plumchrus*) at 0–500 m water column, mesopelagic copepods (Gs: *Gaetanus* spp., Ps: *Pleuromamma scutullata*, Pe: *Paraeuchaeta elongata*, Pb: *Paraeuchaeta birostrata*, Ht: *Heterorhabdus tanneri*) at 0–1,000 m water column, macrozooplankton (Ep: *Euphausia pacifica*, Ti: *Thysanoessa inspinata*, Cc: *Cyphocaris challengeri*, Pa: *Primno abyssalis*, Tp: *Themisto pacifica*, Ad: *Aglantha digitale*, Eh: *Eukrohnia hamata*, Pe: *Parasagitta elegans*) at 0–200 m water column in the Oyashio region during March–April 2007. For details of the mixture ratio of water mass, see Kono and Sato (2010). Significance is marked with asterisks. *: $p<0.05$, **: $p<0.01$.

| Compared parameters | Epipelagic copepods (0–500 m) | | | | | | Mesopelagic copepods (0–1000 m) | | | | | Macrozooplankton (0–200 m) | | | | | | |
|---|---|---|---|---|---|---|---|---|---|---|---|---|---|---|---|---|---|---|
| | Eb | Mp | Mo | Nc | Nf | Np | Gs | Ps | Pe | Pb | Ht | Ep | Ti | Cc | Pa | Tp | Ad | Eh | Pe |
| Abundance vs. | | | | | | | | | | | | | | | | | | | |
| COW ratio of water mass (0-50 m) | 0.416 | 0.369 | 0.422 | −0.247 | 0.526* | 0.282 | 0.423 | 0.189 | 0.750 | 0.836 | −0.198 | −0.284 | 0.264 | 0.218 | 0.539 | 0.646* | 0.735* | 0.041 | 0.848** |
| MKW ratio of water mass (0-50 m) | −0.131 | 0.379 | −0.285 | 0.477 | 0.030 | 0.234 | −0.142 | 0.623 | 0.127 | −0.658 | 0.899* | −0.364 | −0.667* | 0.042 | −0.044 | −0.374 | −0.472 | −0.678* | −0.476 |
| OYW ratio of water mass (0-50 m) | −0.297 | −0.858** | −0.119 | −0.303 | −0.612* | −0.589* | −0.243 | −0.676 | −0.743 | −0.167 | −0.576 | 0.487 | 0.285 | −0.238 | −0.679* | −0.311 | −0.236 | 0.395 | −0.447 |
| Biomass vs. | | | | | | | | | | | | | | | | | | | |
| COW ratio of water mass (0-50 m) | −0.082 | −0.270 | 0.367 | 0.270 | 0.591* | 0.550* | 0.792 | 0.753 | 0.458 | 0.818 | −0.372 | −0.237 | 0.298 | 0.179 | 0.583 | 0.646* | 0.370 | 0.266 | 0.801** |
| MKW ratio of water mass (0-50 m) | 0.228 | 0.298 | −0.325 | 0.259 | −0.195 | −0.124 | 0.265 | 0.200 | −0.673 | −0.589 | 0.841 | −0.374 | −0.650 | −0.024 | −0.310 | −0.431 | −0.064 | 0.232 | −0.362 |
| OYW ratio of water mass (0-50 m) | −0.184 | −0.062 | −0.011 | −0.606* | −0.413 | −0.452 | −0.893 | −0.806 | 0.167 | −0.208 | −0.380 | 0.449 | 0.238 | −0.211 | −0.323 | −0.221 | −0.375 | −0.732* | −0.543 |

reproduction during the phytoplankton bloom period. During the OECOS period, the additional recruitment of overwintering C3–C4 stages to the C6F population from April 20–30 has been reported (Yamaguchi et al., 2010a). In addition, in the Alaskan Gyre, the maturation of an overwintered *E. bungii* population during the spring phytoplankton bloom has also been reported (Miller et al., 1984). Within the overwintered stages (C3–C6), C5F and C6F stages might utilize the early phase of the phytoplankton bloom at the beginning of April for reproduction, and C3 and C4F stages might utilize the phytoplankton bloom in April as an energy source for growth to C6F and gonad maturation (Yamaguchi et al., 2010a). Consequently, these species could experience extended reproduction throughout the phytoplankton bloom period, reflecting the continuous recruitment of the C6F population.

Concerning the life cycle of *M. pacifica* in the Oyashio region, all copepodid stages occur throughout the year, and there are two pronounced generations: the first generation, characterized by rapid growth during the spring phytoplankton bloom (generation length: 2–3 months), and the second generation, characterized by slow development (9–10 months) with overwintering at C5 in deep ocean layers (up to 1,000–2,000 m) (Padmavati et al., 2004). Because the occurrence of the C1 stage of *M. pacifica* was much earlier than that of *E. bungii* and the dominance of C6F stages were observed from March to April 7 (Fig. 9B), the occurrence of the C1 stages likely reflected reproduction prior to the spring phytoplankton bloom. Based on field observations, a low egg hatching rate was reported for *M. pacifica*, likely reflecting the negative effect of diatom aldehyde on copepod development and growth during the spring phytoplankton bloom (Halsband-Lenk, 2005; Hopcroft et al., 2005). Because diatoms are the primary dominant phytoplankton taxon during the spring phytoplankton bloom in the Oyashio region (Isada et al., 2010), the negative effect of diatoms on copepod development might have occurred for *M. pacifica* during the OECOS period, reflecting the decreasing *M. pacifica* biomass observed during April (Fig. 9B).

For *M. okhotensis*, a two-year generation length was estimated, and this species utilizes the spring phytoplankton bloom during the first year for development to C5 and during the next year for reproduction (Padmavati et al., 2004). Because the composition of early copepodid stages was quite low (Fig. 9C), the reproduction of *M. okhotensis* did not occur in the Oyashio region during the OECOS period. For *M. okhotensis* in the Oyashio region, substantial parts of their population would be transported from the neighbouring Sea of Okhotsk (Padmavati et al., 2004). During the OECOS period, one water mass (COW) was derived from the Sea of Okhotsk (Fig. 5A). While both the abundance and biomass of *M. okhotensis* were positively correlated with coefficients for COW ($r$ = 0.422 for abundance, 0.369 for biomass), and

although these correlations were not significant (Table 3), these findings suggest that the effects of transportation from the Sea of Okhotsk might not be as large as previously expected for *M. okhotensis*.

For *N. cristatus*, reproduction occurs below 500 m from October to December, with a resulting peak of C1 observed at the near-surface layer from January to February. This newly recruited population develops to C5 by the end of June, and subsequently migrates down to a deeper layer for diapause from summer to autumn (Miller et al., 1984; Kobari and Ikeda, 1999; Tsuda et al., 2004). During the OECOS period, the development of this newly recruited population from C1 to C4 stages was observed (Fig. 9D). Details on growth rate of *N. cristatus* are discussed in Chapter 4.

*Neocalanus flemingeri* also undergoes seasonal ontogenetic vertical migration. According to Kobari and Ikeda (2001a), the dominant stages of *N. flemingeri* in the Oyashio region shift seasonally: C1 and C2 in March, C3 and C4 in April and C5 in early June, and subsequently populations enter overwintering at C4 or C6 stages at a deep ocean layer from autumn to winter. During the OECOS period, C1, C2 and C3 stages peaked in population structure on April 9, 18 and 25, respectively (Fig. 9E), reflecting the development of *N. flemingeri* from C1 to C3 stages during the spring phytoplankton bloom of the OECOS period.

For *N. plumchrus*, the surface occurrence timing of copepodid stages of this species is much later than that of the sympatric two *Neocalanus* spp., while reproduction at a deep layer continues ca. eight months from October to May in the Oyashio region (Tsuda et al., 1999; Kobari and Ikeda, 2001b). A recent molecular DNA identification study on nauplii (Fujioka et al., 2015) reported that the vertical distribution of N1–N2 was > 250 m, while that of the N3 extended from the surface to a deeper layer and that of N4–N6 occurred only at the surface layer. According to Fujioka et al. (2015), the reproduction of *N. plumchrus* occurs at a deep layer and development ceases at N3, thus N3 acts as a mediator of developmental timing after N4, and subsequently, the initiation of development from N3 to N4 is triggered by the onset of the spring phytoplankton bloom. Because the development of *N. plumchrus* from N4 to N6 occurred at the surface layer in April, these individuals might reach the C1 stage near May (Fig. 1B). For the OECOS period, the first occurrence of *N. plumchrus* after April 7 suggested that these individuals undergo naupliar development (N4–N6) prior to April 7 (Fig. 9F).

Both *Gaetanus simplex* and *G. variabilis* are medium-sized copepods (total lengths ca. 4 mm) belonging to Aetideidae and are distributed throughout the mesopelagic zones of the subarctic Pacific Ocean, Bering Sea and Sea of Okhotsk (Brodskii, 1950). The life cycle of *G. variabilis* in the Oyashio region has been reported as two years, with reproduction timing during the spring phytoplankton bloom (Yamaguchi and Ikeda, 2000a). During the OECOS period, *Gaetanus* spp. was predominantly at C4–C6 stages (Fig. 10A), and the occurrence of spermatophore-attached C6F have been reported (Abe et al., 2012). These findings suggest that reproduction of *Gaetanus* spp. might have occurred during the OECOS period. However, as the naupliar development at *in situ* temperature requires 51 days (Yamaguchi and Ikeda, 2000a), the recruitment of C1 stage individuals might not have been detectable in the present study.

*Pleuromamma scutullata* is distributed at approximately 250–500 m, and this species performs nocturnal DVM and functions as a suspension feeder with a one-year generation length, showing peak reproduction during the spring phytoplankton bloom (Yamaguchi and Ikeda, 2000b). The population structure of *P. scutullata* primarily comprised C5 and C6 stages during the OECOS period (Fig. 10B), consistent with the phenomenon observed during the same season of a previous study (Yamaguchi and Ikeda, 2000b). Together with high *MCS* (Fig. 10B), the dominance of mature specimens in C6F and the occurrence of C6M with spermatophores at 500–750 m during April (Abe et al., 2012) suggest active reproduction for *P. scutullata* in April.

In the Oyashio region, *P. elongata* has a one-year generation length, and reproduction occurs throughout the year, peaking from April – June (Yamaguchi and Ikeda, 2001). The significant increase in abundance, progressive dominance of C1–C3 stages and gradual decrease in *MCS* (Fig. 10C) suggest the continuous recruitment of C1 stages to the *P. elongata* population during the OECOS period. During the OECOS period, the mean composition of egg-carrying C6F individuals (32%) (Abe et al., 2012) is much higher than the annual mean (4.3%, Yamaguchi and Ikeda, 2001). These findings suggest that *P. elongata* undergoes active reproduction during the OECOS period.

The life cycle of *P. birostrata* was also studied in the Oyashio region. These species have a one-year generation length, and reproduction occurred throughout the year, peaking from in April – June (Yamaguchi and Ikeda, 2001). During the OECOS period, the composition of C1–C3 stages was high for *P. birostrata* (52–69%) (Fig. 10D), and the composition of egg-carrying specimens in the C6F population (54%) (Abe et al., 2012) was much higher than the reported annual mean (mean 5% and range 0–33%, Yamaguchi and Ikeda, 2001). Thus, these findings suggest that reproduction of *P. birostrata* was initiated during the OECOS period.

For *H. tanneri*, the generation length is one year, and spermatophore-attached C6F are observed throughout the year, with peak reproduction in December (Yamaguchi and Ikeda, 2000b). The increased inter molt growth of C3–C4 individuals was observed during the summer when the zooplankton biomass was high. Together with the predominance of C6 in the population (Fig. 10E) and the seasonal developmental timing (C3–C4 in summer), *H. tanneri* undergoes reproduc-

tion and the development of early copepodid stages during the spring phytoplankton bloom.

In the Oyashio region, the euphausiid *E. pacifica* reproduce twice a year: March to April and August (Kim et al., 2009). In the present study, the continuous occurrence of spermatophore-attached females was observed after April 17 (Fig. 11A), suggesting that *E. pacifica* reproduction occurred in late April. However, the low composition of spermatophore-attached females (< 5%) and the faster growth rates (0.082 mm *TL* $day^{-1}$) than those of *T. inspinata* (0.022 mm *TL* $day^{-1}$, Kim et al., 2010a) suggest that *E. pacifica* utilized the spring phytoplankton bloom for body development and not reproduction.

*T. inspinata* reproduction occurred throughout the year with a peak from March – May (Kim et al., 2009). Even during the OECOS period, most of the adult females had attached spermatophores (Fig. 11B), suggesting that the spring phytoplankton bloom was used as an energy source for the reproduction of *T. inspinata*.

For *C. challengeri*, the compositions of egg- or juvenile-carrying specimens within mature females increased during April (Abe et al., 2016), and the juvenile composition in the total population rapidly increased in late April (Fig. 12A). This species reproduce throughout the year, peaking from April to July (Yamada and Ikeda, 2000). The population structure and reported reproduction timing suggest active reproduction for *C. challengeri* during the OECOS period.

*T. pacifica* in the Oyashio region has four generations per year, with a reproduction peak in early summer, and peaks in both abundance and biomass during the summer (Yamada et al., 2004). During the OECOS period, increases in the composition of egg- and juvenile-carrying females of *T. pacifica* through April were reported (Abe et al., 2016). These findings suggest that *T. pacifica* underwent reproduction based on their increased mesozooplankton biomass (Fig. 8A).

The life cycle of *A. digitale* lasts one year, with a reproduction peak from June to August in the Oyashio region (Takahashi and Ikeda, 2006). Assuming this life cycle schema, two cohort sizes based on the *BH* were observed, corresponding to those recruited from spring to summer (large-sized *BH* cohort) and late summer to autumn (small-sized *BH* cohort) in the previous year. The composition of mature specimens in the large-sized *BH* cohort increased after April 15 (Fig. 13), suggesting that *A. digitale* grew and matured during the spring phytoplankton bloom.

For *E. hamata*, mature specimens are distributed at depths below 250 m in the subarctic Pacific (Terazaki and Miller, 1986). Because the sampling depths in the present study were much shallower (0–200 m), only small-sized juveniles and immature specimens (stage I) were collected for *E. hamata*. In the Oyashio region, the recruitment of the new generation occurs from spring to summer (Matsumoto, 2008). The high abundance of juveniles in March and mid-April might reflect the recruitment of a new generation of *E. hamata* (Fig. 14A).

Because the nighttime vertical distribution depths for *P. elegans* are much shallower than 200 m (Ozawa et al., 2007), the sampling design of the present study may cover the entire population of *P. elegans* in the Oyashio region. Mature stage IV specimens with *BLs* of approximately 30 mm, were observed on April 30, 2007 (Fig. 14B). The reproduction of *P. elegans* peaks from late spring to summer in the Oyashio region (Terazaki, 1998; Kotori, 1999). These findings suggest the initiation of reproduction for *P. elegans* at end of the April during the OECOS period.

### 3-2-2. Responses of zooplankton for water mass exchange

As previously described, the geographical origins and temperatures of the three water masses observed during the OECOS period varied (Fig. 5). Within the three water masses, COW showed positive correlations with five species, while MKW showed one positive and two negative correlations with species, and OYW showed a negative correlation with six species (Table 3). These findings suggest high zooplankton abundance and biomass under COW conditions. While OYW also originated from the cold-water mass, the lowest experienced temperature may induce the low zooplankton growth rate in OYW. Because the origin of COW was the Sea of Okhotsk, the high primary production of the marginal sea (note that the Sea of Okhotsk is in the southernmost ice coverage ocean in the northern hemisphere) may support sufficient food conditions for the various zooplankton species examined in the present study (Fig. 5).

Because each chaetognath species showed species-specific temperature and salinity ranges, each species is considered an indicator of the water mass (Russell, 1935; Bieri, 1959). During the OECOS period, *P. elegans* showed a high positive correlation with COW. Similar water mass correlations between COW and *P. elegans* were observed for the cnidarian *A. digitale* (Table 3). Both species (*P. elegans* and *A. digitale*) are subarctic/arctic species, with similar geographical distributions and little DVM behaviour (Kotori, 1976; Shiota et al., 2012). However, macrozooplanktonic euphausiids and amphipods showed strong DVM behaviour (Iguchi et al., 1993; Ikeda and Shiga, 1999). The more moderate effects of water-mass exchange on euphausiids and amphipods compared to the other macrozooplankton taxa (Table 3) might reflect the strong DVM behaviours of these individuals, which masked the effects of water-mass exchange at the surface layer.

Because the growth of epipelagic copepods occurred at the surface layer, the surface temperature is considered the most important factor to determine growth and survival during the spring. Within the three water masses, the observed temperature was the lowest for OYW. Thus, it is particularly interesting that most epipelagic copepods showed negative

correlations with OYW (Table 3). The lowest temperature at OYW may induce slower growth and decrease the survival rate of epipelagic copepods in OYW compared with those in the other water masses. However, mesopelagic copepods showed little effect on water-mass exchange (Table 3), likely reflecting the fact that the water mass exchange at the surface layer has less effect on the distribution of mesopelagic copepods.

## 4. Vertical Distribution of Dominant Copepods

### 4–1. Results

For epi- and mesopelagic copepods, day and night vertical stratified samplings were collected with a VMPS (60 μm mesh) between 0 and 1,000 m. Diel and ontogenetic changes in the vertical distribution ($D_{50\%}$) of epipelagic copepods (*E. bungii*, *M. pacifica*, *M. okhotensis*, *N. cristatus*, *N. flemingeri* and *N. plumchrus*) and mesopelagic copepods (*P. scutullata*, *P. elongata* and *P. birostrata*) in the Oyashio region are shown in Figs. 15–17.

#### 4–1–1. Epipelagic copepods

*Eucalanus bungii* had no DVM during all copepodid stages throughout the study period (Kolmogorov-Smirnov test; $p > 0.05$, Fig. 15A). *E. bungii* was concentrated at approximately 250–500 m both day and night on March 8, 2007. The vertical distribution ranges of C3–C6 extended (50–750 m) both day and night on April 5. The vertical distribution of C4–C6 reached the surface by April 11, but C3 stayed in the deep layer. During April 23–29, C6F were consistently distributed at the surface layer. Newly recruited C1–C2 were observed at the surface layer on April 29. On April 29, C1–C4 were distributed near the surface layer. No sexual differences in the vertical distribution were observed for C4–C5, while the C6M remained below 150 m both day and night, and C6M never occurred at the surface layer.

For *M. pacifica*, daytime distribution depths of C1–C3, C4–C5 and C6 on March 8 were at 150–250, 150–500 and 250–500 m, respectively (Fig. 15B). At night, all copepodid stages, except C6M, performed nocturnal ascent and were distributed in the upper 150 m. These strong nocturnal DVMs were observed on April 5 and 11. From April 23–24 and 28–29, DVM was not observed for C1–C5. Only the C6F stage continued a nocturnal ascent on both April 23 and 29. The magnitude of the DVM was 46–359 m (evaluated by day $D_{50\%}$ –night $D_{50\%}$) for C6F. The daytime distribution depths increased with increasing copepodid stages, and the DVM magnitude also increased. The C6M of *M. pacifica* were distributed at 250–500 m depths both day and night and never occurred at the surface layer, consistent with *E. bungii* C6M.

For *M. okhotensis*, adult specimens (C6F/M) did not per-

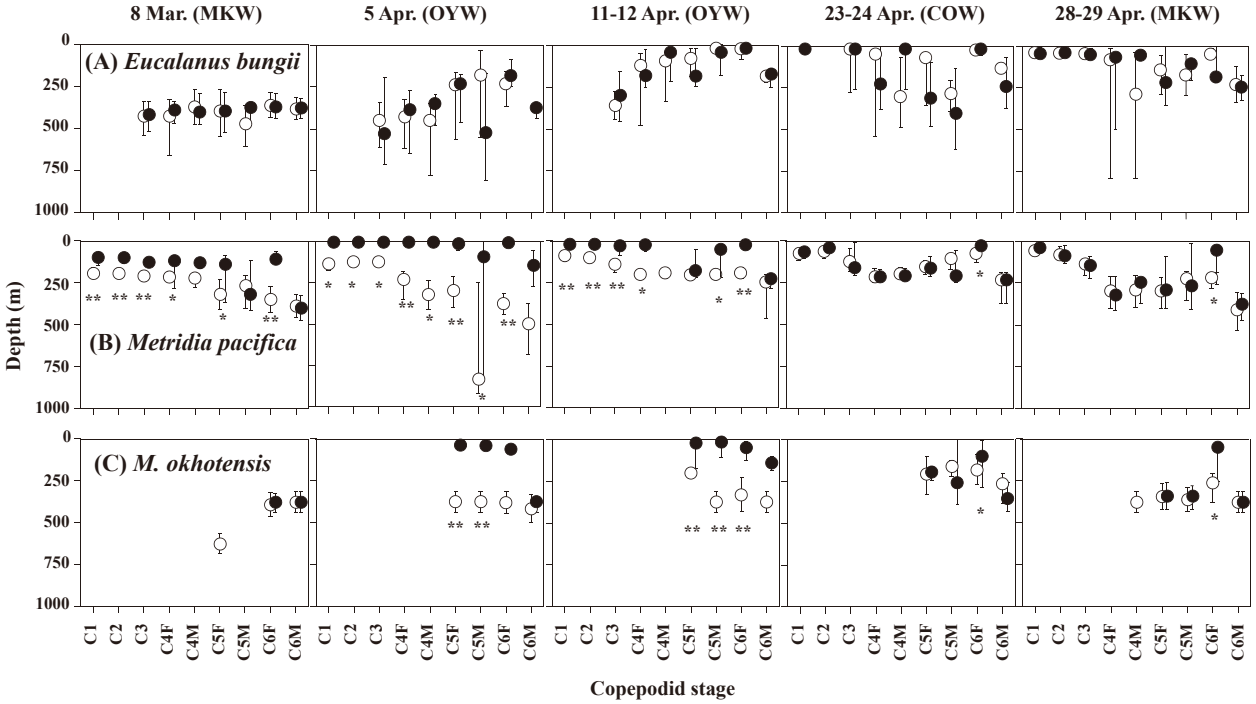


Fig. 15. Ontogenetic changes in the vertical distribution of epipelagic copepods, *Eucalanus bungii* (A), *Metridia pacifica* (B) and *M. okhotensis* (C), in the Oyashio region during March–April 2007. Open and solid symbols denote $D_{50\%}$ of day and night, respectively. Vertical bars indicate the depth ranges of $D_{25\%}$ to $D_{75\%}$. Asterisks indicate the presence of diel vertical migration, detected using the Kolmogorov-Smirnov test. *: $p<0.05$, **: $p<0.01$. Dominant water masses at each date are shown in the parentheses. COW; coastal Oyashio water, MKW; modified Kuroshio water, OYW; Oyashio water.

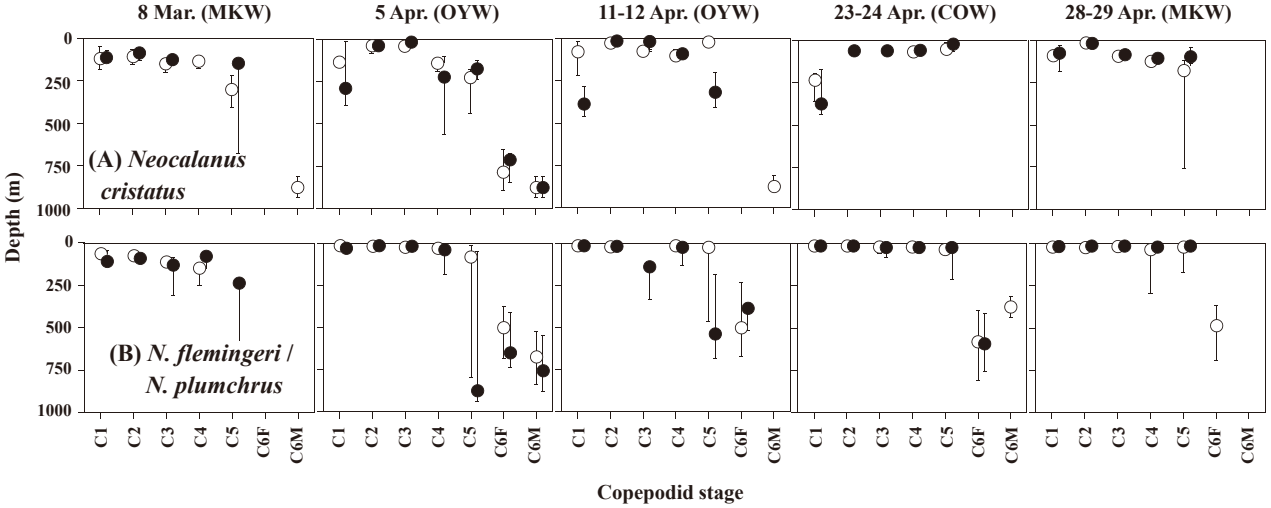


Fig. 16. Ontogenetic changes in the vertical distribution of *Neocalanus* copepods, *N. cristatus* (A) and *N. flemingeri / N. plumchrus* (B), in the Oyashio region during March to April 2007. Open and solid symbols denote $D_{50\%}$ of day and night, respectively. Vertical bars indicate the depth ranges of $D_{25\%}$ to $D_{75\%}$. Note that no diel vertical migration was detected for all species/stages using the Kolmogorov–Smirnov test. Dominant water masses at each date are shown in the parentheses. COW; coastal Oyashio water, MKW; modified Kuroshio water, OYW; Oyashio water.

form DVM on March 8 and remained below 250 m both day and night ($p > 0.05$, Fig. 15C). The nocturnal ascent DVM was observed for C5F/M on April 5 and C5F/M and C6F on April 11. The magnitude of these DVM was 71–358 m. On April 23 and 29, the nocturnal ascent DVM was detected only for C6F. The C6M of *M. okhotensis* was distributed at 250–500 m both day and night throughout the study period.

For *N. cristatus*, C1–C4 was distributed in the upper 250 m both day and night throughout the study period (Fig. 16A). Vertical distributions were concentrated at approximately 100

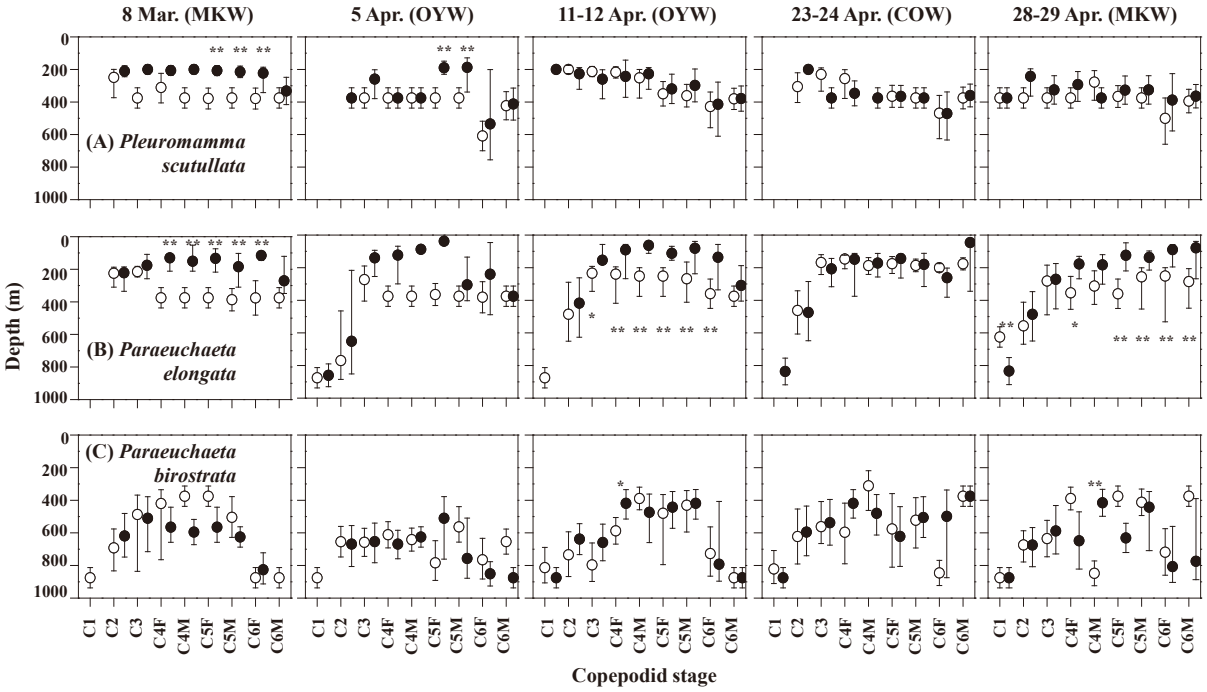


Fig. 17. Ontogenetic changes in vertical distribution of mesopelagic copepods, *Pleuromamma scutullata* (A), *Paraeuchaeta elongata* (B) and *Paraeuchaeta birostrata* (C), in the Oyashio region during March to April 2007. Open and solid symbols denote $D_{50\%}$ of day and night, respectively. Vertical bars indicate depth ranges of $D_{25\%}$ to $D_{75\%}$. Asterisks indicate that the presence of DVM detected using the Kolmogorov–Smirnov test. *: $p<0.05$, **: $p<0.01$. Dominant water masses at each date are shown in the parentheses. COW; coastal Oyashio water, MKW; modified Kuroshio water, OYW; Oyashio water.

m on March 8, but extended to the surface layer after April 5. Throughout the study period, C6 stages occurred below 500 m. No DVM was observed in any copepodid stages of *N. cristatus* during the study period ($p > 0.05$, Fig. 16A).

For *N. flemingeri*, C1–C4 were distributed at 50–250 m and were not observed in surface water both day and night on March 8 (Fig. 16B). *N. plumchrus* was observed after April 11. The C1–C4 stages of both species were distributed near the surface layer after April 5.

#### 4–1–2. Mesopelagic copepods

For *P. scutullata*, C5F/M and C6F showed clear DVM ($p < 0.01$) with a magnitude of 156–171 m on March 8 (Fig. 17A). Nocturnal ascent DVM was observed for C5F/M on April 5 ($p < 0.01$), while no DVM was detected for all copepodid stages after April 11 ($p > 0.05$). The OVM of *P. scutullata* was characterized by a developmental descent with a magnitude of 102–138 m (Fig. 17A).

*Paraeuchaeta elongata* after C4 stages showed clear DVM, characterized by nocturnal ascent with a magnitude of 120–160 m throughout the study period (Fig. 17B). Because C1 and C2 were distributed at the deepest layer, the OVM of *P. elongata* was characterized by developmental ascent with a magnitude of 478–675 m (Fig. 17B).

For *P. birostrata*, DVM was not detected for most dates (Fig. 17C). Concerning OVM, C1 and C6 of *P. birostrata* were distributed at the deepest layers, and C4 and C5 were detected at the shallowest layers. Because of these stage-specific vertical distributions, the OVM of *P. birostrata* comprises a mixture of two patterns: developmental ascent for the early copepodid stages ($D_{50\%}$ of C1 – C4: 339–357 m) and developmental descent for the late copepodid stages ($D_{50\%}$ of C6F – C4: 237–273 m) (Fig. 17C).

### 4–2. Discussion

#### 4–2–1. Epipelagic copepods

The vertical distribution of *E. bungii* showed clear temporal changes. The activation of diapause and the upward migration of overwintered C3–C6F stages were observed on April 5 (Fig. 15A). The timing of upward migration was faster for C6F than for C3–C4 stages, and newly recruited C1–C3 stages were distributed at 0–50 m, while C6M resided at deeper layers throughout the study period (Fig. 15A). The activation of *E. bungii* diapause remains unclear. Based on high-frequency samplings obtained during iron-fertilization experiments in the Gulf of Alaska, the upward migration of *E. bungii* from the subsurface (20–50 m) to the surface layer has been observed during high phytoplankton bloom (Tsuda et al., 2006). During the OECOS period of the present study, the timing of the ascent migration of *E. bungii* corresponded with the timing of the chl *a* peak. For SEEDS I (the highest chl. *a* recorded iron-fertilization experiment), high standing stocks of early copepodid stages of large grazing copepods likely resulted from the reduced mortality rates of these stages, as suspension feeders feed on large diatoms and less predation pressure on eggs and nauplii (Tsuda et al., 2005). For the OECOS period, the surface distribution of C1–C3 might also reflect of abundance of their food phytoplankton and also reflect lower predation pressures.

*Metridia pacifica* has active DVM (Tsuda and Sugisaki, 1994). The daily downward carbon transportation through *M. pacifica* DVM was estimated to be 8.0 mg C $m^{-2}$ $day^{-1}$, and the yearly total was 3.0 g C $m^{-2}$ $year^{-1}$, accounting for 15% of the total passive sinking POC flux at 150 m (Takahashi et al., 2009). For the OECOS period, active DVM was observed, except for C6M from March 8 to April 11. Interestingly, these DVM were only limited for C6F during April 23–24 and 28–29 (Fig. 15B). The other stages were observed at deep layers throughout the day on these dates. These patterns were also observed for the two mesopelagic copepods (*P. scutullata* and *Gaetanus simplex*), as both species performed DVM during the normal season (Abe et al., 2012). The flexibility of DVM behaviour has been well documented for *Metridia* spp. Thus, within the same stage, only less-lipid accumulated specimens perform DVM in *M. pacifica* (≒ *M. lucens*) (Hays et al., 2001), and their DVM patterns varied with the presence/absence of visual vertebrate predators (Osgood and Frost, 1994). Seasonally, the magnitude of DVM is smaller during spring than during summer and winter, reflecting seasonal changes in light penetration, which is smaller during the spring because of the phytoplankton bloom (Takahashi et al., 2009). The continuous DVM of C6F stage *M. pacifica* might reflect reproduction at the surface layer during the spring phytoplankton bloom.

For the congener *M. okhotensis*, nocturnal DVM was observed on April 5 and 11–12, but ceased, except for C6F, after April 23. The active DVM of *M. okhotensis* has been previously reported (Hattori, 1989). The seasonally limited DVM pattern (observed only in April) has also been reported for *M. okhotensis* in the Oyashio region (Padmavati et al., 2004; Takahashi et al., 2008). The continuous DVM behaviour of C6F stages in late April during the OECOS period was similar to that of congener *M. pacifica.* These findings suggest that the DVM patterns of C6F support reproduction at the surface layer.

The vertical distribution of early stages (C1–C3) of *N. cristatus* was at 0–250 m on March 8 and 0–150 m on April 5 and 23, and subsequently a shallower distribution was observed on April 29: 0–25 m for C1–C2 and 50–100 m for C3–C4. These patterns (shallower changes in vertical distribution of early copepodid stages with advances of phytoplankton bloom) were reported during iron-fertilization experiments (SERIES) (Tsuda et al., 2006). Commonly, the C2 stages of *N. cristatus* occurred shallower than the C1 stages (Fig. 16A), likely reflecting the occurrence of reproduction below depths of 1,000 m (Miller et al., 1984; Kobari and Ikeda, 1999). The initial feeding stage is C1 for *N. cristatus,* while other

*Neocalanus* spp. (*N. flemingeri* and *N. plumchrus*) initiate feeding at N4 (Saito and Tsuda, 2000). The first feeding stage of *Neocalanus* spp. shows a broader vertical distribution range (Fujioka et al., 2015). A deeper distribution of C1 compared to C2 in *N. cristatus* might reflect this broader vertical distribution.

A comparison of the vertical distribution depths between three *Neocalanus* spp. and *E. bungii* during the OECOS period revealed that *N. cristatus* and *E. bungii* were distributed deeper than *N. flemingeri* and *N. plumchrus*. As for feeding habits, the late copepodid stages of *N. cristatus* and *E. bungii* feed on sinking particles or aggregations (Dagg, 1993), while major food items of late copepodid stages of *N. flemingeri* and *N. plumchrus* are phytoplankton (Sato et al., 2011). These differences in food preference may contribute to the deeper distribution of *N. cristatus* and *E. bungii* compared to *N. flemingeri* and *N. plumchrus*. The vertical separation of these species pairs was observed: large body-sized *N. cristatus* and *E. bungii* were distributed below 50 m and small body-sized *N. flemingeri* and *N. plumchrus* distributed at the surface layer in the eastern subarctic Pacific during the spring (Mackas et al., 1993). In the Oyashio region, species-specific vertical separation was reported for these four species, from shallow to deep in the following order, *N. plumchrus*, *N. flemingeri*, *E. bungii* and *N. cristatus*, and these vertical segregations contribute to the niche separation of large grazing copepods during the growing season (Sato et al., 2011; Tsuda et al., 2014).

For *N. flemingeri*, the vertical distribution was broader (25-100 m) on March 8, but concentrated at 0-50 m after April 5, similar to the temporal changes observed for *N. cristatus*. Iron-fertilization experiments revealed the upward migration from the sub-surface layer for the C3-C5 stages of *E. bungii* and C2-C4 stages of *N. cristatus* in the North Pacific (Tsuda et al., 2006). The upward migration of *N. flemingeri* during the spring phytoplankton bloom may also reduce the mortality and high survival rate of early copepodid stages.

For *N. plumchrus*, N1-N2 are distributed from deeper layers to 250 m, and N3 was observed at broader depths from deeper layers to the surface layer; the development from N4 to N6 has been observed at the surface layer in April (Fujioka et al., 2015). The observation of copepodid stages of *N. plumchrus* on April 5 might reflect development from N4 to N6 during the spring phytoplankton bloom.

**4-2-2. Mesopelagic copepods**

The DVM magnitude of *P. scutullata* during the OECOS period was 156-188 m (Fig. 17A). These values are within the range of the reported values for this species in the Oyashio region (20-249 m, Yamaguchi and Ikeda, 2000b). The ceased DVM was also observed for *P. scutullata,* but it occurred earlier (from 11 April) than in *M. pacifica* (after April 23, Fig. 15B). The earlier cessation in *P. scutullata* suggests that mesopelagic *P. scutullata* might sensitively respond to increases in passive sinking POC flux. The developmental descent of the OVM was observed for *P. scutullata* throughout the study period (Fig. 17A). Yamaguchi et al. (2004a) examined the OVM patterns of mesopelagic copepods and found that within the mesopelagic copepods, OVM characterized by developmental decent was common for shallower resident species (<1,000 m), while developmental ascent was the common OVM for deeper species (>1,000 m). These shifts in OVM patterns in mesopelagic copepods are consistent with the lifetime fecundity of this species, i.e., shallower resident species have high fecundity with small-sized eggs (*r*-selection), while deeper resident species have lower fecundity with large-sized eggs (*K*-selection). To reduce mortality, the shallower species of early stages tend to be distributed at shallower depths, characterized by high temperatures to achieve faster growth (*r*-selection). For deeper resident species, to avoid predation, early stages occur at deeper depths (*K*-selection) (Yamaguchi et al., 2004a). Because *P. scutullata* were distributed at relatively shallow depths within mesopelagic copepods, their OVM might show a developmental descent pattern (*r*-selection).

In the Oyashio region, vertical separation within the genus has been reported for the three *Paraeuchaeta* spp. (*P. elongata, P. birostrata* and *P. rubra*), and *P. elongata* distributed at the shallowest depths, with a distribution centre at 310 m (Yamaguchi and Ikeda, 2002a). The distribution depths of *P. elongata* in the present study are consistent with these depths. However, *P. birostrata* occurs at deeper depths of approximately 800 m (Yamaguchi and Ikeda, 2002a). In the present study, *P. birostrata* was distributed between 500 and 1,000 m, thus vertical separation within *Paraeuchaeta* species was also observed in the present study (Fig. 17B, C). The vertical separations within the congener species might reduce food competition in the food-limited mesopelagic realm (Yamaguchi and Ikeda, 2002a).

Nocturnal ascent DVM was observed for carnivorous *P. elongata* throughout the study period, except on April 5 and 23-24 (Fig. 17B). As previously described, the ceased DVM reflected particle feeders inhabiting the epipelagic (*M. pacifica*) and mesopelagic (*P. scutullata*) layers after April 11 or 23 during the OECOS period (Abe et al., 2012; Figs. 15B, 17A). However, the ceased DVM was not observed for *P. elongata*. While results of the ceased DVM of suspension feeders in the epipelagic and mesopelagic layers might result from the increasing POC flux after the spring phytoplankton bloom in mid-April, such effects may be limited for carnivorous *P. elongata*, as this species performs continuous DVM, even after the spring phytoplankton bloom.

For *P. birostrata*, the OVM pattern greatly varied from that of *P. elongata*. The OVM pattern of *P. birostrata* reflected a mixture of developmental ascent at early copepodid stages and developmental descent at late copepodid stages (Fig.

17C). For *P. birostrata*, C4 is the shallowest stage throughout the year, and C1 and C6 are the deepest (Yamaguchi and Ikeda, 2002a). This combined OVM pattern is consistent with the findings of the present study. The OVM patterns of *Paraeuchaeta* spp. are associated with the magnitude of the inter-molt growth of each developmental stage, and the shallowest stage shows the highest inter-molt growth within the species (Yamaguchi and Ikeda, 2002b).

## 5. Growth of Dominant Copepods and Macrozooplankton

### 5-1. Results

As previously described (chapter 3), various zooplankton species achieved growth and reproduction in the Oyashio region during the spring phytoplankton bloom. To conduct species-specific comparisons, the growth of each species was calculated according to the standardized carbon-mass specific growth rate (*g*) (see 2-3-5).

#### 5-1-1. Dominant copepods

For the epipelagic *E. bungii*, the composition of C3 showed a rapid decrease on April 25 (Fig. 9A). Two cohorts were recognized for *E. bungii*: overwintered C3 and C4-C5 populations prior to April 25, and newly recruited C1-C2 and C3 populations after April 25 (Fig. 9A). Each cohort was referred to as large-sized (C3-C5) and small-sized (C1-C3) cohorts, respectively. Significant growth was observed for each cohort (Fig. 18, $p < 0.05$). The growth rate (*g*) (mean ± sd) of both small- (Eb1) and large-sized (Eb2) cohorts was 0.061±0.440 and 0.029±0.074 day$^{-1}$, respectively.

The individual biomass of *M. pacifica* was high (3.0 µg C ind.$^{-1}$) on March 8, but low thereafter. For *M. okhotensis*, the individual biomass was high on April 5 (83.2 µg C ind.$^{-1}$), but low and highly variable for the other sampling dates. The individual carbon mass of *N. cristatus* ranged from 26.3 to 201.1 µg C ind.$^{-1}$ (except for C6) and showed significant growth throughout the OECOS period (Nc: $p < 0.05$). The mean growth rate (*g*) of this cohort was 0.064±0.179 day$^{-1}$. The individual carbon mass of *N. flemingeri* and *N. plum-*

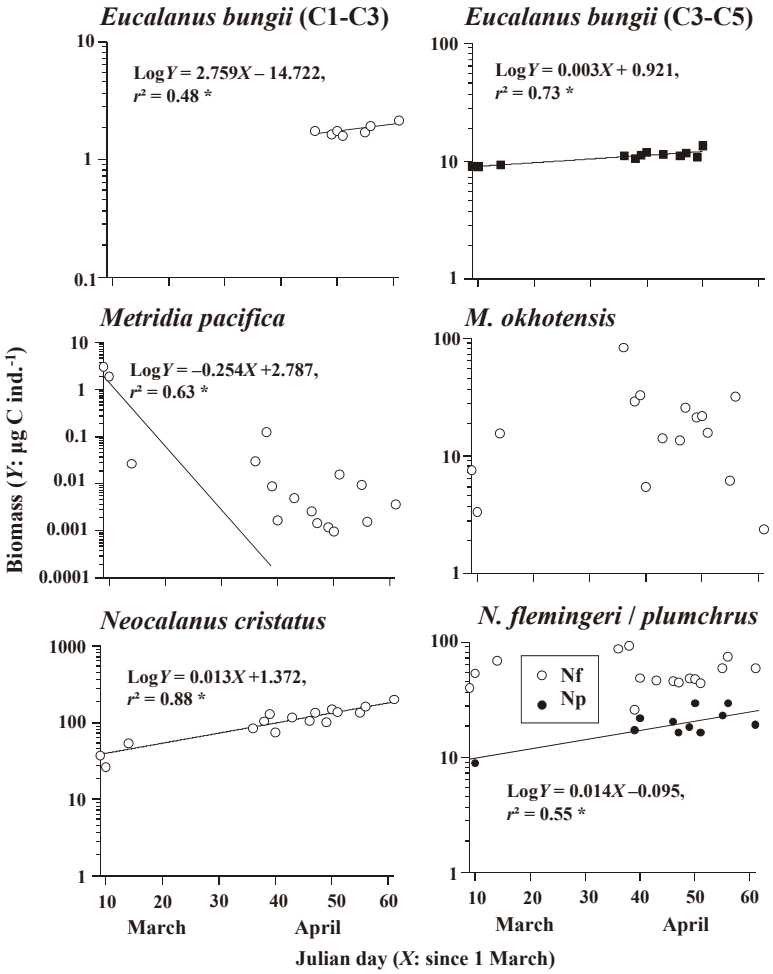


Fig. 18. Temporal changes in the individual biomass calculated based on the mean copepodid stage (CS, cf. Table 2) for epipelagic copepods in the Oyashio region during spring 2007. For cohorts showing significant growth along with date (slope is significantly differed from 0), regressions were shown between biomass (*Y*) and Julian day (*X*). *: $p < 0.05$.

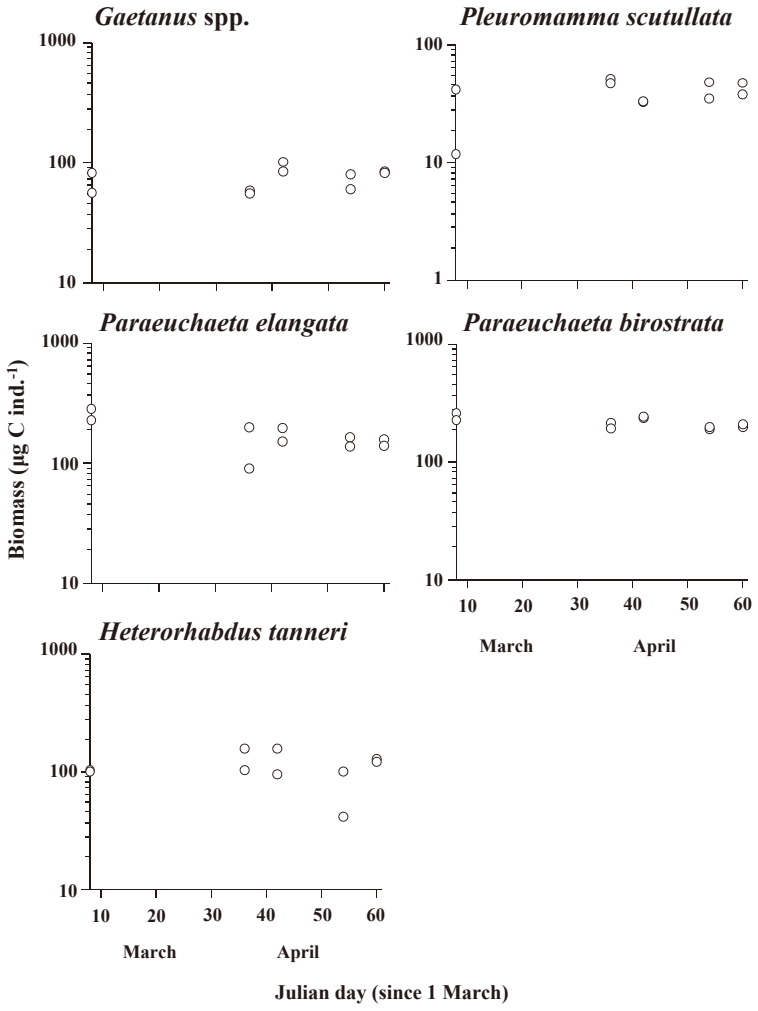


Fig. 19. Temporal changes in individual biomass calculated by the mean copepodid stage (CS, cf. Table 2) for mesopelagic copepods in the Oyashio region during spring in 2007. Note that no significant trends were observed according to the date for all mesopelagic copepods.

*chrus*, except C6, ranged from 25.9 to 93.0 and 2.68 to 16.19 µg C ind.$^{-1}$, respectively. No significant growth was detected for *N. flemingeri*, while significant growth was observed for *N. plumchrus* (Fig. 18, $p < 0.05$). The mean growth rate ($g$) of this cohort was 0.039±0.492 day$^{-1}$.

No mesopelagic copepods examined in the present study showed significant growth during the OECOS period. The individual carbon masses of mesopelagic copepods were 55.2–100.8 µg C ind.$^{-1}$ for *Gaetanus* spp., 11.8–51.6 µg C ind.$^{-1}$ for *P. scutullata*, 89.6–283.7 µg C ind.$^{-1}$ for *P. elongata*, 189.7–258.7 µg C ind.$^{-1}$ for *P. birostrata* and 41.5–156.1 µg C ind.$^{-1}$ for *H. tanneri* (Fig. 19).

**5–1–2. Macrozooplankton**

For macrozooplankton, temporal changes in the individual carbon mass were analysed based on the body length (*BL* or *BH*) of each cohort along the sampling date. The results for euphausiids and amphipods are shown in Fig. 20, and the results for cnidarians and chaetognaths are shown in Fig. 21.

For the euphausiid *E. pacifica*, individual carbon masses of small and large cohorts were 280–1,310 and 3,091–7,024 µg C ind.$^{-1}$, respectively. Significant growth was observed for both cohorts ($p < 0.05$), and the mean growth rate ($g$) was 0.033±0.041 day$^{-1}$. For *T. inspinata*, the individual carbon mass of the small and large cohorts was 0–3,928 and 22,662–30,074 µg C ind.$^{-1}$, respectively. Significant growth was observed for the large-sized cohort ($p < 0.05$), with a mean growth rate ($g$) of 0.022±0.021 day$^{-1}$.

For all amphipod species, no significant growth was detected for all cohorts throughout the study period. For *C. challengeri*, the individual mean carbon mass for each cohort was 40.7, 85.4, 171.6, 367.4, 754.1 and 1,274.2 µg C ind.$^{-1}$ (ordered from small to large body size). For *P. abyssalis*, the individual mean carbon mass for each cohort was 19.5, 47.6, 78.7 and 700.9 µg C ind.$^{-1}$. For *T. pacifica,* the individual mean carbon biomass for each cohort was 21.5, 64.8, 189.9 and 326.0 µg C ind.$^{-1}$.

For the cnidarian *A. digitale*, small- and large-sized cohorts were identified, and no significant growth changes were

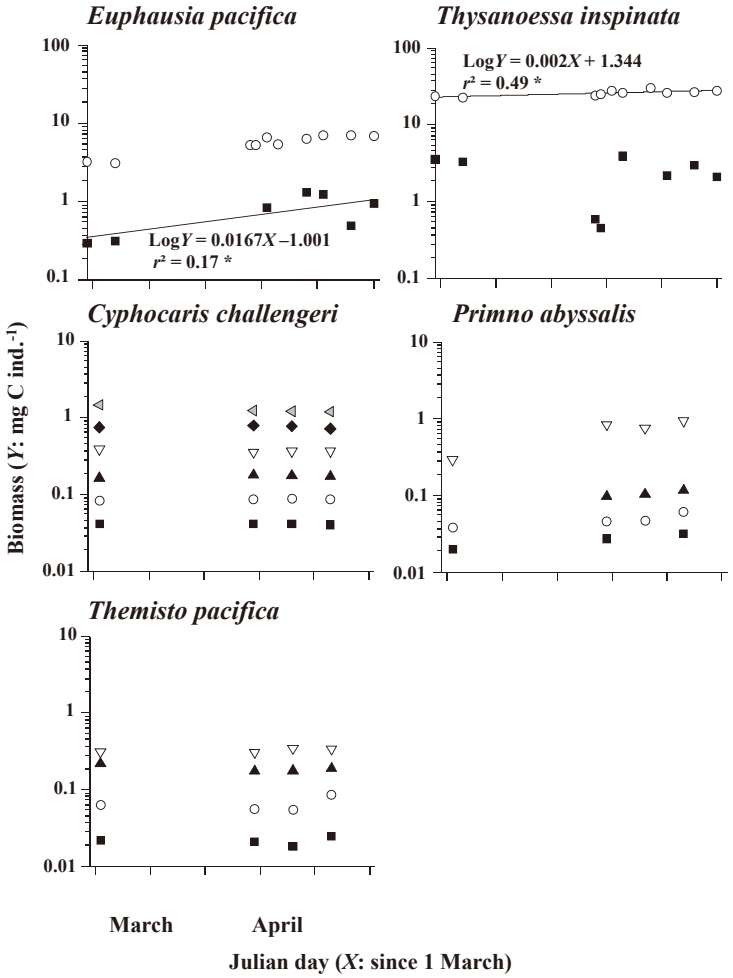


Fig. 20. Temporal changes in individual biomass of macrozooplanktonic *Euphausia pacifica*, *Thysanoessa inspinata*, *Cyphocaris challengeri*, *Primno abyssalis* and *Themisto pacifica* in the Oyashio region during spring in 2007. For cohorts showing significant growth with the date (slope is significantly differed from 0), regressions were calculated between biomass ($Y$) and Julian day ($X$). *: $p < 0.05$.

detected. The individual mean carbon mass of small- and large-sized cohorts was 47.6–134.2 and 200.5–381.6 μg C ind.$^{-1}$, respectively (Fig. 21).

For chaetognaths, the individual mean carbon mass of small- (Eh1), middle- (Eh2) and large-sized (Eh3) cohorts in *E. hamata* ranged from 16.3 to 48.0, 44.0 to 98.5 and 83.8 to 173.0 μg C ind.$^{-1}$, respectively. Significant growth was detected for all cohorts ($p < 0.05$), and the mean growth rate ($g$) of Eh1, Eh2 and Eh3 was 0.081±0.094 (Eh1), 0.100±0.095 (Eh2) and 0.041±0.059 (Eh3) day$^{-1}$, respectively (Fig. 21). The individual mean carbon mass of small-, middle- and large-sized cohorts of *P. elegans* ranged from 208 to 634, 577 to 1273 and 1,065 to 1,745 μg C ind.$^{-1}$, respectively. Significant growth was observed for middle- (Pe1) and large-sized (Pe2) cohorts ($p < 0.05$), and the mean growth rate ($g$) of Pe1 and Pe2 was 0.071±0.085 and 0.049±0.041 day$^{-1}$, respectively (Fig. 21). The growth rates for the body length were 0.039–0.050 mm day$^{-1}$ for *E. hamata* and 0.042–0.101 mm day$^{-1}$ for *P. elegans* (Table 4).

Throughout the OECOS period, significant growth in individual carbon mass was observed for the following taxa/species: copepods (*E. bungii*, *N. cristatus* and *N. plumchrus*), euphausiids (*E. pacifica* and *T. inspinata*) and chaetognaths (*E. hamata* and *P. elegans*). Inter- and intra-species (between cohort) differences were examined using one-way ANOVA, and the results revealed no significant differences in the growth rates for various zooplankton species and taxa during the OECOS period ($p = 0.99$, Table 5).

### 5-2. Discussion

In the present study, significant growth was observed for copepods (*E. bungii*, *N. cristatus* and *N. plumchrus*), euphausiids (*E. pacifica* and *T. inspinata*) and chaetognaths (*E. hamata* and *P. elegans*). Although various copepod species were examined in the present study (eleven species), only three species showed significant growth with time, partly reflecting the morphological characteristics of this taxon. Because copepods have six morphologically different cope-

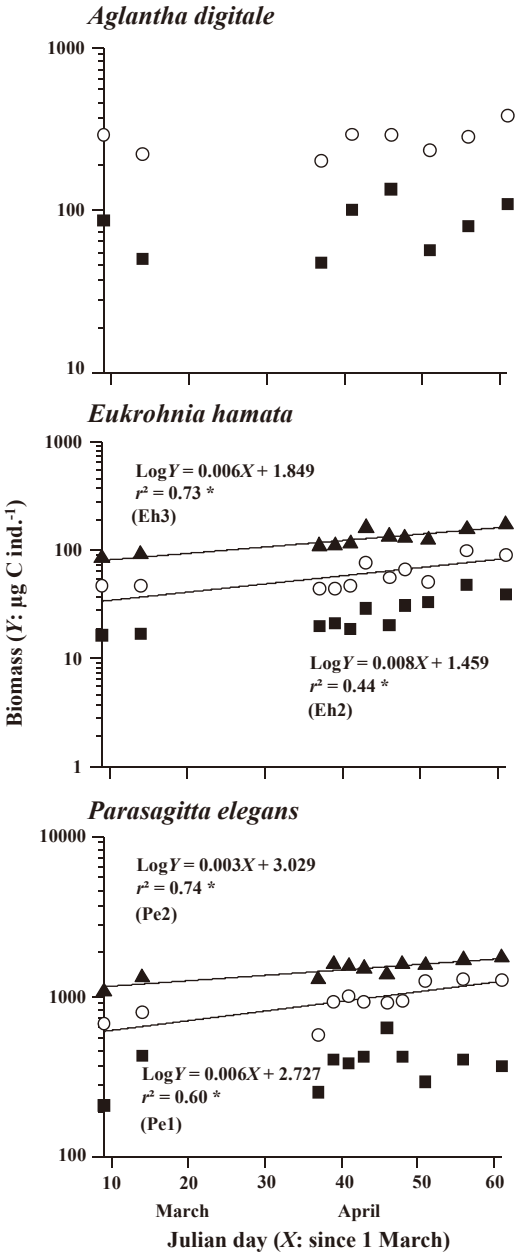


Fig. 21. Temporal changes in individual biomass of macrozooplanktonic *Aglantha digitale*, *Eukrohnia hamata* and *Parasagitta elegans* in the Oyashio region during spring 2007. For cohorts showing significant growth with the date (slope is significantly differed from 0), regressions were calculated between biomass ($Y$) and Julian day ($X$). *: $p < 0.05$.

podid stages, the population structure was divided into six categories. The low resolutions in population structure of copepods may prevent detailed cohort analysis of this taxon. However, fine-scaled body length divisions of macrozooplankton taxa were achieved, facilitating the separation of cohorts for macrozooplankton taxa (Figs. 11–14). These advantages in the population structure analysis (body length measurement) facilitated the detection of significant growth for two dominant macrozooplankton taxa (euphausiids and chaetognaths) in the present study.

### 5–2–1. Growth rate of copepods

Analyses based on the mean copepodid stage (MCS), the growth rates ($g$) of small (C1–C3 population) and large (C3–C5 population) cohorts of *E. bungii*, *N. cristatus* and *N. plumchrus* were 0.061±0.440, 0.029±0.074, 0.064±0.179 and 0.039±0.492 day$^{-1}$, respectively. The body size (copepodid stage), temperature and food (chl *a*) affect the growth rate ($g$) of copepods, which increases with increasing temperature, younger copepodid stages and increasing ambient chl. *a* concentration under laboratory conditions (Liu and Hopcroft, 2006a, 2006b). During the OECOS period, although the differences were insignificant, the growth rate of the small-sized cohort was higher than that of large-sized cohort within *E. bungii*.

During the OECOS period, Kobari et al. (2010c) estimated the stage duration and growth rates of the four dominant copepods (*E. bungii*, *N. cristatus*, *N. flemingeri* and *N. plumchrus*) using on-board rearing experiments. The growth rate of *E. bungii* C2 was 0.04 day$^{-1}$ based on laboratory rearing (Kobari et al., 2010c). This value was slightly lower than that of the small-sized cohort of *E. bungii* based on the cohort analysis evaluated in the present study (0.061 day$^{-1}$). From laboratory rearing, the growth rate of *N. cristatus* was 0.06 day$^{-1}$ (Kobari et al., 2010c). From natural cohort analysis, the $g$ of *N. cristatus* was 0.067 day$^{-1}$ in the Bering Sea shelf (Vidal and Smith, 1986). The estimated value obtained from the cohort analysis during the OECOS period (0.064 day$^{-1}$) was between these two values. Interestingly, within the same OECOS period, the $g$ derived from laboratory rearing (Kobari et al., 2010c) was slightly lower than that using the natural cohort method (the present study). Because of the presence of predators under natural conditions, the predation removal at late copepodid stages may reflect the dominance of early copepodid stages, characterized by a high $g$ (Liu and Hopcroft, 2006a, 2006b). To confirm these hypotheses in copepods, additional data accumulation on $g$ is required using both laboratory rearing and natural cohort methods in the future.

### 5–2–2. Growth rate of macrozooplankton

During the OECOS period, the mean growth rates ($g$) of large-sized cohorts of the euphausiids *E. pacifica* and *T. inspinata* were 0.033 and 0.022 day$^{-1}$, respectively (Fig. 20). For *E. pacifica*, the $g$ at the Oregon coast and Gulf of Alaska (at 5ºC) was 0.0089–0.0135 day$^{-1}$ and 0.0025 day$^{-1}$, respectively (Pinchuk and Hopcroft, 2007; Shaw et al., 2010). The $g$ of *E. pacifica* in the present study was higher than these values. For euphausiids, the $g$ showed an exponentially negative relationship with body mass under constant temperature and a positive relationship with temperature (Ross, 1982; Shaw et al., 2010). Because the mean body mass was higher for *T. inspinata* (Fig. 20), the $g$ of *T. inspinata* may be lower than that of *E. pacifica*. Concerning the horizontal distribu-

Table 4. Growth rates in the body length of *Eukrohnia hamata* and *Parasagitta elegans* from various oceans.

| Chaetognath species | Growth rate (μm day$^{-1}$) | Location | Habitat temperature (°C) and depth | References |
|---|---|---|---|---|
| *Eukrohnia hamata* | 6–20 | Site H, Western North Pacific | 2–17 | Nishiuchi, 1999 |
| | 15 | Site H, Western North Pacific | 2.3–2.9 (>250 m) | Matsumoto, 2008 |
| | 39–50 | St. A–5, Western North Pacific | 1–6 (0–200 m) | This study |
| | 83–100 | Station P, Eastern North Pacific | 3.8–6.0 (100–500 m) | Terazaki and Miller, 1986 |
| *Parasagitta elegans* | 14–44 | High–Arctic fjord, Svalbard | −1.7–4 | Grigor et al., 2014 |
| | 20–70 | Site H, Western North Pacific | 2–17 | Nishiuchi, 1999 |
| | 30–290 | Western North Pacific | 1.25–3.44 (100 m) | Kotori, 1999 |
| | 40–70 | North Sea | 6–17 | Saito and Kiørboe, 2001 |
| | 42–101 | St. A–5, Western North Pacific | 1–6 (0–200 m) | This study |
| | 69 | Conception Bay, Newfoundland | −1.0 | Choe and Deibel, 2000 |
| | 117–150 | Celtic Sea | 7.8–17.1 | Conway and Williams, 1986 |
| | 150 | Oslofjord, southern Norway | | Jakobsen, 1971 |
| | 167–200 | Station P, Eastern North Pacific | 6.0–13.8 (Surface) | Terazaki and Miller, 1986 |

Table 5. Results of one–way ANOVA for the mass–specific growth rate (*g*) of various zooplankton species (cf. Figs. 18–21) in the Oyashio region during March and April in 2007. For one–way ANOVA, the species were applied as independent variables. *df*: degree of freedom, *SS*: sum of squares.

| Parameter | *df* | *SS* | *F* | *p* |
|---|---|---|---|---|
| Species | 10 | 0.004 | 0.111 | 0.999 |
| Error | 70 | 2.750 | | |

tion of *g* in the Gulf of Alaska, a positive correlation with the chl. *a* concentration was observed for the *g* of *T. inermis* (a species having wax ester that mainly feeds on phytoplankton), while no correlation with chl. *a* was observed for *E. pacifica*, which has high *g* during the phytoplankton bloom period (Pinchuk and Hopcroft, 2007). In the present study, as the food concentration was high around the annual peak (spring phytoplankton bloom), the *g* is expected to be high around the bloom, which explains why the *g* value obtained in the present study is higher than the annual data in the eastern North Pacific (Shaw et al., 2010).

For chaetognaths, the growth rate of this taxon is commonly expressed by increases in body length rather than body mass. The specific growth rates of the chaetognath body length from various locations are summarized in Table 4. In the Oyashio region, the growth rate of the chaetognath *E. hamata* body length showed seasonal changes and was higher from the spring to the summer, and lower during the winter (Matsumoto, 2008). In the present study, the growth rates of each *E. hamata* cohort ranged from 39 to 50 μm day$^{-1}$. These values were higher than those obtained on an annual basis in the Oyashio region (6–20 μm day$^{-1}$, Nishiuchi, 1999; Matsumoto, 2008), but lower than the values in the eastern subarctic Pacific (83–100 μm day$^{-1}$, Terazaki and Miller, 1986).

A comparison on growth rates of two sympatric chaetognaths in the present study showed that the growth rate of *P. elegans* (42–101 μm day$^{-1}$) was faster than those of *E. hamata* (39–50 μm day$^{-1}$). In the eastern subarctic Pacific, the growth rate of mesopelagic *E. hamata* (83–100 μm day$^{-1}$) was slower than that of epipelagic *P. elegans* (167–200 μm day$^{-1}$) (Terazaki and Miller, 1986) (Table 4).

Because the vertical distribution of *E. hamata* is deeper than that of *P. elegans* (Ozawa et al., 2007), the temperature of *E. hamata* was lower than that of *P. elegans*. Within chaetognath species (*P. elegans*), the growth rate increases with increasing habitat temperature (Sameoto, 1971). In addition, the abundance and biomass of mesozooplankton and copepods, the major prey of chaetognaths, are high at the surface layer and exponentially decrease with increasing depth in the Oyashio region (Yamaguchi et al., 2002, 2004b). Based on the habitat temperature and food availability, the growth rates of mesopelagic chaetognaths were slower than those of epipelagic species.

## 6. Feeding Ecology, Biomass and Production

### 6–1. Results

In this chapter, because only scarce information is available, the feeding ecology of mesopelagic copepods was examined. For macrozooplankton, the feeding ecologies of two dominant taxa, euphausiids and chaetognaths, were evaluated.

### 6–1–1. Feeding ecology

Within mesopelagic copepods, the gut contents of the suspension feeders, C6F of *G. simplex*, *G. variabilis* and *P. scutullata*, are shown in Table 6. The results of the gut content analyses of suspension feeding copepods, diatoms (mainly *Thalassiosira* spp.), dinoflagellates, cyanophytes, foraminiferans, radiolarians and tintinnids are also shown. Similar results for all three species of protozooplankton (foraminiferans, radiolarians and tintinnids) were observed on March 8, prior to the spring phytoplankton bloom, but not on April 11

Table 6. Gut contents of mesopelagic suspension feeding copepods (*Gaetanus simplex*, *G. variabilis* and *Pleuromamma scutullata*) in the Oyashio region on March 8, and April 11 and 29, 2007. Gut contents were examined for C6F specimens collected from the most abundant depth layer at night. The numbers of examined specimen are shown in the parentheses. For each cell condition, three categories (intact [100%], fragment [50–100%] and broken [0–50%]) were scored. (R.S.): resting spore.

| | *Gaetanus simplex* | | | *Gaetanus variabilis* | | | *Pleuromamma scutullata* | | |
|---|---|---|---|---|---|---|---|---|---|
| | 8 Mar. | 11 Apr. | 29 Apr. | 8 Mar. | 11 Apr. | 29 Apr. | 8 Mar. | 11 Apr. | 29 Apr. |
| Species / taxa | (8) | (12) | (15) | (5) | (10) | (15) | (15) | (7) | (8) |
| Diatoms | | | | | | | | | |
| *Actinocyclus* spp. | 1 | | | | | | 1 | | |
| *Azpeitia tabularis* | 1 | | | | | | | | |
| *Coscinodiscus* spp. | 1 | | | | | | | | 1 |
| *Neodenticula seminae* | | 5 | | | | | | | 1 |
| *Odontella aurita* | | 1 | 2 | | | 3 | | 6 | 14 |
| *Thalassiosira* spp. | 15 | 22 | 20 | 5 | 4 | 30 | 4 | 5 | 56 |
| Unidentified pennate diatoms | | 1 | 1 | 2 | 1 | 2 | 1 | | 1 |
| *Chaetoceros furcellatus* (R.S.) | | 2 | 2 | | | 10 | | | 3 |
| Dinoflagellates | | | | | | | | | |
| *Ceratium fusus* | 1 | | | | | | | | |
| Unidentified dinoflagellates | | | | | | | | 1 | |
| Dinoflagellate cyst | | | 1 | | | | | | |
| Cyanophytes | 5 | 2 | | | | | | | |
| Foraminiferans | 9 | | | | | | 1 | | |
| Radiolarians | 2 | | | | | | | | |
| Tintinnids | | | | | | 2 | 1 | | |
| Intact (100%) | 10 | 16 | 16 | 3 | 1 | 8 | 4 | 4 | 52 |
| Fragment (50–100%) | 6 | 7 | 3 | | | 15 | 3 | 4 | 10 |
| Broken (0–50%) | 19 | 10 | 7 | 4 | 4 | 24 | 1 | 4 | 14 |

Table 7. Gut contents of mesopelagic carnivorous copepods (*Paraeuchaeta elongata* and *Heterorhabdus tanneri*) in the Oyashio region during spring 2007. Note that only amorphous materials for the other species and dates were observed, and these results were not included in this table. For comparison, although prey calanoid copepods observed only as mandible blade (*MB*), their prosome and total lengths (*PL* and *TL*) were calculated using the described equations (Dalpadado et al., 2008 for *MB–PL*, Yamaguchi unpublished for *PL–TL*).

| | Length (μm) | | |
|---|---|---|---|
| Species / taxa and stage | *MB* | *PL* | *TL* |
| *Paraeuchaeta elongata* C6F (29 April) | | | |
| *Metridia pacifica* C2 | 48 | 547 | 913 |
| Copepod nauplii | – | – | 118 |
| *Neocalanus cristatus* C1 or *Neocalanus plumchrus* C2 | 70 | 970 | 1,131 |
| | 72 | 1,008 | 1,176 |
| *Triconia borealis* C6M | – | 325 | 415 |
| *Heterorhabdus tanneri* C6F (29 April) | | | |
| *Metridia pacifica* C4 | 75 | 1,066 | 1,780 |

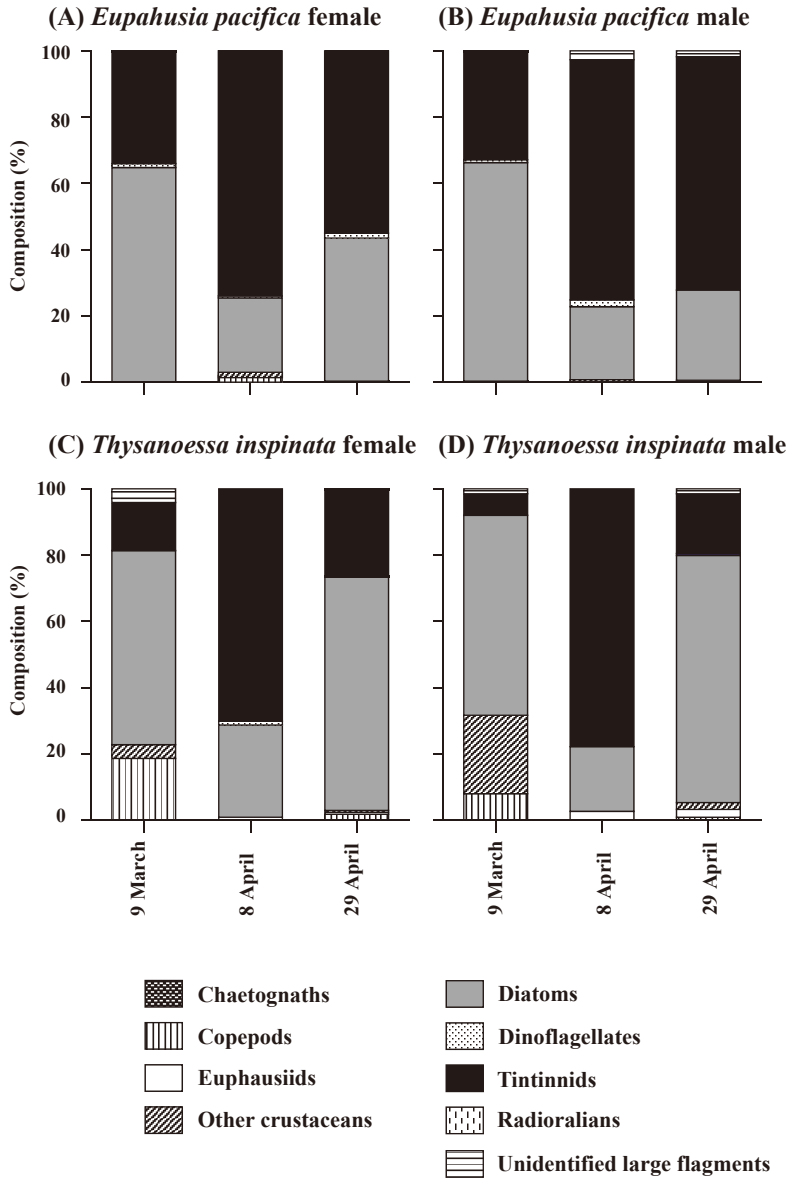


Fig. 22. Temporal changes in the gut content compositions regarding the number for euphausiids, *Euphausia pacifica* female (A), *E. pacifica* male (B), *Thysanoessa inspinata* female (C) and *T. inspinata* male (D), in the Oyashio region from March–April in 2007.

during the spring phytoplankton bloom. From all species, the resting spores of *Chaetoceros furcellatus* with intact cell conditions were observed on April 29. The cell conditions of the food items also varied with copepod species. The proportion of intact cells was highest for *P. scutullata* (33–68%), followed by *G. simplex* (29–62%), and the least proportion of intact cells was for *G. variabilis* (17–43%). The proportion of broken (0–50%) cell showed the opposite pattern: the proportion was lowest in *P. scutullata* (13–33%), higher in *G. simplex* (27–54%), and highest in *G. variabilis* (51–80%).

For carnivorous mesopelagic copepods, most of the gut contents were amorphous materials, and species identification from these materials was possible only for *P. elongata* and *H. tanneri* on April 29, 2007 (Table 7). As for the prey items of *P. elongata* C6F, early copepodid stages (C1–C2) of dominant epipelagic copepods (*M. pacifica* and *Neocalanus* spp.), nauplii and poecilostomatoid copepods were also observed. From the gut contents of *H. tanneri* C6F, the mandible blade of *M. pacifica* C4 was observed. Notably, the total length (*TL*) of the prey organisms was smaller in *P. elongata* C6F (118–1,131 μm) than in *H. tanneri* C6F (1,780 μm) (Table 7).

The gut contents of two euphausiid species (*E. pacifica* and *T. inspinata*) on March 9, April 8, and April 29 are shown in Fig. 22. Within the food items, the dominant taxa of *E. pacifica* were diatoms on March 9 and tintinnids on April 8 and 29 (Fig. 22A, B). Numerically, diatoms were dominant in *Chaetoceros* spp. and *Thalassiosira* spp., tintinnids were

Table 8. Composition of the number of food items (%) observed in the stomachs of euphausiids (*Euphausia pacifica* and *Thysanoessa inspinata*) in the Oyashio region at each sampling date from March–April in 2007. For each date, the guts of 15 specimens were examined for each female and male.

| | *Euphausia pacifica* | | | | | | *Thysanoessa inspinata* | | | | | |
|---|---|---|---|---|---|---|---|---|---|---|---|---|
| | Female | | | Male | | | Female | | | Male | | |
| | 9 Mar. | 8 Apr. | 29 Apr. | 9 Mar. | 8 Apr. | 29 Apr. | 9 Mar. | 8 Apr. | 29 Apr. | 9 Mar. | 8 Apr. | 29 Apr. |
| Food item (%) | | | | | | | | | | | | |
| Chaetognaths | – | – | – | – | – | – | – | – | 0.1 | – | – | – |
| Copepods | | | | | | | | | | | | |
| *Metridia* spp. | – | – | – | 0.1 | – | – | – | – | – | – | – | – |
| *Neocalanus* spp. | – | – | – | – | – | – | 2.1 | – | – | – | – | 0.5 |
| *Oithona* spp. | – | – | – | 0.1 | – | – | – | – | 0.1 | – | – | 0.5 |
| Unidentified copepods | – | 0.6 | 0.3 | 0.1 | – | 0.6 | 10.4 | – | 0.5 | 1.6 | – | – |
| fragments | – | 0.6 | 0.3 | – | – | 0.6 | 6.3 | – | 1.0 | 6.3 | – | – |
| Euphausiids | | | | | | | | | | | | |
| Unidentified euphausiids | – | – | – | 0.0 | – | – | – | 1.0 | 0.6 | – | 2.8 | 2.5 |
| Other crustacean fragments | – | 1.2 | 0.3 | 0.0 | 0.9 | – | 4.2 | – | 0.6 | 23.8 | – | 2.0 |
| Unidentified nauplii | – | – | – | 0.0 | – | – | – | 1.0 | – | – | – | – |
| Diatoms | | | | | | | | | | | | |
| *Actinoptychus* spp. | 0.1 | – | – | 0.0 | – | – | – | – | – | – | – | 2.5 |
| *Chaetoceros* spp. | 4.1 | 0.3 | 0.3 | 4.3 | – | 1.2 | – | – | 0.2 | 9.5 | – | 1.5 |
| *Coscinodiscus* spp. | 0.2 | – | – | 0.1 | – | – | – | 1.0 | 3.1 | – | – | – |
| *Odontella aurita* | – | 0.9 | 0.3 | 0.0 | 1.8 | 1.2 | – | 14.3 | 2.4 | – | – | – |
| *Thalasiossira* spp. | 3.9 | 20.9 | 37.7 | 3.1 | 18.2 | 22.9 | – | 6.7 | 46.2 | – | 11.1 | – |
| *Paralia sulcata* | 4.3 | – | – | 0.6 | – | – | 2.1 | – | – | 4.8 | – | 12.7 |
| *Rhizosolenia* spp. | 0.2 | – | – | 0.2 | – | – | – | – | – | – | – | – |
| *Skeletonema* spp. | – | – | – | 0.0 | – | – | – | – | 0.4 | – | – | – |
| Pennate diatoms | 0.4 | 0.3 | – | 0.1 | – | – | 6.3 | – | – | 1.6 | – | 2.0 |
| Unidentified diatom fragments | 51.3 | 2.1 | 4.6 | 57.7 | 2.7 | 1.8 | 50.0 | 5.7 | 18.3 | 44.4 | 8.3 | 55.9 |
| Dinoflagellates | | | | | | | | | | | | |
| *Ceratium* spp. | 0.3 | – | – | 0.0 | – | – | – | – | – | – | – | – |
| *Dinophysis parvula* | 0.3 | – | – | 0.0 | – | – | – | – | – | – | – | – |
| *Dinophysis rotundata* | – | – | – | 0.6 | – | – | – | – | – | – | – | – |
| *Protoperidinium* spp. | 0.3 | – | – | 0.1 | – | – | – | – | – | – | – | – |
| Unidentified dinoflagellate fragments | 0.4 | 0.6 | 1.4 | 0.1 | 1.8 | – | – | 1.0 | 0.1 | – | – | 0.5 |
| Tintinnids | | | | | | | | | | | | |
| *Acanthostomella norvegica* | 4.8 | 25.7 | 8.3 | 3.8 | 11.8 | 12.9 | 2.1 | 8.6 | 2.3 | 3.2 | 27.8 | 1.0 |
| *Amplectella* sp. | – | – | – | 0.0 | – | – | – | 4.8 | – | – | – | – |
| *Ascampbelliella protuberans* | – | – | – | 0.0 | – | – | – | 1.0 | – | – | – | – |
| *Codonellopsis frigida* | 1.2 | 2.4 | 2.3 | 0.7 | 1.8 | 1.8 | – | 1.0 | 0.9 | – | – | 2.0 |
| *Leprotintinnus pellucidus* | – | – | – | 0.0 | – | – | – | 1.0 | – | – | – | – |
| *Parafavella denticulata* | 0.6 | 1.5 | 2.3 | 0.3 | 2.7 | 15.9 | – | 7.6 | 1.0 | – | – | 0.5 |
| *Parafavella joergensenii* | 3.9 | – | – | 4.1 | – | – | 2.1 | 5.7 | 1.6 | – | – | 1.5 |
| *Parafavella ventricosa* | – | – | – | 0.0 | – | – | – | 2.9 | 0.5 | – | – | 0.5 |
| *Parafavella* spp. | 6.4 | 6.9 | 10.0 | 6.4 | 9.1 | 11.2 | 4.2 | 16.2 | 11.0 | 1.6 | 8.3 | 6.4 |
| *Ptychocylis obtusa* | 16.8 | 36.1 | 32.0 | 17.5 | 46.4 | 28.2 | 6.3 | 21.0 | 8.7 | 1.6 | 41.7 | 6.4 |
| Radioralians | 0.2 | – | – | 0.2 | – | – | – | – | – | – | – | – |
| Unidentified large fragments | – | – | – | 0.0 | 2.7 | 1.8 | 4.2 | – | 0.4 | 1.6 | – | 1.5 |
| Total food items (*n*) | 893 | 335 | 350 | 1,033 | 110 | 170 | 48 | 105 | 931 | 63 | 36 | 204 |

dominant in *Ptychocylis obtusa* throughout the study period (Table 8). For *T. inspinata,* diatoms were the dominant food items on March 9 and April 29, while tintinnids were the dominant food on April 8 (Fig. 22C, D). No sexual differences in the food items were detected for both species. As for special characteristics of food items of *T. inspinata*, the proportion of copepods in all food items was high: 13.9% (mature female) and 2.3% (mature male) on March 9. Because these proportions were based on number, when evaluating the proportions in mass, the importance of crustaceans might be more evident. Copepods (*Metridia* spp., *Neocalanus* spp. and *Oithona* spp.), chaetognaths and euphausiids were observed in the gut contents of *T. inspinata* (Table 8), and *T. inspinata* fed on larger-sized food items compared with those of *E. pacifica.* For the copepod prey of *E. pacifica*, only small-sized *Metridia* spp. and *Oithona* spp. showed

Table 9. Composition of the number of food items (%) observed in the gut of chaetognaths (*Eukrohnia hamata*, *Parasagitta elegans* and *Pseudosagitta scrippsae*) in the Oyashio region from March–April in 2007. NPC: number of prey per chaetognath.

| | *E. hamata* | *P. elegans* | *P. scrippsae* |
|---|---|---|---|
| Food item (%) | | | |
| Copepods | | | |
| *Eucalanus bungii* | – | 12.5 | – |
| *Eucalanus bungii* C2 | – | – | 2.1 |
| *Eucalanus bungii* C3 | – | – | 2.1 |
| *Eucalanus bungii* C5F | – | 1.1 | 4.2 |
| *Eucalanus bungii* C6F | – | 10.2 | 2.1 |
| *Neocalanus cristatus* | – | 1.1 | – |
| *Neocalanus cristatus* C4 | – | 2.3 | – |
| *Neocalanus* sp. | – | 1.1 | – |
| *Metridia pacifica* | – | – | 6.3 |
| *Metridia pacifica* C5F | – | – | 6.3 |
| *Metridia pacifica* C6F | – | – | 12.5 |
| *Pleuromamma scutullata* C6F | – | – | 2.1 |
| *Pseudocalanus* sp. | – | – | 2.1 |
| Unidentified copepods | 26.7 | 50.0 | 16.7 |
| Chaetognaths | | | |
| *Eukrohnia hamata* | 6.7 | – | 8.3 |
| *Parasagitta elegans* | – | – | 4.2 |
| Appendicularians | 6.7 | – | – |
| Unidentified organisms | 60.0 | 21.6 | 31.3 |
| Number of individual food containing (*n*) | 15 | 88 | 48 |
| Number of total individual examined (*n*) | 1,938 | 1,301 | 143 |
| Grand mean of NPC | 0.008 | 0.068 | 0.336 |

small compositions.

The gut contents of three chaetognaths (*E. hamata*, *P. elegans* and *P. scrippsae*) are shown in Table 9. The most numerous food items of *P. elegans* were copepods (78.4%) (Table 9). Within the food items of *P. elegans*, the copepod *E. bungii* composed 23.8%, followed by *Neocalanus* spp. (4.5%). The food items of *P. scrippsae* also primarily comprised copepods (56.5%), while the prey copepod species varied with those in *P. elegans*. Thus, within the food items of *P. scrippsae*, *Metridia* spp. was the most dominant (25.1%), followed by *E. bungii* (10.5%). Because *E. hamata* predominantly comprised smaller *BL* specimens, amorphous items were dominant (60.0%) in these food items. Throughout the study period, the total mean number of food items per chaetognath (NPC) was 0.008 prey ind.$^{-1}$ in *E. hamata*, 0.068 prey ind.$^{-1}$ in *P. elegans*, and 0.336 prey ind.$^{-1}$ in *P. scrippsae*.

**6–1–2. Biomass and production**

The monthly mean biomass of epi- and mesopelagic copepods and macrozooplankton species in March (prior to the spring phytoplankton bloom) and April (phytoplankton bloom period) are shown in Fig. 23. The biomass of whole net zooplankton community was 2,692 mg C m$^{-2}$ in March. Within the species examined in the present study, the highest biomass (1,131 mg C m$^{-2}$) was recorded for *M. pacifica* in March, corresponding to 46% of all net zooplankton biomasses (Fig. 23). Following *M. pacifica*, *N. cristatus* and *E. bungii* were also abundant, accounting for 354 mg C m$^{-2}$ (12%) and 312 mg C m$^{-2}$ (11%), respectively in March. However, the composition of mesopelagic copepods and macrozooplankton in the total zooplankton biomass was low in March.

In April, the total zooplankton biomass slightly increased to 3,807 mg C m$^{-2}$, which was 30% higher than in March (Fig. 23). The dominant species in April greatly varied with those in March. The biomass of *M. pacifica* decreased to 337 mg C m$^{-2}$ (one-fourth of that in March), and the biomass of epipelagic copepod *N. cristatus*, mesopelagic copepods *P. elongata* and *P. birostrata* and macrozooplanktonic euphausiid *E. pacifica* and *T. inspinata* and chaetognath *P. elegans* increased. Among these species, the biomass of *E. pacifica* was 896 mg C m$^{-2}$ (= 4.6 times higher than in March), composing the highest proportion (24%) of the total zooplankton biomass in April (Fig. 23).

Production showed a similar species-composition pattern

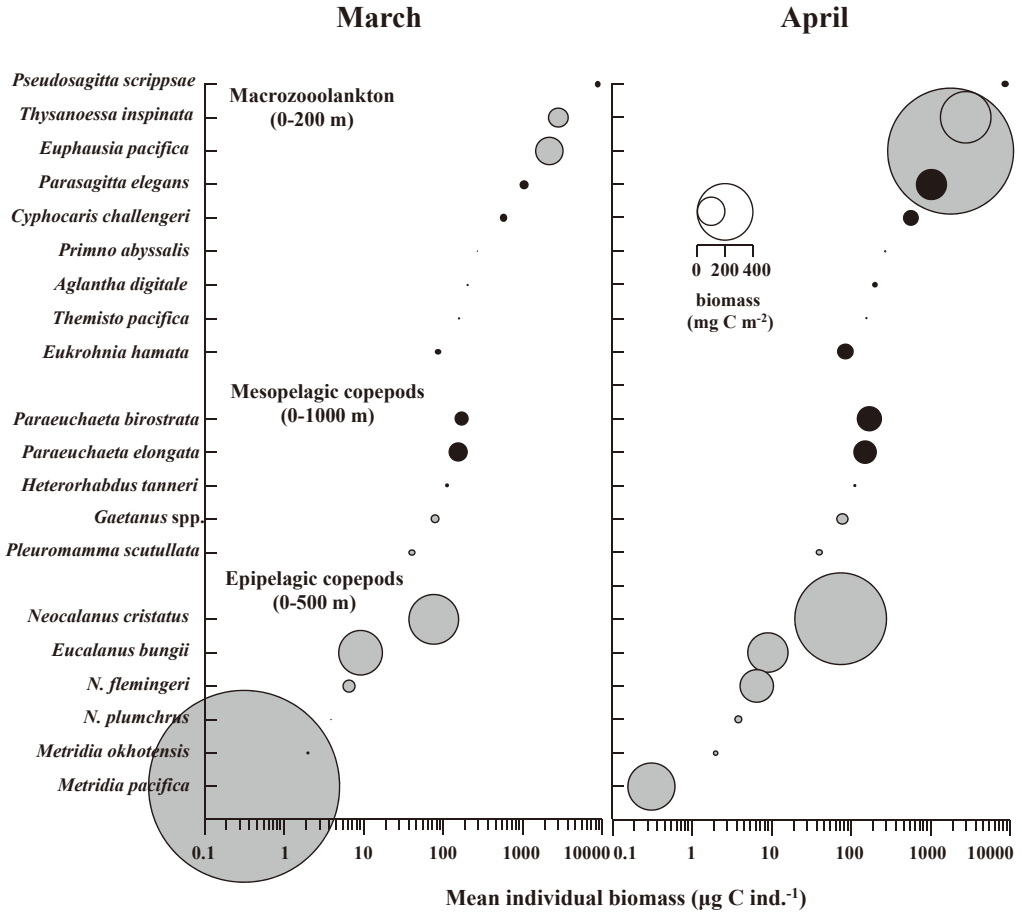


Fig. 23. Monthly mean biomass of various meso- / macrozooplankton species in the Oyashio region during March (before bloom) and April (after bloom) 2007. The sizes of the circles are the mean biomasses (mg C $m^{-2}$) of each species in each month. Grey and black circles indicate suspension feeders (grey) or carnivores (black), respectively. Species were arranged in the order of the mean individual biomass (cf. Figs. 18–21) within each functional group (epipelagic, mesopelagic copepods and macrozooplankton). Note that the quantified depth ranges varied with groups.

with that in biomass, but compositions of carnivores were less (Fig. 24). The total zooplankton production was 42.3 mg C $m^{-2}$ $day^{-1}$ in March, comprising 48% (20.5 mg C $m^{-2}$ $day^{-1}$) *M. pacifica.* Following *M. pacifica*, *N. cristatus* and *E. bungii* produced 5.1 and 4.5 mg C $m^{-2}$ $day^{-1}$, respectively, accounting for 12.0% and 10.6% of the total production, respectively. The total zooplankton production in April was 43.3 mg C $m^{-2}$ $day^{-1}$, with similar values in March. In addition, the species composition significantly varied, and the composition of *M. pacifica* decreased 12.3% in April. However, the compositions of the two dominant euphausiids increased, accounting for 25.0% of the total zooplankton production for *E. pacifica* and 10.3% for *T. inspinata*.

## 6–2. Discussion

### 6–2–1. Feeding ecology

Concerning the feeding ecology of mesopelagic suspension feeding copepods, the protozooplankton in the gut contents in March might reflect the relatively small sinking flux of phytoplankton to deeper layers before the initiation of the spring phytoplankton bloom. However, the occurrence of resting diatom spores on April 29 might reflect changes in food items, which respond quickly to the changes in sinking particles from the surface layer. The species-specific differences in cell conditions regarding food items might reflect the species-specific vertical distribution of each species. Thus, the distribution depths were in the order of *P. scutullata* < *G. simplex* < *G. variabilis* (Abe et al., 2012), consistent with the proportion of intact cells detected in their guts, i.e., highest for shallower living *P. scutullata* (33–68%), followed by the intermediate-depth inhabiting *G. simplex* (29–62%) and smallest for the deep inhabiting *G. variabilis* (17–43%) (Table 6). The results of the gut content analysis revealed that the taxonomic accounts of food items were similar for mesopelagic suspension feeding copepods; however, increases in the proportion of broken cells with increasing depths might reflect the coprophagy and repacking of suspension feeding copepods in overlaying layers (Sasaki et al., 1988; Yamaguchi et al., 2002).

For mesopelagic suspension feeding copepods, the food

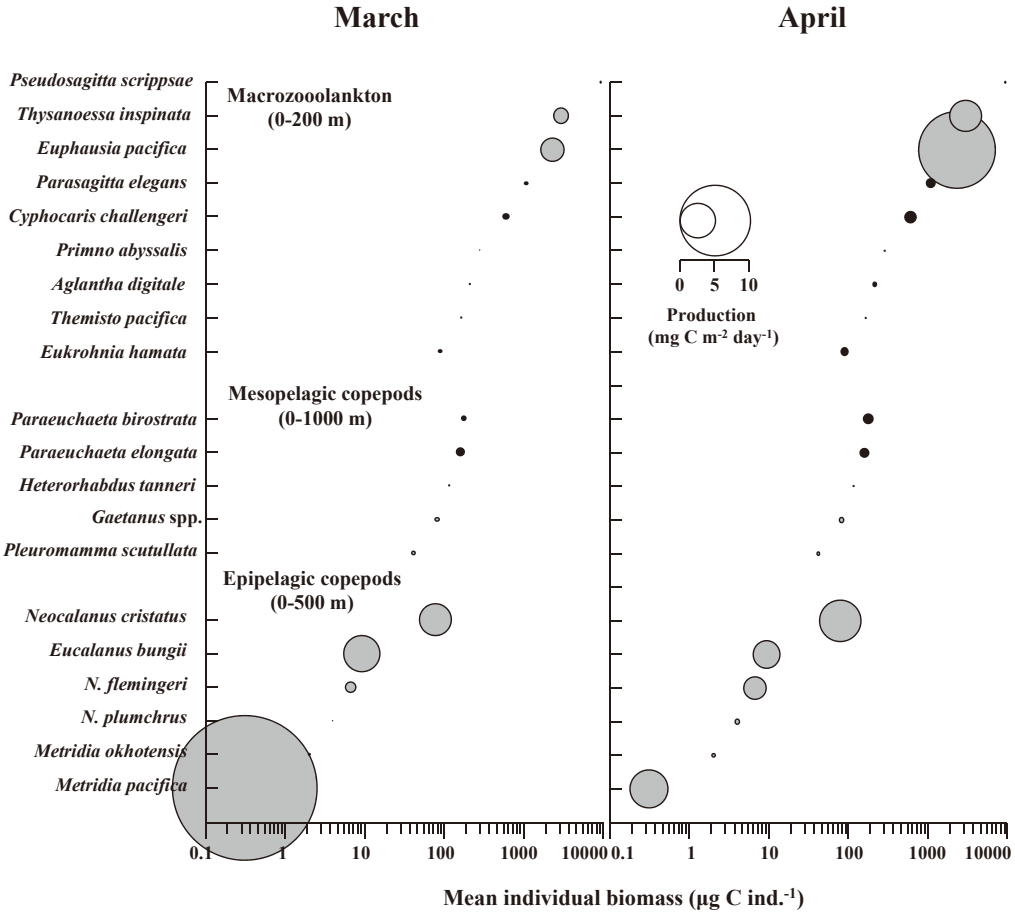


Fig. 24. Monthly mean production of various meso- / macrozooplankton species in the Oyashio region during March (before bloom) and April (after bloom) 2007. The sizes of the circles are the mean production (mg C $m^{-2}$ $day^{-1}$) of each species in each month. Grey and black circles indicate suspension feeders (grey) or carnivores (black), respectively. Species were arranged in the order of the mean individual biomass (cf. Figs. 18–21) within the each functional group (epipelagic, mesopelagic copepods and macrozooplankton). Note that the quantified depth ranges varied with groups.

requirements were estimated from empirical metabolic models calculated based on habitant temperature and body mass (for detailed method, see Yamaguchi et al., 2010b). Thus, the estimated ingestion rate of mesopelagic suspension feeding copepods (20.6 mg C $m^{-2}$ $day^{-1}$) was lower than the carbon mass flux at a depth of 500 m (approximately 100 mg C $m^{-2}$ $day^{-1}$ estimated from primary production), accounting for approximately 20% of the available particle carbon mass flux per depth (Abe et al., 2012). These findings suggest that mesopelagic suspension feeding copepods could obtain a sufficient amount of food at 500 m in April without any DVM. Thus, the ceased DVM observed for mesopelagic suspension feeding copepods after mid-April (Fig. 17A) might reflect increasing food availability at lower depths, resulting from the initiation of the spring phytoplankton bloom in early April (Fig. 6A).

For carnivorous copepods, the size of the prey animal is associated with the body size of the predator. According Hansen et al. (1994), the mean ratio in body size between predator: prey is 18:1, ranging from 10:1 to 30:1. Based on these ratios, the sizes of the prey items of C6F of *P. elongata* (*PL*: 4.95 mm, Yamaguchi and Ikeda, 2002b) and *H. tanneri* (*PL*: 2.92 mm, Yamaguchi and Ikeda, 2000b) were 165–495 and 97–292 µm, respectively. These values roughly correspond to the observed values for *P. elongata* (118–1,176 µm), while the food item size of *H. tanneri* (1,780 µm) is 6–19 times (=1,780 / 92 or 1,780 / 292) larger than the predicted prey animal sizes (Table 7). The anomalous large food item of *H. tanneri* might be associated with its specialized feeding modes (injecting venom or anaesthetic into the prey) (Nishida and Ohtsuka, 1996). The mandible blade of *Heterorhabdus* spp. has evolved to inject venom or anaesthetic into prey (Nishida and Ohtsuka, 1996); thus, the feeding mode and prey animals of Heterorhabdidae were significantly different from those of Euchaetidae. The inter-moult growth of Heterorhabdidae is higher than 900% in body mass (Yamaguchi and Ikeda, 2000b). However, the inter-molt growth of sympatric carnivorous Euchaetidae is approximately 400% in

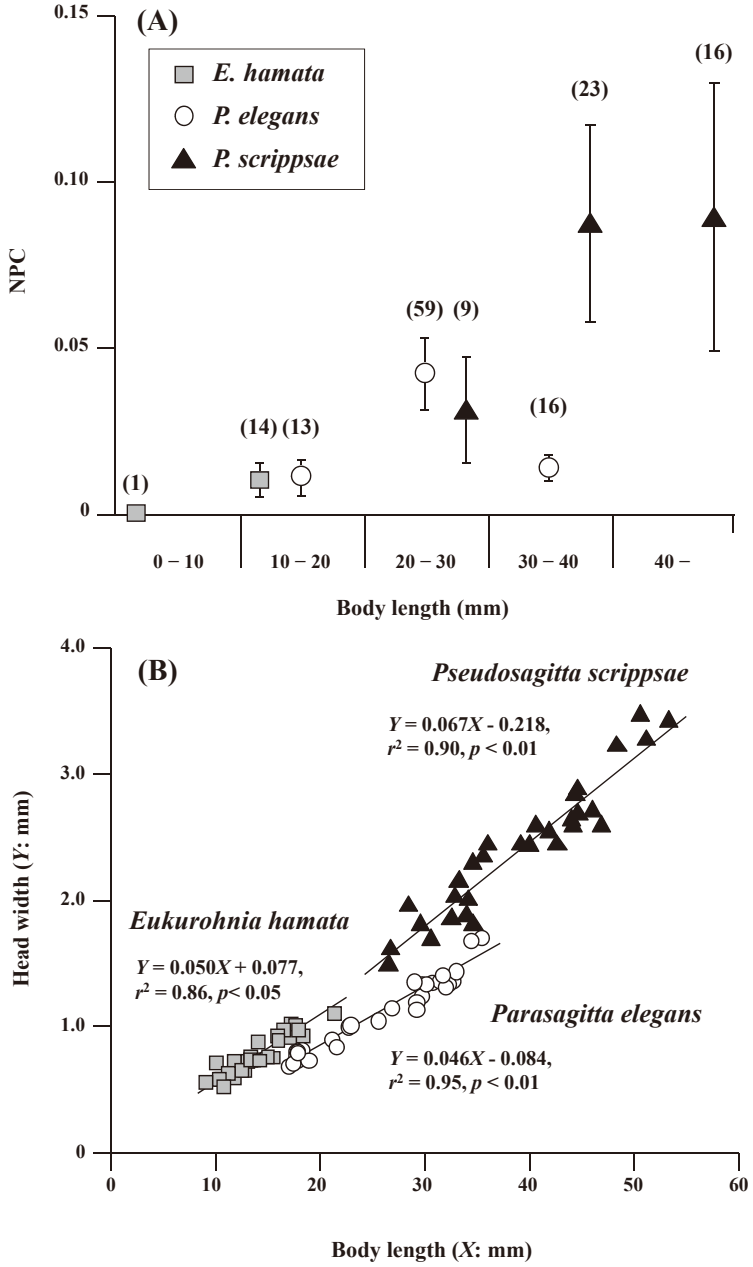


Fig. 25. Mean (symbols) and standard deviation (bars) of NPC presented with each 10 mm body length class of three chaetognaths in the Oyashio region during March–April 2007 (A). Relationship between the head width and body length of three chaetognaths in the Oyashio region during March–April 2007 (B). For (A), the numbers in the parentheses indicate the sample sizes. For (B), regressions are shown with species.

body mass (Yamaguchi and Ikeda, 2002b). These findings suggest that the specialized feeding mode of Heterorhabdidae may enable the capture of large-sized prey and also contribute to the increased inter-molt growth of this family (Yamaguchi and Ikeda, 2000b).

Based on the results of the gut content analyses, euphausiids were also found to feed on various zooplankton taxa, even during the spring phytoplankton boom (Table 8). For food items of *E. pacifica* from Sanriku, Nakagawa et al. (2001, 2002) reported that diatoms were dominant, while heterotrophs, particularly copepods, were important regarding carbon mass. In the present study, the compositions of the copepods in food items were low (0–1.0% for *E. pacifica*, 0–15.5% for *T. inspinata*, Table 8, Fig. 22); however, based on mass, the compositions increased, reflecting the large body size of copepods. The intensity of the carnivores varied with species and occurrence of large-sized zooplankton in the gut of *T. inspinata* (Table 8, Fig. 22). These results might reflect the larger body sizes of *T. inspinata* compared with those of *E. pacifica* (Fig. 20) and their predatory morphology, that is, the second thoracic legs of *T. inspinata*, were extremely elongated and developed. Because the major food items of *T.*

*inspinata* showed increased temporal changes (Fig. 22), they may have flexibility in feeding, that is, they may feed on large-sized crustaceans, such as copepods, before the bloom and shift to numerous diatoms and tintinnids after the bloom.

For chaetognaths, the mean NPC (no. prey ind.$^{-1}$) was highest for *P. scrippsae* (0.336), followed by *P. elegans* (0.068) and *E. hamata* (0.008) (Table 9). Because these NPC values reflect species differences in *BL*, to obtain accurate species comparisons, standardization of NPC values based on *BL* is needed. Comparison of the NPC, standardized using a 10-mm *BL* interval, showed that the NPC increased with increasing *BL*, except for the 30-40 mm *BL* of *P. elegans* (Fig. 25A). Highly significant correlations were observed between the *BL* and head width (*HW*) for all chaetognath species ($p < 0.05$, Fig. 25B). These findings suggest that wider body-sized organisms are available as food for larger *BL* chaetognath specimens. Increases in the composition of large-sized food items with increasing *BL* have been reported for *P. elegans* in the Gulf of Alaska and North Sea (Brodeur and Terazaki, 1999; Saito and Kiørboe, 2001). The highest NPC of *P. scrippsae* observed in the present study (Table 9) might be associated with the largest *BL* of this species. The large *BL* of *P. scrippsae* might have enabled the ingestion of a wide-size range of prey during the study period. Notably, the gut passage-time of the large *BL P. scrippsae* was longer than that for other species and thus might increase the NPC of this species.

As remarkable characteristics of food items, the most important food organisms (25.1%) of *P. scrippsae* were the copepods *Metridia* spp. (Table 9). However, for the sympatric chaetognath species, no *M. pacifica* was observed in the food items of the smaller body-sized *E. hamata* (*BL*: 5.8 - 23.7 mm) and *P. elegans* (11.0 - 41.3 mm) (Table 9). The swimming behaviour of *Metridia* spp. is continuously cruising, and its swimming speed is 2.3-5.4 mm sec.$^{-1}$ (Wong, 1988). *Metridia* spp. performs strong DVM (Takahashi et al., 2009; Yamaguchi et al., 2010b), and the speed of the DVM behaviour is 6.4-9.2 mm sec.$^{-1}$ (Hattori, 1989). While the swimming speed is faster for *Metridia* spp., the large body sized of *P. scrippsae* (*BL*: 12.0 - 55.0 mm) might enable feeding on *Metridia* spp.

**6-2-2. Biomass and Production**

For the biomass composition of species, the highest biomass was observed for the small-sized copepod of *M. pacifica* in March (46%, Fig. 23). These findings suggest that the abundance of *M. pacifica* was extremely high (Fig. 9B) prior to the initiation of the spring phytoplankton bloom in the Oyashio region. The composition of C6F was high for *M. pacifica* in March (Fig. 9B), and the dominance of large-sized C6F in the population might also reflect the high biomass observed in March. In April, the abundance of *M. pacifica* remained at the same level as that in March and the population primarily comprised small-sized early copepodid stages (Fig. 9B); thus, the overall biomass decreased in April (Fig. 23).

Most species, that showed increased biomass from March to April (i.e., the epipelagic copepod *N. cristatus*, mesopelagic copepods *P. elongata* and *P. birostrata*, euphausiids *E. pacifica* and *T. inspinata* and chaetognath *P. elegans*), exhibited significant growth during the OECOS period (Figs. 18-21), suggesting that the increases in biomass might reflect increases in growth, but not increases in reproductive activities.

Notably, increases in the zooplankton biomass from March to April in the Oyashio region were not explained only by internal growth. Particularly in April, various macrozooplankton species had high abundance and biomass (Figs. 11-14). These results reflected the dominance of each species in COW, which was not observed in March (Table 3). Thus, the total zooplankton biomass in the Oyashio region was similar between March and April, while the species composition significantly varied, i.e., the copepod *M. pacifica* was dominant in March and the euphausiid *E. pacifica* was dominant in April (Fig. 23). Because ecological information on euphausiids is limited and there is even less information for copepods, additional information is required for future studies.

Production estimation in the present study was achieved using physiological metabolic methods based on empirical models (Ikeda and Motoda, 1978). The metabolic rates were estimated according to Ikeda (2014), applying four independent variables (body mass, temperature, distribution depth and taxa), while previous formulae applied only two independent variables (only body mass and temperature) (Ikeda, 1985; Ikeda et al., 2001). Although applying four independent variables in the new calculation resulted in a high biomass for mesopelagic copepods in April (Fig. 23), production in this species was estimated to be lower, reflecting deeper distribution depths (Fig. 24). For chaetognaths, although a high biomass was recorded in April (Fig. 23), lower production might reflect an independent variable (taxa) (Fig. 24). Thus, the estimation of a more accurate metabolic rate on zooplankton might be achieved using a Global-Bathymetric Model (Ikeda, 2014), adding two independent variables (depth and taxa) to the formula.

For parameters governing zooplankton production, the estimation methods for metabolic rates have advanced over the past four decades. To estimate the feeding rates (food requirements) from the metabolic rates, two parameters, gross growth efficiency ($K_1$= production / feeding) and assimilation efficiency (*A%*= assimilation / feeding), are needed. While the estimation of both parameters by laboratory experiments is difficult, the assimilation efficiency could be estimated using the ratio method (Conover, 1966a, 1966b) based on measurements of the organic matter contents in food and faecal pellets. In the Oyashio region, the assimilation efficiency

of the two dominant copepods (*Neocalanus* spp. and *E. bungii*) ranged from 34 to 66%, with phytoplankton as food and showed a significantly negative relationship with the ash content of the phytoplankton ($r^2$ = 0.79 – 0.87, $p < 0.001$, Abe et al., 2013). Because the phytoplankton species composition temporally varied during the spring phytoplankton bloom (Fig. 6B), a changing effect on the assimilation efficiency might have occurred during the OECOS period. In future studies, the development of a convenient method for the estimation of the gross growth efficiency ($K_1$) is also needed to accurately estimate zooplankton production.

## 7. Synthesis

In this chapter, the responses of each zooplankton species on the spring phytoplankton bloom in the Oyashio region are described. For epipelagic copepods for which data sets are available for other oceanic locations (North Atlantic and North Pacific), the responses to phytoplankton blooms are compared between locations. Moreover, I further discuss the issues highlighted and remaining points in the present study and propose directions for future studies.

### 7–1. Responses of zooplankton on a phytoplankton bloom during OECOS period

Temporal changes in chl *a* and microzooplankton biomass and the responses of each zooplankton species during the OECOS period are summarized in Fig. 26.

Concerning hydrography, three water masses (COW, MKW and OYW) were exchanged in the short-term during the spring phytoplankton bloom. Because of the intrusions of COW, sufficient nutrients originated from the Sea of Okhotsk, and phytoplankton peaked on April 7–8 and 23. Microzooplankton showed peaks one day after chl *a* peaks, and the biomasses paralleled the temporal changes in chl *a* (Fig. 26).

For the zooplankton population structure, the development of the copepod *N. cristatus* from C1 to C4 and the growth of two euphausiids (*E. pacifica* and *T. inspinata*) and two chaetognaths (*E. hamata* and *P. elegans*) are shown (Figs. 18–21). The mass-specific growth rate (*g*) showed no significant differences between species (Table 5). These results suggest that there were no food limitations for various feeding modes of zooplankton during the spring phytoplankton bloom period.

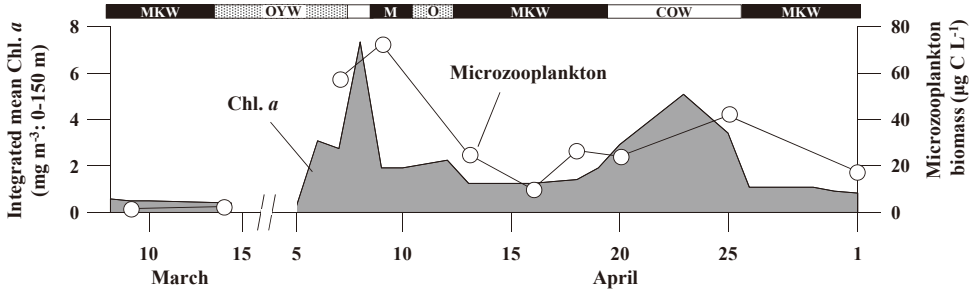


- **Population structure**
  - Constant growth: *Neocalanus cristatus* (C1-C4), *Euphausia pacifica*, *Thysanoessa inspinata*, *Eukrohnia hamata* (Cohort 1-3), *Parasagitta elegans* (Cohort 1-2)
  - Weight-specific growth rate (*g*) were similar for these species
- **Vertical distribution**
  - Arousal from resting: *Eucalanus bungii* (5 April)
  - Cease DVM: *Metridia pacifica* except C6F (after 23 April), *Pleuromamma scutullata* (after 11 April)
  - Continuous DVM: *Paraeuchaeta elongata* (C4-C6F)
- **Reproduction**
  - Epipelagic copepod: *Eucalanus bungii* (after 10 April)
  - Mesopelagic copepods: *Gaetanus* spp., *P. scutullata* and *Paraeuchaeta* spp. (activate after mid-April)
  - Euphausiids: *Thysanoessa inspinata*
  - Amphipods: *C. challengeri, P. abyssalis* and *T. pacifica* (April)
- **Feeding**
  - Food availability increased for mesopelagic suspension copepods after bloom
  - Kept species-specific pattern within taxa: euphausiids and chaetognaths
- **Community structure**
  - March: *Metridia pacifica* predominated
  - April: *Euphausia pacifica* dominated

Fig. 26. Schematic diagram showing ecological responses (population structure, vertical distribution, reproduction, feeding and community structure) of meso- / macrozooplankton in the Oyashio region during the spring phytoplankton bloom of 2007.

From the vertical distribution of copepods, temporal changes in the vertical distribution were observed for *E. bungii*, *M. pacifica* and *P. scutullata* (Figs. 15, 17). For *E. bungii*, upward migration through activation from resting depths was observed on April 5. Ceased DVM was observed for *M. pacifica* and *P. scutullata* after phytoplankton bloom. *P. scutullata* ceased DVM before *M. pacifica* did, and the epipelagic *M. pacifica* C6F continued DVM. The continuous DVM of *M. pacifica* C6F might reflect reproduction at the surface layer. The mesopelagic carnivorous copepod *P. elongata* performed DVM throughout the study period.

For the reproduction of zooplankton, arousal from diapause was observed for *E. bungii* on April 5, and reproduction was initiated with the phytoplankton bloom peak (April 7–8), and subsequently, the newly recruited population peaked on April 12 (Fig. 9A). For various mesopelagic copepods, the composition of spermatophore-attached C6F increased in April and reproduction likely started in April (Abe et al., 2012). Because the highest composition of mature females with attached-spermatophores was observed in the *T. inspinata* population (more than 40% of the population), their reproduction might have occurred during the study period (Fig. 11B). For amphipods, the occurrence of egg-carrying females might reflect reproduction of *C. challengeri* and *T. pacifica* in April.

Concerning the feeding ecology, mesopelagic suspension feeding copepods fed on protozooplankton species prior to the phytoplankton bloom and on diatom resting spores after the bloom. Based on the cell condition, repacking and coprophagy were observed (Table 6). Species-specific differences in feeding modes were recognized for carnivorous copepods, euphausiids and chaetognaths during the study period (Tables 6–9).

For the total zooplankton biomass, the small-sized copepod *M. pacifica* dominated in March (Fig. 23). Both the biomass and production values in April were similar to those in March, while the species composition significantly varied; the composition of *M. pacifica* decreased, and a high composition of the macrozooplanktonic euphausiid *E. pacifica* was observed in April.

### 7-2. Comparison with other locations

High-frequency samplings of zooplankton during the spring phytoplankton bloom were conducted in the North Atlantic Norwegian Sea (St. M) and the North Pacific (SEEDI, SEEDII, SERIES), and comparative population data on copepods were available for each location (Fig. 1A).

The feeding, growth and reproduction of the dominant copepod *Calanus finmarchicus* have been reported based on high-frequency samplings (continued for approximately 80 days) from March 23 to June 9, 1997, in the Norwegian Sea (Irigoien et al., 1998; Meyer-Harms et al., 1999; Niehoff et al., 1999; Hirche et al., 2001; Ohman and Hirche, 2001). A significant difference in the ecology between *C. finmarchicus* in the North Atlantic and *Neocalanus* spp. in the North Pacific shows that the former reproduces at the surface layer during the phytoplankton bloom (Fig. 1C). Temporal changes in the abundance, population structure and individual mass at each location are shown in Fig. 27.

The abundance of *C. finmarchicus* in the Norwegian Sea was approximately 10 times higher than that of two dominant copepods (*E. bungii* and *N. cristatus*) in the Oyashio region (Fig. 27A), partly reflecting the quantitative abundance of *C. finmarchicus*, based not only on copepodid stages but also on eggs and nauplii (Niehoff et al., 1999; Hirche et al., 2001). However, a high abundance of *C. finmarchicus* was also observed during the late post bloom period when copepodid stages dominated; thus, the differences in copepods abundance might reflect inter-oceanic differences. Differences in copepod body size (smaller for *C. finmarchicus* in the North Atlantic) might reflect inter-oceanic differences in quantitative abundance.

The population structure of *C. finmarchicus* was dominated by eggs, nauplii and adults before the bloom, but the composition of these components gradually decreased after the bloom and the composition of the copepodid stages increased (Fig. 27B). Based on population structure data, the MCS of *C. finmarchicus* was also calculated, and minimum MCS values were observed on May 5. Thus, the significant recruitment of a new generation likely occurred on May 5, and their populations were divided into two cohorts: the N1–C3 cohort prior to May 5 and the C1–C5 cohort after May 5. The MCS of each cohort was calculated, and the individual mass was also calculated from the MCS using the formula:

$$Y = 0.0463 \times e^{0.794X}$$

where $X$ indicates the developmental stage from N1 as 1, and $Y$ is the individual mass (μg C ind.$^{-1}$). This formula was developed based on individual carbon mass data on *C. finmarchicus* according to Hirche et al. (2001). Significant positive increases were observed for *C. finmarchicus*. Within the species, the slope (growth rates) of the early copepodid stages that develop during the phytoplankton bloom was higher than that for the later copepodid stage (Fig. 27C).

Temporal changes in the abundance, population structure and individual carbon mass of *E. bungii* and *N. cristatus* during the OECOS and three iron-fertilization experiments in the subarctic Pacific (SEEDS I, SEEDS II, SERIES) are shown in Fig. 28. For the temporal changes of individual carbon mass are shown in Fig. 28E, and the *X*-axis (date) shows the peak of bloom (chl *a*) as occurring on the same Julian day. The highest chl *a* content was observed in SEEDS I (～18.0 mg m$^{-3}$), and moderate values were observed in the OECOS (0.2–7.3 mg m$^{-3}$) and SERIES (1.4–6.0 mg m$^{-3}$), while the lowest value was observed in SEEDS II (0.8–2.5 mg m$^{-3}$). The results of iron-fertilization experiments showed high abundances of copepods during SEEDS II (biomass was

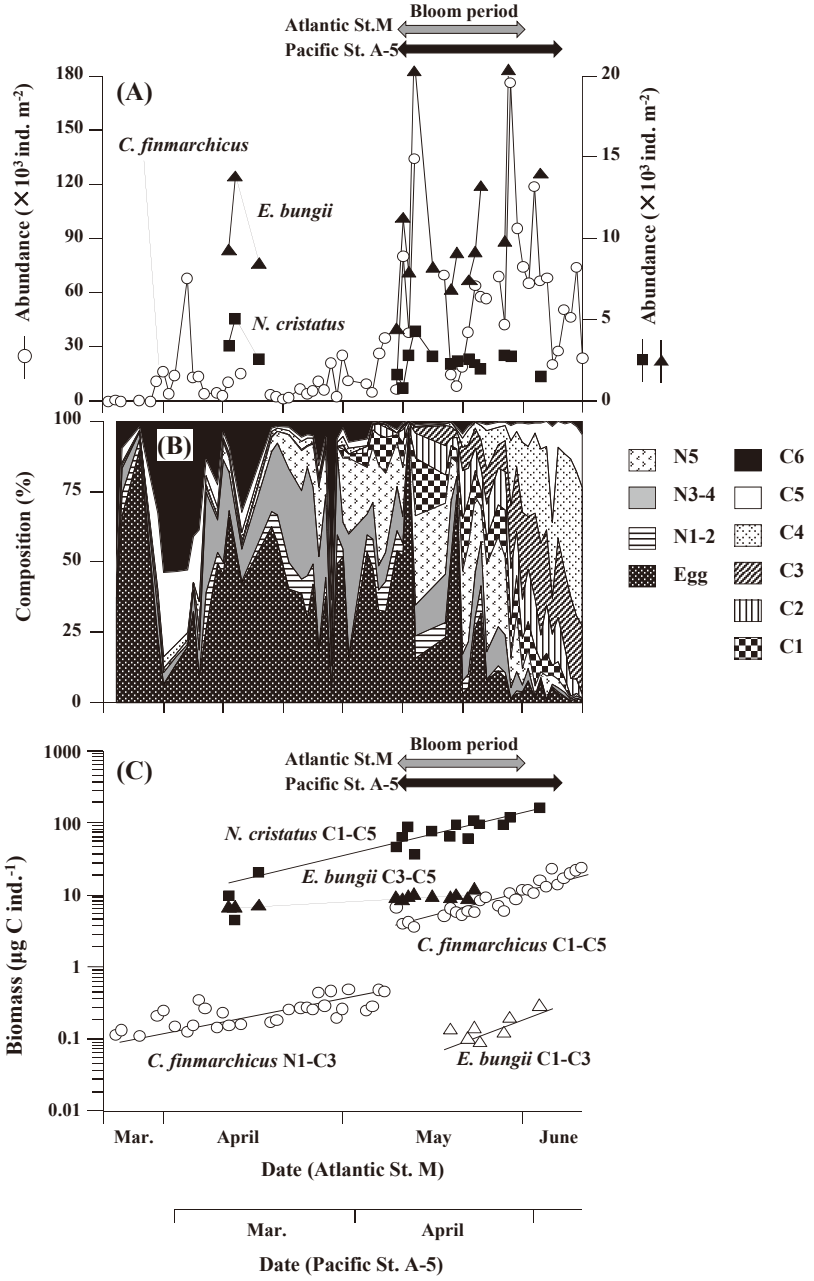


Fig. 27. Comparisons of the population parameters of dominant copepods during the phytoplankton bloom in the North Atlantic Norwegian Sea (*Calanus finmarchicus*) and North Pacific (*Eucalanus bungii* and *Neocalanus cristatus*). Abundance of each species (A), developmental stage composition in abundance of *C. finmarchicus* (B) and temporal changes in individual biomass calculated from the mean copepodid stage of each species (C). Note that the date (*X*-axis) scales are adjusted according to the time that the phytoplankton bloom started in each region.

approximately 3–5 times higher than those of SEEDS I) (Tsuda et al., 2009). Compared with the results of these oceanic iron fertilization experiments, the copepod abundance in the Oyashio region during the OECOS was substantially high. Thus, the abundance of *E. bungii* and *N. cristatus* during the OECOS was approximately 2–4 times higher than that recorded in the three iron-fertilization projects (Fig. 28A).

The mass-specific growth rate (*g*) of epipelagic copepods, evaluated using high-frequency samplings, is summarized in Table 10. For *E. bungii*, newly recruited C1 stage individuals were observed for studies in the western subarctic Pacific (OECOS, SEEDS I and SEEDS II). For SERIES in the eastern subarctic Pacific, the composition of *E. bungii* C1–C3 decreased and that of C5 increased after phytoplankton bloom (Fig. 28D). For several locations, growth of C1–C2 stages (OECOS) or C1–C3 stages (SEEDS II) was observed (Fig. 28E), and the mass-specific growth rates (*g*) were higher for newly recruited younger generations (Table 10).

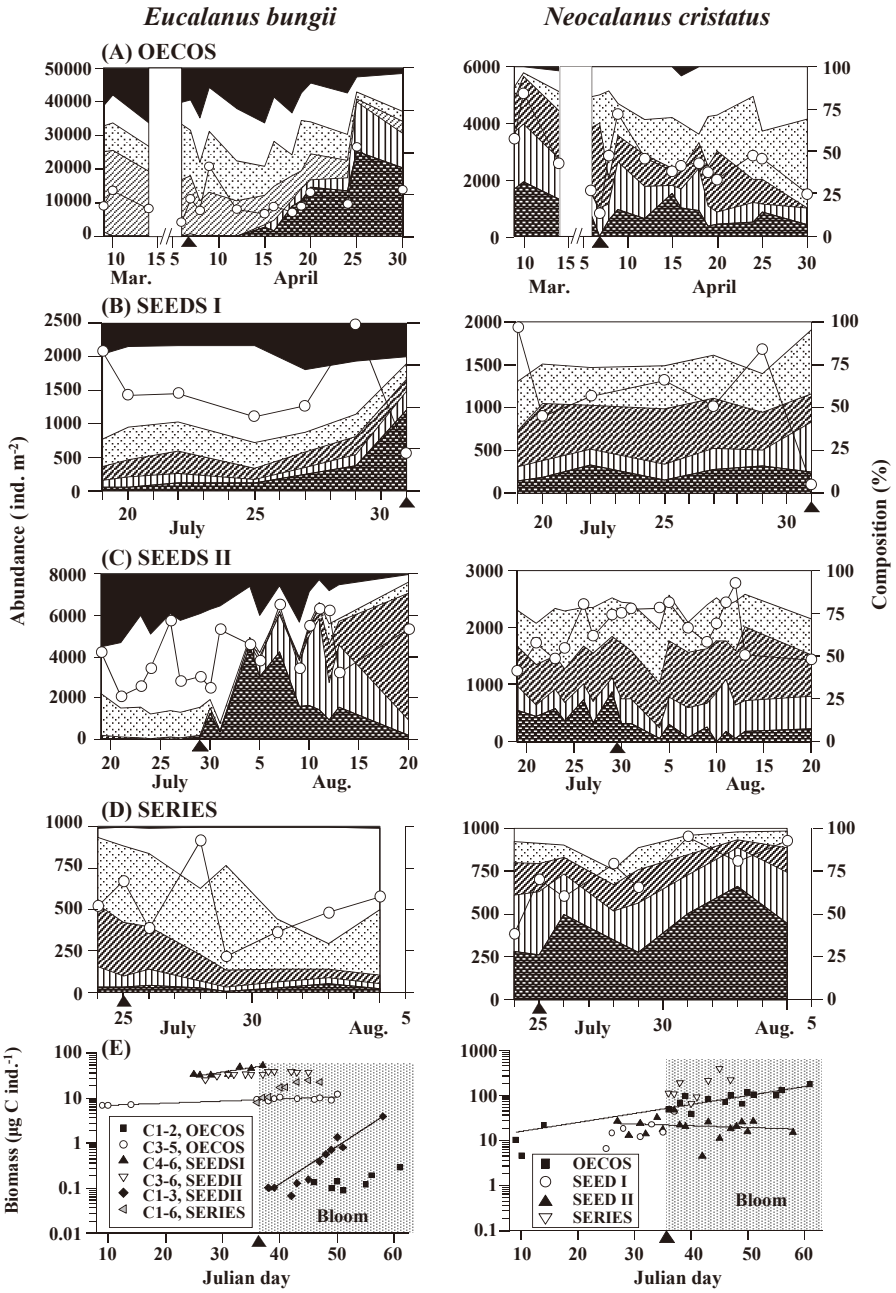


Fig. 28. Comparison of the population structure of *Eucalanus bungii* (left panels) and *Neocalanus cristatus* (right panels) during the phytoplankton bloom, as evaluated by various high-frequency time-series samplings in the North Pacific. OECOS (A), SEEDS I (B), SEEDS II (C), SERIES (D). Temporal changes in individual biomass calculated by the mean copepodid stage (E). Note that the date (*X*-axis) scales of (E) are adjusted for the time that the phytoplankton bloom started in each region. The positions of the large black triangles shown the chl *a* peak for each region.

For *N. cristatus*, significant increases in MCS were observed for all locations, except SEEDS II, and a significant increase in individual carbon mass was observed for the OECOS period (Fig. 28E). Concerning the *g* of the *N. cristatus* C1-C5 cohort, the lowest value was observed for OECOS (0.064±0.179 day$^{-1}$), followed by SERIES (0.080±0.275 day$^{-1}$), and the highest value was observed for SEEDS I (0.116±0.172 day$^{-1}$), characterized by high chl *a* values (Table 10).

The *g* values of epipelagic copepods during the spring phytoplankton bloom varied from 0.002 (*N. cristatus* in SEEDS II, Tsuda et al., 2009) to 0.210 (*C. finmarchicus* egg-C3 natural cohort at St. M, Niehoff et al., 1999) (Table 10). Within the four species examined, *C. finmarchicus* and *E. bungii* showed arousal from diapause, migration to the surface layer and reproduction at the surface layer. Because of these life

Table 10. Comparison of the mean mass-specific growth rate ($g$) of dominant copepods: (*Calanus finmarchicus* in the North Atlantic, *Eucalanus bungii*, *Neocalanus cristatus* and *N. plumchrus* in the North Pacific) during the phytoplankton bloom.

| Species | Cohort stage | Mass-specific growth rate ($g$) | Method | Study period | Location | References |
|---|---|---|---|---|---|---|
| *Calanus finmarchicus* | C1-C5 | 0.044±0.253 | Natural cohort | May-June | Norwegian Sea, St. M | Niehoff et al., 1999 |
| | egg-C3 | 0.210±1.058 | Natural cohort | May-June | Norwegian Sea, St. M | Niehoff et al., 1999 |
| *Eucalanus bungii* | C4-C6 | 0.013±0.059 | Natural cohort | July | western subarctic Pacific, SEEDSI | Tsuda et al., 2005 |
| | C3-C5 | 0.020±0.041 | Natural cohort | July-Aug. | western subarctic Pacific, SEEDSII | Tsuda et al., 2009 |
| | C3-C5 | 0.029±0.074 | Natural cohort | Mar.-Apr. | Oyashio region, OECOS | This study |
| | C2 | 0.04 | Incubation | Mar.-Apr. | Oyashio region, OECOS | Kobari et al., 2010c |
| | C1-C3 | 0.041±0.137 | Natural cohort | July-Aug. | western subarctic Pacific, SEEDSII | Tsuda et al., 2009 |
| | C1-C2 | 0.061±0.440 | Natural cohort | Mar.-Apr. | Oyashio region, OECOS | This study |
| | C1-C6 | 0.072±0.081 | Natural cohort | July-Aug. | eastern subarctic Pacific, SERIES | Tsuda et al., 2006 |
| *Neocalanus cristatus* | C1-C5 | 0.002±0.292 | Natural cohort | July-Aug. | western subarctic Pacific, SEEDSII | Tsuda et al., 2009 |
| | C5 | 0.05 | Natural cohort | Mar.-June | Bering Sea shelf | Vidal and Smith, 1986 |
| | C3 | 0.06 | Incubation | Mar.-Apr. | Oyashio region, OECOS | Kobari et al., 2010c |
| | C1-C5 | 0.064±0.179 | Natural cohort | Mar.-Apr. | Oyashio region, OECOS | This study |
| | C3 | 0.07 | Natural cohort | Mar.-June | Bering Sea shelf | Vidal and Smith, 1986 |
| | C4 | 0.07 | Natural cohort | Mar.-June | Bering Sea shelf | Vidal and Smith, 1986 |
| | C2 | 0.08 | Natural cohort | Mar.-June | Bering Sea shelf | Vidal and Smith, 1986 |
| | C1-C5 | 0.080±0.275 | Natural cohort | July-Aug. | eastern subarctic Pacific, SERIES | Tsuda et al., 2006 |
| | C1-C5 | 0.116±0.172 | Natural cohort | July | western subarctic Pacific, SEEDSI | Tsuda et al., 2005 |
| *Neocalanus plumchrus* | C4 | 0.02 | Incubation | Mar.-Apr. | Oyashio region, OECOS | Kobari et al., 2010c |
| | C3 | 0.03 | Incubation | Mar.-Apr. | Oyashio region, OECOS | Kobari et al., 2010c |
| | C1-C5 | 0.039±0.492 | Natural cohort | Mar.-Apr. | Oyashio region, OECOS | This study |
| | C5 | 0.04 | Natural cohort | Mar.-June | Bering Sea shelf | Vidal and Smith, 1986 |
| | C4 | 0.048 | Incubation | May | eastern subarctic Pacific | Miller and Nielsen, 1988 |
| | C4 | 0.07 | Incubation | Mar.-May | Gulf of Alaska | Liu and Hopcroft, 2006a |
| | C4 | 0.11 | Natural cohort | Mar.-June | Bering Sea shelf | Vidal and Smith, 1986 |
| | C3 | 0.11 | Incubation | Mar.-May | Gulf of Alaska | Liu and Hopcroft, 2006a |
| | C2 | 0.12 | Incubation | Mar.-May | Gulf of Alaska | Liu and Hopcroft, 2006a |
| | C1 | 0.12 | Incubation | Mar.-May | Gulf of Alaska | Liu and Hopcroft, 2006a |
| | C3 | 0.133 | Natural cohort | Mar.-June | Bering Sea shelf | Vidal and Smith, 1986 |
| | C2 | 0.141 | Natural cohort | Mar.-June | Bering Sea shelf | Vidal and Smith, 1986 |
| | C1 | 0.143 | Natural cohort | Mar.-June | Bering Sea shelf | Vidal and Smith, 1986 |

cycle patterns, the growth and maturation of adult cohorts and growth of newly recruited cohorts can be traced within the same time frame (Fig. 27C). Common for both species, the $g$ of the newly recruited cohort was approximately 5 times higher than that of the adult cohorts (Table 10). Within the same species, $g$ was exponentially higher for early copepodid stages according to laboratory experiments (Liu and Hopcroft, 2006a, 2006b). Thus, observed differences in $g$ between adult and newly recruited cohorts were consistent with the results based on laboratory experiments. Within the chl *a* range during OECOS (~8 mg $m^{-3}$), no species differences were observed for $g$ (Table 5). However, the highest $g$ of *N. cristatus* was observed for SEEDS I, characterized by a high chl *a* value. These findings suggest that the $g$ value might increase with increasing chl *a* within the observed chl *a* range (~18 mg $m^{-3}$).

### 7-3. Future prospects

In the present study, the responses of various meso- and macrozooplankton species to the spring phytoplankton bloom were evaluated. Within the copepods, *E. bungii* showed arousal from diapause, migration from resting depths to the surface and reproduction. *N. cristatus* showed continuous growth, and *M. pacifica* and *P. scutullata* showed ceased DVM during the spring phytoplankton bloom period (Fig. 26). The ceased DVM reflected the effect of the spring phytoplankton bloom on the mesopelagic ecosystem.

As a feature of the present study, the responses to the spring phytoplankton bloom and water mass exchanges of various macrozooplankton species were evaluated. Particularly, the macrozooplanktonic euphausiid *E. pacifica* was shown to be the most dominant zooplankton species in biomass and production in April (Figs. 23, 24). Previously, zooplankton studies in the Oyashio region primarily focused on mesozooplankton, such as copepods, which are relatively easy to collect (Ikeda et al., 2008). Because the present study revealed the importance of macrozooplankton or micronekton, samplings using large-mouth devices, such as Bongo nets, MOCNESS and MOHT, are required in future studies.

As a future direction, the development of methods to accurately measure the gross growth efficiency ($K_1$) of zooplankton is important. The lack of available $K_1$ data prevents the accurate estimation of zooplankton production using physiological methods. As a solution for these issues, the RNA:

DNA ratio, amount of hormones and enzyme activities were measured, but the precision of these measurements was relatively low; thus, these issues are still problematic (Runge and Roff, 2000).

From high-frequency samplings, such as those obtained in the present study, temporal resolution was improved. However, the analytical levels of spatial- and vertical-resolutions remain low. In the OECOS, large temporal changes in the vertical distribution of epi- and mesopelagic copepods were evaluated using high-frequency samplings by VMPS. Notably, the minimum sampling depth interval of VMPS was 25 m in the present study. Because there is such a low vertical resolution, the problem of a low spatial and vertical resolution remains when attempting to obtain adequate comparisons with high-resolution CTD data commonly collected at an interval of 1 m.

To obtain high spatial-resolution zooplankton data, traditional plankton net towing can be used. Indeed, VPR (Video Plankton Recorder) or UVP (Underwater Video Profiler), which obtain zooplankton visual data with fine spatial and vertical resolutions, is a solution to this problem. Because VPR could obtain zooplankton data with no physical damage, small-scale distributions of various doliolid generations have been reported in the Oyashio-Kuroshio frontal region (Takahashi et al., 2013, 2015) and the ecology of small poecilostomatoid copepods (*Oncaea* spp.) attached on appendicularian houses (Nishibe et al., 2015).

In a Norwegian fjord and the Greenland Sea, zooplankton responses to the spring phytoplankton bloom have been evaluated by VPR (Norrbin et al., 2009; Sainmont et al., 2014). Because large body-sized copepods, such as *Neocalanus* spp. and *E. bungii*, were dominant in the Oyashio region, VPR analysis might be suitable for zooplankton studies in this region. From VPR samplings, we obtained temperature and depth data as well as zooplankton individual size data (= biomass) within the same time frame. These findings suggest that we could obtain all four of the independent variables (body mass, temperature, distribution depth and taxa) required for calculating the metabolic rate using the Global Bathymetric Model (Ikeda, 2014) within one VPR cast.

Combining image analysis methods, such as VPR, with physiological production estimation methods (Ikeda and Motoda, 1978; Ikeda, 2014) will enable the accurate estimation and mapping of zooplankton secondary production. From such analyses, zooplankton production estimations are possible at high resolution (e.g., 1 m interval), such as physical oceanographic CTD data. Today, nearly 150 years have passed since the German scientist Dr. Victor Hensen (Taniguchi, 1994) initiated modern plankton studies (ca. 1870). However, the method for plankton net sampling and the microscopic analysis of the net samples have changed little from that time. From a historical perspective, we are in a transitional period of zooplankton quantification methods from the use of plankton net samplings to visual analysing methods that cause no physical damage to zooplankton with high spatial and vertical resolutions. Thus, high-frequency samplings using imaging instruments, such as VPR or UVP, might provide spatial and temporal high-resolution zooplankton data as well as provide new insights into the zooplankton realm in future studies.

## 8. Summary

In marine ecosystems, zooplankton play an important role in the transfer production of both the grazing food chain and microbial food web for higher trophic revels. In addition to a food mediator role, zooplankton accelerate the vertical material flux, termed the "Biological pump". In the Oyashio region, western subarctic Pacific, nearly half of the annual primary production occurs from April to May. During this same period, zooplankton grow faster. However, it is difficult to generate an accurate evaluation of zooplankton growth rates using the ordinary sampling interval (once per month) from previous studies. For an accurate evaluation of the growth rates of zooplankton, high frequency time-series samplings during the spring phytoplankton bloom are needed. The OECOS is an international research programme for the evaluation of zooplankton responses to the spring phytoplankton bloom using high-frequency time-series samplings.

During the OECOS period, high frequency oceanographic observations, including CTD casts (approximately every day), water samplings and various net samplings, were conducted at St. A-5 in the Oyashio region from March 8 to May 1, 2007. In the present study, short-term changes in phytoplankton, protozooplankton and meso- and macrozooplankton abundance, biomass, population structure, vertical distribution, growth rates and feeding ecology were studied during the OECOS period. Based on these phenological descriptions, the present study aimed to evaluate the lower trophic levels during the spring phytoplankton bloom in the Oyashio region. For comparison, copepod data collected from other high-frequency time-series samplings during the phytoplankton bloom (SEEDS I, SEEDS II, SERIES and St. M) were gathered and compared with those of the OECOS. A thorough comparison of the five time-series data and characteristics of zooplankton responses to the phytoplankton bloom were conducted.

Throughout the OECOS period, three dominant water masses (COW, MKW and OYW) occurred at the surface layer (0-50 m) over a short period of time. Because the COW contains sufficient nutrients originating from the Sea of Okhotsk, phytoplankton peaks were observed at the COW on April 7-8 and 23. The composition of diatoms was more than 74% of the chl *a* content during April, and centric diatoms predominated throughout the study period. The domi-

nant species changed from *Thalassiosira* spp. to *Chaetoceros* spp. after April 20. Peaks of microzooplankton biomass were observed on April 7 and 25, and both thecate and athecate dinoflagellates dominated in the microzooplankton community. The mesozooplankton wet mass at 0–150 m ranged from 7.6–147.7 g WM $m^{-2}$. The wet zooplankton biomass was low in March, but increased after April 8.

For the zooplankton population structure, the copepod *N. cristatus* developed from C1 to C4. Significant growth of two euphausiids (*E. pacifica* and *T. inspinata*) and two chaetognaths (*E. hamata* and *P. elegans*) was observed. A comparison of the mass-specific growth rate (*g*) showed no significant differences between species. These findings suggest that there was no food limitation for all feeding modes of zooplankton during the spring phytoplankton bloom in the Oyashio region.

For the reproduction of zooplankton, reproduction of the epipelagic copepod *E. bungii* was initiated in response to the phytoplankton bloom peak on April 7–8, and newly recruited early copepodid stages were observed on April 12. For mesopelagic copepods, increases in the composition of spermatophore-attached C6F in April suggested the initiation of reproduction. Throughout the study period, most adult females of *T. inspinata* had spermatophores, and the high proportion of attached-spermatophore females to the total population (>40%) suggested that spawning had occurred. For amphipods, the reproduction of *C. challengeri* and *T. pacifica* was initiated in April.

In response to water masses, various species showed high abundance and biomass under COW-dominated conditions and low abundance and biomass under OYW-dominated conditions. Few species showed any correlations with MKW. Zooplanktonic responses to high abundance under COW and low abundance under OYW might reflect the different characteristics of each water mass. The results of FRA-ROMS analyses revealed that the temperature of OYW was lowest and induced low zooplankton growth rates. However, the geographical origin of COW is the Sea of Okhotsk, a marginal sea with high primary productivity, providing high zooplankton survival and growth rates.

Temporal changes in the vertical distribution were observed for *E. bungii*, *M. pacifica* and *P. scutullata*. For *E. bungii*, the arousal from diapause and upward migration to the surface layer was initiated on April 5. DVM ceased for *M. pacifica* and *P. scutullata* after 23 and 11 April, respectively. In *P. scutullata*, this cessation was observed for all copepodid stages. However, in *M. pacifica*, the cessation was observed in all stages except C6F, which performed DVM throughout the study period. The continuous DVM behaviour of *M. pacifica* C6F might reflect reproduction at the surface layer. The ceased DVM of suspension feeding copepods might reflect increasing POC flux, which enables the acquisition of sufficient food at greater depths, without any DVM in April. For the mesopelagic carnivorous copepod *P. elongata*, continuous DVM was observed throughout the study period.

Gut content analyses were conducted on mesopelagic copepods and macrozooplanktonic euphausiids and chaetognaths. Mesopelagic suspension-feeding copepods primarily fed on protozooplankton prior to the onset of the phytoplankton bloom, while resting spores of diatoms were observed in the gut contents after the phytoplankton bloom. Within the gut contents, the cell conditions were mostly intact for shallower dwelling species, and the composition of broken cells increased for deeper living species. These results might reflect the coprophagy and repacking of mesopelagic suspension-feeding copepods. For mesopelagic carnivorous copepods, the species-specific preferences of euphausiids and chaetognaths in the feeding ecology were observed throughout the study period.

Within the biomass and production of the total zooplankton community, the small-sized copepod *M. pacifica* was dominant in March. Both the biomass and production values in April were similar to those in March, while the species composition significantly varied, that is, the composition of *M. pacifica* decreased and the macrozooplanktonic euphausiid *E. pacifica* was the most dominant species in April.

A comparison of the mass-specific growth rate (*g*) of epipelagic copepods at various locations showed that *g* varied from 0.002 to 0.210. For *C. finmarchicus* in the North Atlantic and *E. bungii* in the North Pacific, overwintered adult generations reproduced at the surface layer. Common for these species, *g* of the newly recruited generation cohort was approximately 5 times higher than that of the adult cohort. The highest *g* of *N. cristatus* was observed for SEEDS I, characterized by the highest chl *a,* suggesting that the *g* values increased with increasing chl *a* within the observed chl *a* range (～18 mg $m^{-3}$).

As a feature of the present study, the response to the spring phytoplankton bloom and water masses on macrozooplankton, with limited ecological information taxa, was evaluated. Particularly, the euphausiid *E. pacifica* was the most dominant zooplankton species both in biomass and production after the spring phytoplankton bloom. Previous zooplankton studies in the Oyashio region primarily focused on mesozooplankton, such as copepods. However, because of their importance, studies on macrozooplankton and micronekton are needed in the future. From high-frequency time-series sampling, such as the OECOS project, the time-resolution analysis was significantly improved, but the problems of low analytical levels of spatial- and vertical-resolution remain. Thus, the application of visual imaging instruments, such as VPR (Video Plankton Recorder) and UVP (Underwater Video Profiler), which collect zooplankton data continuously, has been suggested as a solution for increasing the spatial- and vertical resolution of zooplankton data analysis in future studies.

## 9. Acknowledgements

I would like to express my sincere thanks to Professor Ichiro Imai who provided detailed guidance, advice and reviewed this manuscript. I would also like to thank Professor Tetsuya Takatsu and Associate Professor Atsushi Yamaguchi for their valuable comments and review of the manuscript.

I would like to thank the captains, officers, crew and researchers on board T/S *Oshoro-Maru*, Hokkaido University and R/V *Hakuho-Maru*, JAMSTEC for assistance during the field sampling. The OECOS is a project endorsed by PICES. Part of this study was supported by a Grant-in-Aid for Scientific Research (A) 24248032, (B) 16H02947 and Innovative Areas 24110005 from the Japanese Society for the Promotion of Science (JSPS). This work was partially conducted for the Arctic Challenge for Sustainability (ArCS) project.

I thank Emeritus Professor Tsutomu Ikeda for the planning and fulfilment of the project and Dr. Barbara Niehoff (Alfred Wegener Institute for Polar and Marine Research), Professor Atsushi Tsuda (Atmosphere and Ocean Research Institute, The University of Tokyo), Associate Professor Koji Suzuki (Hokkaido University), Associate Professor Naoshi Ota (Ishinomaki Senshu University), Associate Professor Kosei Komatsu (Atmosphere and Ocean Research Institute, The University of Tokyo) and Dr. Rui Saito (Ehime University) for kindly providing published/unpublished data. I would also like to express my sincere appreciation to Associate Professor Yoshizumi Nakagawa (Tokyo University of Agriculture), Dr. Yuichiro Yamada (Kitasato University) and Dr. Hiroomi Miyamoto (Tohoku National Fisheries Research Institute) for kind advice on species identification of macrozooplankton taxa. Professor Tokihiro Kono (Tokai University) provided advice on mixing ratio of water masses.

I am deeply grateful to all of the scientists and students who participated in the OECOS project. Particularly, I would like to thank alumni members of the Plankton Laboratory of Hokkaido University: Dr. Hye Seon Kim, Dr. Yuka Onishi, Ms. Aya Omata, Ms. Momoka Kawai, Ms. Mariko Kaneda and Mrs. Erika Ishiwatari-Hida, who performed analysis of the samples used in the present study. I would also like to thank all of the members of Plankton Laboratory of Hokkaido University for providing assistance and advice on the present study. Finally, I express my sincere thanks to my parents and family for giving me the opportunity to study at Hokkaido University as well as continuous encouragement and support throughout this study.

## 10. References

Abe, Y., Ishii, K., Yamaguchi, A. and Imai, I. (2012) Short-term changes in population structure and vertical distribution of mesopelagic copepods during the spring phytoplankton bloom in the Oyashio region. *Deep-Sea Res. I*, **65**, 100-112.

Abe, Y., Natsuike, M., Matsuno, K., Terui, T., Yamaguchi, A. and Imai, I. (2013) Variation in assimilation efficiencies of dominant *Neocalanus* and *Eucalanus* copepods in the subarctic Pacific: consequences for population structure models. *J. Exp. Mar. Biol. Ecol*., **449**, 321-329.

Abe, Y., Yamaguchi, A., Matsuno, K., Kono, T. and Imai, I. (2014) Short-term changes in population structure of Hydromedusa *Aglantha digitale* during the spring phytoplankton bloom in the Oyashio region. *Bull. Fish. Sci. Hokkaido Univ*., **64**, 71-81.

Abe, Y., Yamada, Y., Saito, R., Matsuno, K., Yamaguchi, A., Komatsu, K. and Imai, I. (2016) Short-term changes in abundance and population structure of dominant pelagic amphipod species in the Oyashio region during the spring phytoplankton bloom. *Reg. Stud. Mar. Sci*., **3**, 154-162.

Alvariño, A. (1962) Two new Pacific chaetognaths: their distribution and relationship to allied species. *Bull. Scripps Inst. Oceanog. Tech. Ser*., **8**, 1-50.

Arashkevich, Y.G. (1969) The food and feeding of copepods in the northwestern Pacific. *Oceanology*, **9**, 695-709.

Bieri, R. (1959) The distribution of the planktonic Chaetognatha in the Pacific and their relationship to the water masses. *Limnol. Oceanogr*., **4**, 1-28.

Brodeur, R. and Terazaki, M. (1999) Springtime abundance of chaetognaths in the shelf region of the northern Gulf of Alaska, with observations on the vertical distribution and feeding of *Sagitta elegans*. *Fish. Oceanogr*., **8**, 93-103.

Brodskii, K.A. (1950) *Calanoida of the Far Eastern Seas and Polar Basin of the USSR*. Nauka, Moscow (in Russian). Translated to English in 1967, Israel Program of Scientific Translation, Jerusalem.

Choe, N. and Deibel, D. (2000) Seasonal vertical distribution and population dynamics of the chaetognath *Parasagitta elegans* in the water column and hyperbenthic zone of Conception Bay, Newfoundland. *Mar. Biol*., **137**, 847-856.

Conover, R.J. (1966a) Assimilation of organic matter by zooplankton. *Limnol. Oceanogr*., **11**, 338-345.

Conover, R.J. (1966b) Factors affecting the assimilation of organic matter by zooplankton and the question of superfluous feeding. *Limnol. Oceanogr*., **11**, 346-354.

Conover, R.J. (1988) Comparative life histories in the genera *Calanus* and *Neocalanus* in high latitudes of the northern hemisphere. *Hydrobiologia*, **167/168**, 127-142.

Conway, D.V.P. and Williams, R. (1986) Seasonal population structure, vertical distribution and migration of the chaetognath *Sagitta elegans* in the Celtic Sea. *Mar. Biol*., **93**, 377-387.

Dagg, M.J. (1993) Grazing by the copepod community does not control phytoplankton production in the subarctic Pacific Ocean. *Prog. Oceanogr*., **32**, 163-183.

Dalpadado, P., Yamaguchi, A., Ellertsen, B. and Johannessen, S. (2008) Trophic interactions of macro-zooplankton (krill and amphipods) in the marginal ice zone of the Barents Sea. *Deep-Sea Res. II*, **55**, 2266-2274.

Endo, Y. and Komaki, Y. (1979) Larval stages of euphausiids with descriptions of those of *Thysanoessa longipes* Brandt. *Bull. Japan Sea Reg. Fish. Res. Lab*., **30**, 97-110.

Fraley, C., Raftery, A.E., Murphy, T.B. and Scrucca, L. (2012) mclust Version 4 for R: Normal mixture modeling for model-based clustering, classification, and density estimation. *Technical Report No. 597*. Department of Statistics, University of Washington.

Fujii, Y. and Kamachi, M. (2003) Three-dimensional analysis of

temperature and salinity in the equatorial Pacific using a variational method with vertical coupled temperature-salinity empirical orthogonal function modes. *J. Geophys. Res*., **108**, 3297, doi:10.1029/2002JC001745.

Fujioka, H.A., Machida, R. and Tsuda, A. (2015) Early life history of *Neocalanus plumchrus* (Calanoida: Copepoda) in the western subarctic Pacific. *Prog. Oceanogr*., **137**, 196-208.

Grigor, J.J., Søreide, J.E. and Varpe, Ø. (2014) Seasonal ecology and life history strategy of the high-latitude predatory zooplankter *Parasagitta elegans*. *Mar. Ecol. Prog. Ser*., **499**, 77-88.

Halsband-Lenk, C. (2005) *Metridia pacifica* in Dabob Bay, Washington: The diatom effect and the discrepancy between high abundance and low egg production rates. *Prog. Oceanogr*., **67**, 422-441.

Hansen, B., Bjørnsen, P.K. and Hansen, P.J. (1994) The size ratio between planktonic predators and their prey. *Limnol. Oceanogr*., **39**, 395-403.

Hattori, H. (1989) Bimodal vertical distribution and diel migration of the copepods *Metridia pacifica*, *M. okhotensis* and *Pleuromamma scutullata* in the western North Pacific Ocean. *Mar. Biol*., **103**, 39-50.

Hays, G.C., Kennedy, H. and Frost, B.W. (2001) Individual variability in diel vertical migration of a marine copepods: why some individuals remain at depth when others migrate. *Limnol. Oceanogr*., **39**, 1621-1629.

Hirche, H.J., Brey, T. and Niehoff, B. (2001) A high-frequency time series at Ocean Weather Ship Station M (Norwegian Sea): population dynamics of *Calanus finmarchicus*. *Mar. Ecol. Prog. Ser*., **219**, 205-219.

Hopcroft, R.R., Clarke, C., Byrd, A.G. and Pinchuk, A.I. (2005) The paradox of *Metridia* spp. egg production rates: A new technique and measurements from the coastal Gulf of Alaska. *Mar. Ecol. Prog. Ser*., **286**, 193-201.

Ichinomiya, M., Gomi, Y., Nakamachi, M., Ota, T. and Kobari, T. (2010) Temporal patterns in silica deposition among siliceous plankton during the spring bloom in the Oyashio region. *Deep-Sea Res. II*, **57**, 1665-1670.

Iguchi, N., Ikeda, T. and Imamura, A. (1993) Growth and life cycle of a euphausiids crustacean (*Euphausia pacifica* Hansen) in Toyama Bay, southern Japan Sea. *Bull. Japan Sea Nat. Fish. Res. Inst.*, **43**, 69-81 (in Japanese with English abstract).

Ikeda, T. (1985) Metabolic rates of epipelagic marine zooplankton as a function of body mass and temperature. *Mar. Biol*., **85**, 1-11.

Ikeda, T. (2014) Respiration and ammonia excretion by marine metazooplankton taxa: synthesis toward a global-bathymetric model. *Mar. Biol*., **161**, 2753-2766.

Ikeda, T. and Motoda, S. (1978) Estimated zooplankton production and their ammonia excretion in the Kuroshio and adjacent seas. *Fish. Bull*., **76**, 357-367.

Ikeda, T. and Shiga, N. (1999) Production, metabolism and production/biomass (P/B) ratio of *Themisto japonica* (Crustacea: Amphipoda) in Toyama Bay, southern Japan Sea. *J. Plankton Res*., **21**, 299-308.

Ikeda, T. and Takahashi, T. (2012) Synthesis towards a global-bathymetric model of metabolism and chemical composition of marine pelagic chaetognaths. *J. Exp. Mar. Biol. Ecol*., **424-425**, 78-88.

Ikeda, T., Kanno, Y., Ozaki, K. and Shinada, A. (2001) Metabolic rates of epipelagic marine copepods as a function of body mass and temperature. *Mar. Biol*., **139**, 587-596.

Ikeda, T., Yamaguchi, A. and Matsuishi, T. (2006) Chemical composition and energy content of deep-sea calanoid copepods in the Western North Pacific Ocean. *Deep-Sea Res. I*, **53**, 1792-1809.

Ikeda, T., Shiga, N. and Yamaguchi, A. (2008) Structure, biomass distribution and trophodynamics of the pelagic ecosystem in the Oyashio region, western subarctic Pacific. *J. Oceanogr*., **64**, 339-354.

Ikeda, T., Yamaguchi, A. and Miller, C.B. (2010) Oceanic ecosystem comparison subarctic-Pacific (OECOS): West. *Deep-Sea Res. II*, **57**, 1593-1594.

Imao, F. (2005) Zooplankton community structure and functional role in carbon cycle of the Oyashio region, western North Pacific. Master thesis, Hokkaido University (in Japanese).

Irigoien, X., Head, R., Klenke, U., Meyer-Harms, B., Harbour, D., Niehoff, B., Hirche, H.J. and Harris, R. (1998) A high frequency time series at weathership M, Norwegian Sea, during the 1997 spring bloom: feeding of adult female *Calanus finmarchicus*. *Mar. Ecol. Prog. Ser*., **172**, 127-137.

Isada, T., Hattori-Saito, A., Saito, H., Ikeda, T. and Suzuki, K. (2010) Primary productivity and its bio-optical modeling in the Oyashio region, NW Pacific during the spring bloom 2007. *Deep-Sea Res. II*, **57**, 1653-1664.

Jakobsen, T. (1971) On the biology of *Sagitta elegans* Verrill and *Sagitta setosa*. J. Müller in inner Oslofjord. *Norw. J. Zool*., **19**, 201-225.

Johnson, T.B. and Terazaki, M. (2003) Species composition and depth distribution of chaetognaths in a Kuroshio warm-core ring and Oyashio water. *J. Plankton Res*., **25**, 1279-1289.

Kim, H.S., Yamaguchi, A. and Ikeda, T. (2009) Abundance, biomass and life cycle patterns of euphausiids (*Euphausia pacifica*, *Thysanoessa inspinata* and *T. longipes*) in the Oyashio region, western subarctic Pacific. *Plankton Benthos Res*., **4**, 43-52.

Kim, H.S., Yamaguchi, A. and Ikeda, T. (2010a) Population dynamics of the euphausiids *Euphausia pacifica* and *Thysanoessa inspinata* in the Oyashio region during the 2007 spring phytoplankton bloom. *Deep-Sea Res. II*, **57**, 1727-1732.

Kim, H.S., Yamaguchi, A. and Ikeda, T. (2010b) Metabolism and elemental composition of the euphausiids *Euphausia pacifica* and *Thysanoessa inspinata* during the phytoplankton bloom season in the Oyashio region, western subarctic Pacific Ocean. *Deep-Sea Res. II*, **57**, 1733-1741.

Kobari, T. and Ikeda, T. (1999) Vertical distribution, population structure and life cycle of *Neocalanus cristatus* (Crustacea: Copepoda) in the Oyashio region, with notes on its regional variations. *Mar. Biol*., **134**, 683-696.

Kobari, T. and Ikeda, T. (2001a) Life cycle of *Neocalanus flemingeri* (Crustacea: Copepoda) in the Oyashio region, western subarctic Pacific, with notes on its regional variations. *Mar. Ecol. Prog. Ser*., **209**, 243-255.

Kobari, T. and Ikeda, T. (2001b) Ontogenetic vertical migration and life cycle of *Neocalanus plumchrus* (Crustacea: Copepoda) in the Oyashio region, with notes on regional variations in body sizes. *J. Plankton Res*., **23**, 287-302.

Kobari, T., Mitsui, K., Ota, T., Ichinomiya, M. and Gomi, Y. (2010a) Response of heterotrophic bacteria to the spring phytoplankton bloom in the Oyashio region. *Deep-Sea Res. II*, **57**, 1671-1678.

Kobari, T., Inoue, Y., Nakayama, Y., Okamura, T., Ota, Y., Nishibe, Y. and Ichinomiya, M. (2010b) Feeding impacts of ontogenetically migrating copepods on the spring phytoplankton bloom in the Oyashio region. *Deep-Sea Res. II*, **57**, 1703-1714.

Kobari, T., Ueda, A. and Nishibe, Y. (2010c) Development and growth of ontogenetically migrating copepods during the spring phytoplankton bloom in the Oyashio region. *Deep-Sea Res.*

*II*, **57**, 1715–1726.

Kono, T. and Sato, M. (2010) A mixing analysis of surface water in the Oyashio region: Its implications and application to variations of the spring bloom. *Deep–Sea Res. II*, **57**, 1595–1607.

Kotori, M. (1976) The biology of Chaetognatha in the Bering Sea and the northern North Pacific Ocean, with emphasis on *Sagitta elegans*. *Mem. Fac. Fish. Hokkaido Univ*., **23**, 95–183.

Kotori, M. (1999) Life cycle and growth rate of the chaetognath *Parasagitta elegans* in the northern North Pacific Ocean. *Plankton Biol. Ecol*., **46**, 153–158.

Lalli, C. and Parsons, T. (1998) *Biological Oceanography: An Introduction: 2nd Edition*. Pergamon Press Ltd., Oxford.

Liu, H. and Hopcroft, R.R. (2006a) Growth and development of *Neocalanus flemingeri/plumchrus* in the northern Gulf of Alaska: validation of the artificial–cohort method in cold waters. *J. Plankton Res*., **28**, 87–101.

Liu, H. and Hopcroft, R.R. (2006b) Growth and development of *Metridia pacifica* (Copepoda: Calanoida) in the northern Gulf of Alaska. *J. Plankton Res*., **28**, 769–781.

Liu, H., Suzuki, K. and Saito, H. (2004) Community structure and dynamics of phytoplankton in the western subarctic Pacific Ocean: A synthesis. *J. Oceanogr*., **60**, 119–137.

Longhurst, A.R. (1991) Role of the marine biosphere in the global carbon cycle. *Limnol. Oceanogr*., **36**, 1507–1526.

Longhurst, A.R. and Harrison, W.G. (1989) The biological pump: Profiles of plankton production and consumption in the upper ocean. *Prog. Oceanogr*., **22**., 47–123.

Mackas, D.L., Sefton, H., Miller, C.B. and Raich, A. (1993) Vertical habitat partitioning by large calanoid copepods in the oceanic subarctic Pacific during spring. *Prog. Oceanogr*., **32**, 259–294.

Makarov, R.R. and Denys, C.J.I. (1981) Stages of sexual maturity of *Euphausia superba* Dana. pp. 13, *BIOMASS Handbook 11*. Scientific Committee on Antarctic Research, Cambridge.

Marin, V. (1987) The oceanographic structure of the eastern Scotia Sea–IV. Distribution of copepod species in relation to hydrography in 1981. *Deep–Sea Res. I*, **34**, 105–121.

Matsumoto, Y. (2008) Life cycle and production of chaetognath *Eukrohnia hamata* in the Oyashio region, western North Pacific. Master thesis, Hokkaido University (in Japanese).

McLaren, I.A. (1969) Population and production ecology of zooplankton in Ogac Lake, a landlocked fjord on Baffin Island. *J. Fish. Res. Bd. Can*., **26**, 1485–1559.

Meyer–Harms, B., Irigoien, X., Head, R. and Harris, R. (1999) Selective feeding on natural phytoplankton by *Calanus finmarchicus* before, during, and after the 1997 spring bloom in the Norwegian Sea. *Limnol. Oceanogr*., **44**, 154–165.

Miller, C.B. and Nielsen, R.D. (1988) Development and growth of large, calanoid copepods in the ocean subarctic Pacific, May 1984. *Prog. Oceanogr*., **20**, 275–292.

Miller, C.B., Frost, B.W., Batchelder, H.P., Clemons, M.J. and Conway, R.E. (1984) Life histories of large, grazing copepods in a subarctic ocean gyre: *Neocalanus plumchrus*, *Neocalanus cristatus*, and *Eucalanus bungii* in the Northeast Pacific. *Prog. Oceanogr*., **13**, 201–243.

Montagnes, D.J.S. and Lynn, D.H. (1991) Taxonomy of choreotrichs, the major marine planktonic ciliates, with emphasis on the aloricate forms. *Mar. Microb. Food Webs*, **5**, 59–74.

Motoda, S. (1957) North Pacific standard plankton net. *Inform. Bull. Planktol. Japan*, **4**, 13–15 (in Japanese with English abstract).

Motoda, S. (1959) Devices of simple plankton apparatus. *Mem. Fac. Fish. Hokkaido Univ*., **7**, 73–94.

Nagasawa, S. and Marumo, R. (1972) Feeding of a pelagic chaetognath, *Sagitta nagae* Alvariño in Suruga Bay, central Japan. *J. Oceanogr. Soc. Japan*, **28**, 181–186.

Nagasawa, S. and Marumo, R. (1976) Further studies on the feeding habits of *Sagitta nagae* Alvariño in Suruga Bay, Central Japan. *J. Oceanogr. Soc. Japan*, **32**, 209–218.

Nakagawa, Y., Endo, Y. and Taki, K. (2001) Diet of *Euphausia pacifica* Hansen in Sanriku waters off north–eastern Japan. *Plankton Biol. Ecol*., **48**, 68–77.

Nakagawa, Y., Endo, Y. and Taki, K. (2002) Contributions of heterotrophic and autotrophic prey to the diet of euphausiid, *Euphausia pacifica* in the coastal waters off northeastern Japan. *Polar Biosci*., **15**, 52–65.

Nakayama, Y., Kuma, K., Fujita, S., Sugie, K. and Ikeda, T. (2010) Temporal variability and bioavailability of iron and other nutrients during the spring phytoplankton bloom in the Oyashio region. *Deep–Sea Res. II*, **57**, 1618–1629.

Niehoff, B., Klenke, U., Hirche, H.J., Irigoien, X., Head, R. and Harris, R. (1999) A high frequency time series at Weathership M, Norwegian Sea, during the 1997 spring bloom: the reproductive biology of *Calanus finmarchicus*. *Mar. Ecol. Prog. Ser*., **176**, 81–92.

Nishibe, Y., Kobari, T. and Ota, T. (2010) Feeding by the cyclopoid copepod *Oithona similis* on the microplankton assemblage in the Oyashio region during spring. *Plankton Benthos Res*., **5**, 74–78.

Nishibe, Y., Takahashi, K., Ichikawa, T., Hidaka, K., Kurogi, H., Segawa, K. and Saito, H. (2015) Degradation of discarded appendicularian houses by oncaeid copepods. *Limnol. Oceanogr*., **60**, 967–976.

Nishida, S. and Ohtsuka, S. (1996) Specialized feeding mechanism in the pelagic copepod genus *Heterorhabdus* (Calanoida: Heterorhabdidae), with special reference to the Mandibular tooth and labral glands. *Mar. Biol*., **126**, 619–632.

Nishiuchi, K. (1999) Life history and annual variation in carnivorous zooplankton Chaetognaths in the northern North Pacific. Ph.D. Thesis, Hokkaido University (in Japanese).

Norrbin, F., Eilertsen, H.C. and Degerlund, M. (2009) Vertical distribution of primary producers and zooplankton grazers during different phases of the Arctic spring bloom. *Deep–Sea Res. II*, **56**, 1945–1958.

Ohman, M.D. and Hirche, H.J. (2001) Density–dependent mortality in an oceanic copepod population. *Nature*, **412**, 638–641.

Okamoto, S., Hirawake, T. and Saitoh, S. (2010) Interannual variability in the magnitude and timing of the spring bloom in the Oyashio region. *Deep–Sea Res. II*, **57**, 1608–1617.

Omori, M. (1969) Weight and chemical composition of some important oceanic zooplankton in the North Pacific Ocean. *Mar. Biol*., **3**, 4–10.

Omori, M. and Ikeda, T. (1984) *Methods in Marine Zooplankton Ecology*. John Wiley and Sons, New York.

Øresland, V. (1987) Feeding of the chaetognaths *Sagitta elegans* and *S. setosa* at different seasons in Gullmars fjorden, Sweden. *Mar. Ecol. Prog. Ser*., **39**, 67–79.

Osgood, K.E. and Frost, B.W. (1994) Ontogenetic diel vertical migration behaviors of the marine planktonic copepods *Calanus pacificus* and *Metridia lucens*. *Mar. Ecol. Prog. Ser*., **104**, 13–25.

Ozawa, M., Yamaguchi, A., Ikeda, T., Watanabe, Y. and Ishizaka, J. (2007) Abundance and community structure of chaetognaths from the epipelagic through abyssopelagic zones in the western North Pacific and its adjacent seas. *Plankton Benthos Res*., **2**,

184–197.
Padmavati, G. (2002) Abundance, vertical distribution and life cycle of *Metridia pacifica* and *M. okhotensis* (Copepoda: Calanoida) in the Oyashio region, western subarctic Pacific Ocean. Ph. D thesis, Hokkaido University, 83 pp.
Padmavati, G., Ikeda, T. and Yamaguchi, A. (2004) Life cycle, population structure and vertical distribution of *Metridia* spp. (Copepoda: Calanoida) in the Oyashio region (NW Pacific Ocean). *Mar. Ecol. Prog. Ser*., **270**, 181–198.
Parsons, T.R. and Lalli, C.M. (1988) Comparative oceanic ecology of the plankton communities of the subarctic Atlantic and Pacific oceans. *Oceanogr. Mar. Biol. Ann. Rev*., **26**, 317–359.
Pennak, R.W. (1943) An effective method of diagramming diurnal of zooplankton organisms. *Ecology*, **24**, 405–407.
Pinchuk, A.I. and Hopcroft, R.R. (2007) Seasonal variations in the growth rates of euphausiids (*Thysanoessa inermis*, *T. spinifera*, and *Euphausia pacifica*) from the northern Gulf of Alaska. *Mar. Biol*., **151**, 257–269.
Raymont, J.E.G. (1983) *Plankton and Productivity in the Oceans. Second Edition, Vol. 2. Zooplankton*. Pergamon Press, Oxford.
Ross, R.M. (1982) Energetics of *Euphausia pacifica*. I. Effects of body carbon and nitrogen and temperature on measured and predicted production. *Mar. Biol*., **68**, 1–13.
Runge, J.A. and Roff, J.C. (2000) The measurement of growth and reproduction rates. pp. 401–454, Harris, R.P., Wiebe, P.H., Lenz, J., Skjoldal, H.R. and Huntley, M. (eds.), *ICES Zooplankton Methodology Manual*, Academic Press, San Diego.
Runge, J.A., Pepin, P. and Silvert, W. (1987) Feeding behavior of the Atlantic mackerel *Scomber scombrus* on the hydromedusa *Aglantha digitale*. *Mar. Biol*., **94**, 329–333.
Russell, F.S. (1935) On the value of certain plankton animals as indicators of water movements in the English Channel and North Sea. *J. Mar. Biol. Ass. U.K*., **20**, 309–332.
Sainmont, J., Gislason, A., Heuschele, J., Webster, C.N., Sylvander, P., Wang, M. and Varpe, Ø. (2014) Inter- and intra-specific diurnal habitat selection of zooplankton during the spring bloom observed by Video Plankton Recorder. *Mar. Biol*., **161**, 1931–1941.
Saito, H. and Kiørboe, T. (2001) Feeding rates in the chaetognath *Sagitta elegans*: effects of prey size, prey swimming behaviour and small-scale turbulence. *J. Plankton Res*., **23**, 1385–1398.
Saito, H. and Tsuda, A. (2000) Egg production and early development of the subarctic copepods *Neocalanus cristatus*, *N. plumchrus* and *N. flemingeri*. *Deep-Sea Res. I*, **47**, 2141–2158.
Saito, H., Tsuda, A. and Kasai, H. (2002) Nutrient and plankton dynamics in the Oyashio region of the western subarctic Pacific Ocean. *Deep-Sea Res. II*, **49**, 5463–5486.
Sameoto, D.D. (1971) Life history, ecological production, and an empirical mathematical model of the population of *Sagitta elegans* in St. Margaret's Bay, Nova Scotia. *J. Fish. Res. Bd. Can*., **28**, 971–985.
Sasaki, H., Hattori, H. and Nishizawa, S. (1988) Downward flux of particulate organic matter and vertical distribution of calanoid copepods in the Oyashio Water in summer. *Deep-Sea Res*., **35A**, 505–515.
Sato, K., Yamaguchi, A., Ueno, H. and Ikeda, T. (2011) Vertical segregation within four grazing copepods in the Oyashio region during early spring. *J. Plankton Res*., **33**, 1230–1238.
Sato, M. and Furuya, K. (2010) Pico- and nanophytoplankton dynamics during the decline phase of the spring bloom in the Oyashio region. *Deep-Sea Res. II*, **57**, 1643–1652.
Shaw, C.T., Peterson, W.T. and Feinberg, L.R. (2010) Growth of *Euphausia pacifica* in the upwelling zone off the Oregon coast. *Deep-Sea Res. II*, **57**, 584–598.
Shiota, T., Yamaguchi, A., Saito, R. and Imai, I. (2012) Geographical variations in abundance and body size of the hydromedusa *Aglantha digitale* in the northern North Pacific and its adjacent seas. *Bull. Fish. Sci. Hokkaido Univ*., **62**, 63–69.
Shoden, S., Ikeda, T. and Yamaguchi, A. (2005) Vertical distribution, population structure and life cycle of *Eucalanus bungii* (Copepoda: Calanoida) in the Oyashio region, with notes on its regional variations. *Mar. Biol*., **146**, 497–511.
Sokal, R.P. and Rohlf, F.J. (1995) *Biometry: the Principles and Practice of Statistics in Biological Research, 3rd ed.* W.H. Freeman and Company, New Pork, 887 pp.
Strüder-Kypke, M.C., Kypke, E.R., Agatha, S., Warwick, J. and Montagnes, D.J.S. (2001) The user-friendly guide to coastal planktonic ciliates. Available at: www.liv.ac.uk/ciliate.
Sugie, K., Kuma, K., Fujita, S., Nakayama, Y. and Ikeda, T. (2010a) Nutrient and diatom dynamics during late winter and spring in the Oyashio region of the western subarctic Pacific Ocean. *Deep-Sea Res. II*, **57**, 1630–1642.
Sugie K., Kuma, K., Fujita, S. and Ikeda, T. (2010b) Increase in Si: N drawdown ratio due to resting spore formation by spring bloom-forming diatoms under Fe- and N-limited conditions in the Oyashio region. *J. Exp. Mar. Biol. Ecol*., **382**, 108–116.
Sugie K., Kuma, K., Fujita, S., Ushizaka, S., Suzuki, K. and Ikeda, T. (2011) Importance of intracellular Fe pools on growth of marine diatoms by using unialgal cultures and the Oyashio region phytoplankton community during spring. *J. Oceanogr*., **67**, 183–196.
Suh, H.L., Soh, H.Y. and Hong, S.Y. (1993) Larval development of the euphausiid *Euphausia pacifica* in the Yellow Sea. *Mar. Biol*., **115**, 625–633.
Suzuki, R. and Ishimaru, T. (1990) An improved method for the determination of phytoplankton chlorophyll using N, N-dimethylformamide. *J. Oceanogr. Soc. Japan*, **46**, 190–194.
Takahashi, D. and Ikeda, T. (2006) Abundance, vertical distribution and life cycle patterns of the hydromedusa *Aglantha digitale* in the Oyashio region, western subarctic Pacific. *Plankton Benthos Res*., **1**, 91–96.
Takahashi, K., Kuwata, A., Saito, H. and Ide, K. (2008) Grazing impact of the copepod community in the Oyashio region of the western subarctic Pacific Ocean. *Prog. Oceanogr*., **78**, 222–240.
Takahashi, K., Kuwata, A., Sugisaki, H., Uchikawa, K. and Saito, H. (2009) Downward carbon transport by diel vertical migration of the copepods *Metridia pacifica* and *Metridia okhotensis* in the Oyashio region of the western subarctic Pacific Ocean. *Deep-Sea Res. I*, **56**, 1777–1791.
Takahashi, K., Ichikawa, T., Saito, H., Kakehi, S., Sugimoto, Y., Hidaka, K. and Hamasaki, K. (2013) Sapphirinid copepods as predators of doliolids: Their role in doliolid mortality and sinking flux. *Limnol. Oceanogr*., **58**, 1972–1984.
Takahashi, K., Ichikawa, T., Fukugama, C., Yamane, M., Kakehi, S., Okazaki, Y., Kubota, H. and Furuya, K. (2015) In situ observations of a doliolid bloom in a warm water filament using a video plankton recorder: Bloom development, fate, and effect on biogeochemical cycles and planktonic food webs. *Limnol. Oceanogr*., **60**, 1763–1780.
Taniguchi, A. (1994) Hundred year of planktology. *JAMSTEC*, **6**, 1–9 (in Japanese).
Terazaki, M. (1996) Order Chaetognatha. In: Chihara, M. and Murano, M. (Eds.), *An Illustrated Guide to Marine Plankton in*

*Japan*. Tokai University Press, Tokyo, pp. 1271–1289.

Terazaki, M. (1998) Life history and distribution, seasonal variability and feeding of the pelagic chaetognath *Sagitta elegans* in the subarctic Pacific: A review. *Plankton Biol. Ecol*., **45**, 1–17.

Terazaki, M. and Miller, C.B. (1986) Life history and vertical distribution of pelagic chaetognaths at Ocean Station P in the subarctic Pacific. *Deep-Sea Res*., **33**, 323–337.

Terazaki, M. and Tomatsu, C. (1997) A vertical multiple opening and closing plankton sampler. *J. Adv. Mar. Sci. Tech. Soc*., **3**, 127–132.

Thomson, J.M. (1947) The chaetognaths of southern Australia. *Com. Sci. Ind. Res. Bull. (Div. Fish. Rept. No. 14)*, **222**, 1–43.

Tokioka, T. (1974) On the specific validity in species pairs or trios of plankton animals, distributed respectively in different but adjoining water masses, as seen in chaetognaths. *Publ. Seto Mar. Biol. Lab*., **21**, 393–408.

Tsuda, A. and Sugisaki, H. (1994) *In situ* grazing rate of the copepod population in the western subarctic North Pacific during spring. *Mar. Biol*., **120**, 203–210.

Tsuda, A., Saito, H. and Kasai, H. (1999) Life histories of *Neocalanus flemingeri* and *Neocalanus plumchrus* (Calanoida: Copepoda) in the western subarctic Pacific. *Mar. Biol*., **135**, 533–544.

Tsuda, A., Saito, H. and Kasai, H. (2004) Life histories of *Eucalanus bungii* and *Neocalanus cristatus* (Copepoda: Calanoida) in the western subarctic Pacific Ocean. *Fish. Oceanogr.*, **13**, 10–20.

Tsuda, A., Saito, H., Nishioka, J. and Ono, T. (2005) Mesozooplankton responses to iron-fertilization in the western subarctic Pacific (SEEDS2001). *Prog. Oceanogr*., **64**, 237–251.

Tsuda, A., Saito, H., Nishioka, J., Ono, T., Noiri, Y. and Kudo, I. (2006) Mesozooplankton response to iron enrichment during the diatom bloom and bloom decline in SERIES (NE Pacific). *Deep-Sea Res. II*, **53**, 2281–2296.

Tsuda, A., Takeda, S., Saito, H., Nishioka, J., Kudo, I., Nojiri, Y., Suzuki, K., Uematsu, M., Wells, M.L., Tsumune, D., Yoshimura, T., Aono, T., Aramaki, T., Cochlan, W.P., Hayakawa, M., Imai, K., Isada, T., Iwamoto, Y., Johnson, W.K., Kameyama, S., Kato, S., Kiyosawa, H., Kondo, Y., Levasseur, M., Machida, R., Nagao, I., Nakagawa, F., Nakanishi, T., Nakatsuka, S., Narita, A., Noiri, Y., Obata, H., Ogawa, H., Oguma, K., Ono, T., Sakuragi, T., Sasakawa, M., Sato, M., Shimamoto, A., Takata, H., Trick, C.G., Watanabe, Y.Y., Wong, C.S. and Yoshie, N. (2007) Evidence for the grazing hypothesis: Grazing reduces phytoplankton responses of the HNLC ecosystem to iron enrichment in the western subarctic Pacific (SEEDS II). *J. Oceanogr*., **63**, 983–994.

Tsuda, A., Saito, H., Machida, R.J. and Shimode, S. (2009) Meso- and microzooplankton responses to an in situ iron fertilization experiment (SEEDS-II) in the northwest subarctic Pacific. *Deep-Sea Res. II*, **56**, 2767–2778.

Tsuda, A., Saito, H. and Kasai, H. (2014) Vertical distributions of large ontogenetically migrating copepods in the Oyashio region during their growing season. *J. Oceanogr*., **70**, 123–132.

Ueda, A., Kobari, T. and Steinberg, D.K. (2008) Body length, weight and chemical composition of ontogenetically migrating copepods in the Western Subarctic Gyre of the North Pacific Ocean. *Bull. Plankton Soc. Japan*, **55**, 107–114 (in Japanese with English abstract).

Venrick, E.L. (1986) The Smirnov statistics: an incorrect test for vertical distribution patterns. *Deep-Sea Res*., **33A**, 1275–1277.

Vidal, J. and Smith, S.L. (1986) Biomass, growth, and development of populations of herbivorous zooplankton in the south eastern Bering Sea during spring. *Deep-Sea Res*., **33A**, 523–556.

Wong, C.K. (1988) The swimming behavior of the copepod *Metridia pacifica*. *J. Plankton Res*., **10**, 1285–1290.

Yamada, Y. and Ikeda, T. (2000) Development, maturation, brood size and generation length of the mesopelagic amphipod *Cyphocaris challengeri* (Gammaridea: Lysianassidae) off southwest Hokkaido, Japan. *Mar. Biol*., **137**, 933–942.

Yamada, Y. and Ikeda, T. (2001a) Notes on early development and secondary sexual characteristics of the mesopelagic amphipod *Cyphocaris challengeri* (Gammaridea; Lysianassidae). *B ull. Fish. Sci. Hokkaido Univ*., **52**, 55–59.

Yamada, Y. and Ikeda, T. (2001b) Notes on early development and secondary sexual characteristics of the mesopelagic amphipod *Primno abyssalis* (Hyperiidea: Phrosinidae). *Bull. Fac. Fish. Hokkaido Univ*., **52**, 61–65.

Yamada, Y. and Ikeda, T. (2004) Some diagnostic characters for the classification of two sympatric hyperiid amphipods, *Themisto pacifica* and *T. japonica*, in the western North Pacific. *Bull. Fish. Sci. Hokkaido Univ*., **54**, 59–65.

Yamada, Y. and Ikeda, T. (2006) Production, metabolism and trophic importance of four pelagic amphipods in the Oyashio region, western subarctic Pacific. *Mar. Ecol. Prog. Ser*., **308**, 155–163.

Yamada, Y., Ikeda, T. and Tsuda, A. (2002) Abundance, growth and life cycle of the mesopelagic amphipod *Primno abyssalis* (Hyperiidea: Phrosinidae) in the Oyashio region, western subarctic Pacific. *Mar. Biol*., **141**, 333–341.

Yamada, Y., Ikeda, T. and Tsuda, A. (2004) Comparative life-history study on sympatric hyperiid amphipods (*Themisto pacifica* and *T. japonica*) in the Oyashio region, western North Pacific. *Mar. Biol*., **145**, 515–527.

Yamaguchi, A. and Ikeda, T. (2000a) Vertical distribution, life cycle and developmental characteristics of the mesopelagic calanoid copepod *Gaidius variabilis* (Aetideidae) in the Oyashio region, western North Pacific Ocean. *Mar. Biol*., **137**, 99–109.

Yamaguchi, A. and Ikeda, T. (2000b) Vertical distribution, life cycle and body allometry of two oceanic calanoid copepods (*Pleuromamma scutullata* and *Heterorhabdus tanneri*) in the Oyashio region, western North Pacific Ocean. *J. Plankton Res*., **22**, 29–46.

Yamaguchi, A. and Ikeda, T. (2001) Abundance and population structure of three mesopelagic *Paraeuchaeta* species (Copepoda: Calanoida) in the Oyashio region, western subarctic Pacific Ocean with notes on their carcasses and epizoic ciliates. *Plankton Biol. Ecol*., **48**, 104–113.

Yamaguchi, A. and Ikeda, T. (2002a) Vertical distribution patterns of three mesopelagic *Paraeuchaeta* species (Copepoda: Calanoida) in the Oyashio region, western subarctic Pacific Ocean. *Bull. Fish. Sci. Hokkaido Univ*., **53**, 1–10.

Yamaguchi, A. and Ikeda, T. (2002b) Reproductive and developmental characteristic of three mesopelagic *Paraeuchaeta* species (Copepoda: Calanoida) in the Oyashio region, western subarctic Pacific Ocean. *Bull. Fish. Sci. Hokkaido Univ*., **53**, 11–21.

Yamaguchi, A., Watanabe, Y., Ishida, H., Harimoto, T., Furusawa, K., Suzuki, S., Ishizaka, J., Ikeda, T. and Takahashi, M. (2002) Community and trophic structures of pelagic copepods down to the greater depths in the western subarctic Pacific (WEST-COSMIC). *Deep-Sea Res. I*, **49**, 1007–1025.

Yamaguchi, A., Ikeda, T., Watanabe, Y. and Ishizaka, J. (2004a)

Vertical distribution patterns of pelagic copepods as viewed from the predation pressure hypothesis. *Zool. Stud*., **43**, 475–485.

Yamaguchi, A., Watanabe, Y., Ishida, H., Harimoto, T., Furusawa, K., Suzuki, S., Ishizaka, J., Ikeda, T. and Takahashi, M. (2004b) Latitudinal differences in the planktonic biomass and community structure down to the greater depths in the western North Pacific. *J. Oceanogr*., **60**, 773–787.

Yamaguchi, A., Onishi, Y., Omata, A., Kawai, M., Kaneda, M. and Ikeda, T. (2010a) Population structure, egg production and gut content pigment of large grazing copepods during the spring phytoplankton bloom in the Oyashio region. *Deep-Sea Res. II*, **57**, 1679–1690.

Yamaguchi, A., Onishi, Y., Omata, A., Kawai, M., Kaneda, M. and Ikeda, T. (2010b). Diel and ontogenetic variations in vertical distributions of large grazing copepods during the spring phytoplankton bloom in the Oyashio region. *Deep-Sea Res. II*, **57**, 1691–1702.